Peroxyl radical reactions with carotenoids in microemulsions: Influence of microemulsion composition and the nature of peroxyl radical precursor

Ali El-Agamey, David J. Mcgarvey

PII: S0891-5849(15)01100-4
DOI: http://dx.doi.org/10.1016/j.freeradbiomed.2015.10.427
Reference: FRB12647

To appear in: *Free Radical Biology and Medicine*

Received date: 27 July 2015
Revised date: 10 October 2015
Accepted date: 26 October 2015

Cite this article as: Ali El-Agamey and David J. Mcgarvey, Peroxyl radical reactions with carotenoids in microemulsions: Influence of microemulsion composition and the nature of peroxyl radical precursor, *Free Radical Biology and Medicine,* http://dx.doi.org/10.1016/j.freeradbiomed.2015.10.427

Peroxyl radical reactions with carotenoids in microemulsions: Influence of microemulsion composition and the nature of peroxyl radical precursor

ALI EL-AGAMEY*[1, 2] & DAVID J MCGARVEY[1]

[1]*School of Physical and Geographical Sciences, Keele University, Keele, Staffordshire ST5 5BG, UK*

[2]*Chemistry Department, Faculty of Science, Damietta University, New Damietta, Damietta, Egypt.*

Abstract

The reactions of acetylperoxyl radicals with different carotenoids (7,7'-dihydro-β-carotene and ζ-carotene) in SDS and CTAC microemulsions of different compositions were investigated using laser flash photolysis (LFP) coupled with kinetic absorption spectroscopy. The primary objective of this study was to explore the influence of microemulsion composition and the type of surfactant used on the yields and kinetics of various transients formed from the reaction of acetylperoxyl radicals with carotenoids. Also, the influence of the site (hydrocarbon phases or aqueous phase) of generation of the peroxyl radical precursor was examined by using 4-acetyl-4-phenylpiperidine hydrochloride (APPHCl) and 1, 1-diphenylacetone (11DPA) as water-soluble and lipid-soluble peroxyl radical precursors, respectively. LFP of peroxyl radical precursors with 7,7'-dihydro-β-carotene (77DH) in different microemulsions gives rise to the formation of three distinct transients namely addition radical (λ_{max} = 460 nm), near infrared transient1 (NIR, λ_{max} = 700 nm) and 7,7'-dihydro-β-carotene radical cation ($77DH^{\bullet+}$, λ_{max} = 770 nm). In addition, for ζ-carotene (ZETA) two transients

(near infrared transient1 (NIR1, λ_{max} = 660 nm) and ζ-carotene radical cation (ZETA$^{\bullet+}$, λ_{max} = 730-740 nm)) are generated following LFP of peroxyl radical precursors in the presence of ζ-carotene (ZETA) in different microemulsions. The results show that the composition of the microemulsion strongly influences the observed yield and kinetics of the transients formed from the reactions of peroxyl radicals (acetylperoxyl radicals) with carotenoids (77DH and ZETA). Also, the type of surfactant used in the microemulsions influences the yield of the transients formed. The dependence of the transient yields and kinetics on microemulsion composition (or the type of surfactant used in the microemulsion) can be attributed to the change of the polarity of the microenvironment of the carotenoid. Furthermore, the nature of the peroxyl radical precursor used (water-soluble or lipid-soluble peroxyl radical precursors) has little influence on the yields and kinetics of the transients formed from the reaction of peroxyl radicals with carotenoids. In the context of the interest in carotenoids as radical scavenging antioxidants, the fates of the addition radicals (formed from the reaction of carotenoid with peroxyl radicals) and carotenoid radical cations are discussed.

Keywords: carotenoid; peroxyl radical; radical cation; microemulsion; laser flash photolysis

Introduction

Many studies have been reported about the free radical reactions with carotenoids in organic solvents. These studies have shown that carotenoids can

efficiently scavenge different types of radicals [1-10]. The mechanism of the reaction depends on the type of reacting radical, the carotenoid and the solvent [1,2,5,8,9,11-15]. For example, in non-polar solvents, carotenoids (CAR) can scavenge peroxyl radicals ($ROO^{\bullet}$) via addition and/or hydrogen abstraction pathways (Eqs. 2-3) [4-7]. However, in polar solvents, the reaction can proceed via addition, hydrogen abstraction and electron-transfer pathways (Eqs. 1-3) depending on the type of the reacting free radical and the carotenoid [1-3,5,16,17].

$$CAR + ROO^{\bullet} \longrightarrow CAR^{\bullet +} + ROO^{-} \quad \text{Electron transfer} \qquad (1)$$

$$CAR + ROO^{\bullet} \longrightarrow CAR^{\bullet} + ROOH \quad \text{Hydrogen abstraction} \qquad (2)$$

$$CAR + ROO^{\bullet} \longrightarrow ROOCAR^{\bullet} \quad \text{Addition} \qquad (3)$$

Time-resolved peroxyl radical studies with carotenoids in micelles and microemulsions are very limited [18,19] although they can be used as simple models for cellular membranes [20-22]. Microemulsions are composed of water, oil (usually a hydrocarbon solvent such as cyclohexane), a cofactor (*e.g.* an alcohol with a relatively long hydrocarbon chain such as 1-pentanol) and surfactant. Microemulsions can be classified according to the water to oil ratio into (1) water-in-oil (W/O) (2) oil-in-water (O/W). However, at intermediate ratios of water to oil, bicontinuous structures are formed where water and oil channels are separated by a monolayer of surfactant molecules [21]. Earlier studies have shown the schematic representations for W/O, O/W and bicontinuous microemulsions [21,23]. Unlike micelles, microemulsions have the advantage of

the ability to dissolve large amounts of hydrophobic substances and to accommodate long molecules due to the presence of the oil and cofactor [24].

Hill *et al* studied the reactions of trichloromethylperoxyl radicals with different carotenoids in 2% TX-100 micelles [18]. The reaction gives rise to near infrared (NIR) absorbing species (NIR1) and carotenoid radical cation ($CAR^{\bullet+}$), which absorbs at longer wavelengths than that of NIR1. Subsequently, the NIR1 transient decays slowly to form more $CAR^{\bullet+}$ (Scheme 1). In addition, using pulse radiolysis, the reactions of retinoids with trichloromethylperoxyl radicals in Triton X-100 micelles gave rise to the formation of at least two transient products [19b]. One of them was identified as the corresponding retinoid cation radical ($\lambda_{max} \approx$ 590 nm). Furthermore, there is only one study, using pulse radiolysis, for the reaction of peroxyl radicals with carotenoids in microemulsions. Adhikari *et al* [19a] reported similar reaction mechanisms to that described by Hill (See Scheme 1) for the reactions of halogenated peroxyl radicals with β–carotene (β-CAR) in microemulsions (sodium lauryl sulphate (3.23% w/v), cyclohexane (75% v/v), water (6.45% v/v) and 1-pentanol (15.32% v/v)) (Fig. 1).

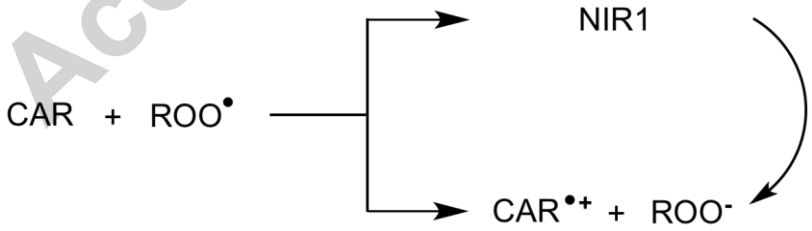

Scheme 1

In the work reported here, the influence of microemulsion composition on the reactions of acetylperoxyl radicals with 77DH and ZETA (See Fig. 1) and of

the resulting addition radicals has been investigated to explore the influence of microenvironment polarity on the transients formed. Also, water-soluble and lipid-soluble peroxyl radical precursors have been used in order to examine the influence of the site of peroxyl radical generation [25]. The carotenoids used in this study (77DH and ZETA) are selected because their radical spectra are well-resolved. Also, the different compositions of microemulsions used in this study and the pseudoternary phase diagram for the four components (SDS, 1-butanol, water and cyclohexane) have been reported by Martinez *et al* [21].

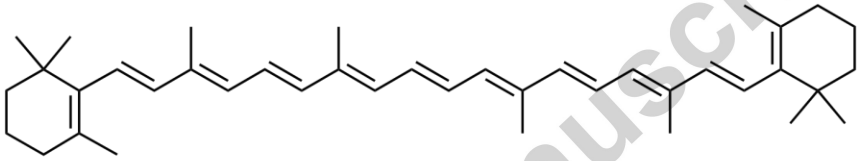

β-Carotene (β-CAR)

ζ-Carotene (ZETA)

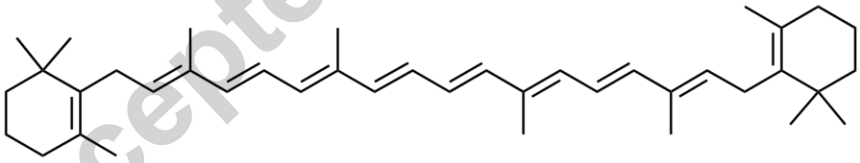

7,7'-Dihydro-β-carotene (77DH)

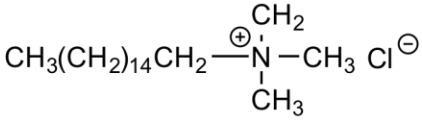

cetyltrimethylammonium chloride (CTAC)

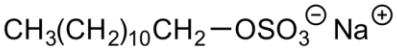

Sodium dodecyl sulfate (SDS)

Fig. 1. Structure of the carotenoids and surfactants.

(single-column fitting image)

Materials and Methods

Materials

1-Butanol (BDH), sodium dodecyl sulfate (BDH), cyclohexane (Aldrich, HPLC grade), 4-acetyl-4-phenylpiperidine hydrochloride (Aldrich), benzene (sigma-Aldrich, spectroscopic grade), 1, 1-diphenylacetone (Lancaster), and cetyltrimethylammonium chloride (Acros) were used as received. The carotenoids, 7,7'-dihydro-β-carotene (77DH) and ζ-carotene (ZETA), were kindly supplied by DSM Nutritional Products and used as received. For microemulsion solutions, ultra pure water (conductivity < 0.067 μS/ cm, Elga UK) was used.

Laser Flash Photolysis

The details of the laser flash photolysis system have been described previously [26a,26b]. Unless otherwise stated, 266 nm laser energies were in the range 2-4 mJ $pulse^{-1}$ with a beam diameter of ~4 mm. Quartz sample cells (2 mm excitation pathlength × 10 mm monitoring pathlength) fitted with vacuum taps (where necessary) were employed for the laser flash photolysis measurements. If necessary, (for example, during acquisition of transient absorption spectra) fresh solution was introduced into the sample cell following each exposure to the laser.

Preparation of Microemulsions

Stock solutions of carotenoids and peroxyl radical precursors were prepared in benzene and methanol respectively. Then volumes containing the required carotenoid and peroxyl radical precursor concentrations were evaporated using a rotary evaporator. The film of carotenoid and peroxyl radical precursor was dissolved in 1-butanol and cyclohexane (calculated as weight percentage of microemulsion composition, see table 1). Subsequently, the surfactant and water were added and the solution was stirred until a clear microemulsion solution was obtained.

Results and Discussion

(a) Generation of radicals.

Laser flash photolysis of 4-acetyl-4-phenylpiperidine hydrochloride (APPHCl) gives rise to acetyl radical and an alkyl substituted benzyl radical via α–cleavage within the very short-lived excited state (singlet or triplet) [26a]. In the presence of oxygen, both radicals react with oxygen to form acetylperoxyl radical ($ACP^{\bullet}$) and a benzylperoxyl radical, respectively (Scheme 2). $ACP^{\bullet}$ is mainly responsible for any observed reaction with carotenoids since it is much more reactive than the benzylperoxyl radical [26a,27].

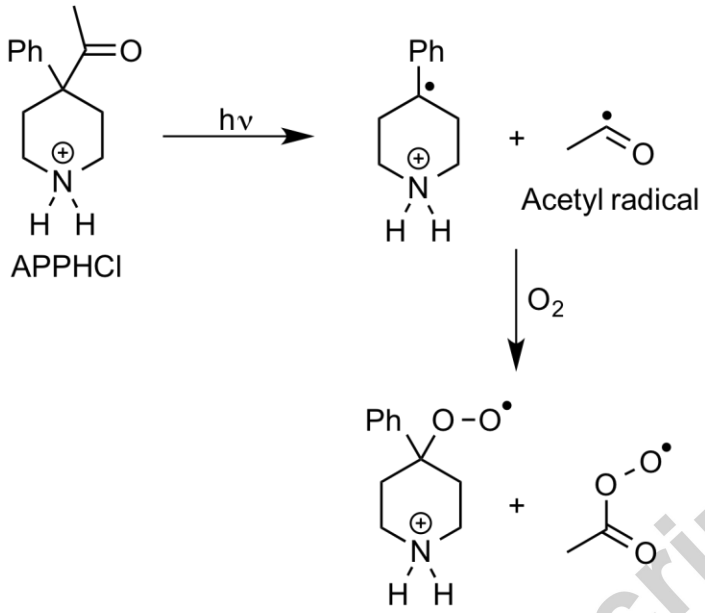

Scheme 2

Similarly, in air-saturated solutions, 1, 1-diphenylacetone (11DPA) undergoes α–cleavage to form acetyl and diphenylmethyl radicals, which react rapidly with oxygen to form ACP$^{\bullet}$ and diphenylmethylperoxyl radical (Scheme 3) [27]. Also, ACP$^{\bullet}$ is principally responsible for the reactions with carotenoids observed on the timescales studied due to the reactivity difference between the resulting peroxyl radicals *i.e.* ACP$^{\bullet}$ is much more reactive than diphenylmethylperoxyl radical [27].

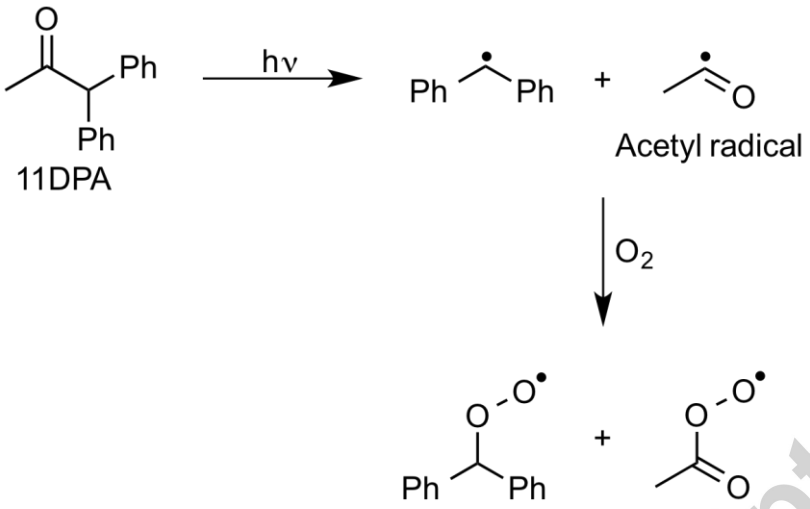

Scheme 3

(b) Influence of microemulsion composition.

(i) 7,7'-Dihydro-β-carotene (77DH). LFP (266 nm) of 77DH and APPHCl or 11DPA in air-saturated SDS microemulsions is shown in Figs. 2 and S1. The compositions of different SDS microemulsions are shown in Table 1.

Table 1: Composition (as weight %) of different microemulsions used in this study [21].

Microemulsion	Surfactant[a]	BU[a,c]	W[c]	CH[c]
A (W/O)	8	16	7	69
B[b]	10	20	23	47
C[b]	10	20	39	31
D[b]	10	20	55	15
E (O/W)	8	16	72	4

[a] The ratio of surfactant to BU in different microemulsion is 1:2.
[b] The microemulsions B, C and D are bicontinuous microemulsions.
[c] BU = 1-butanol; W = water; CH = cyclohexane.

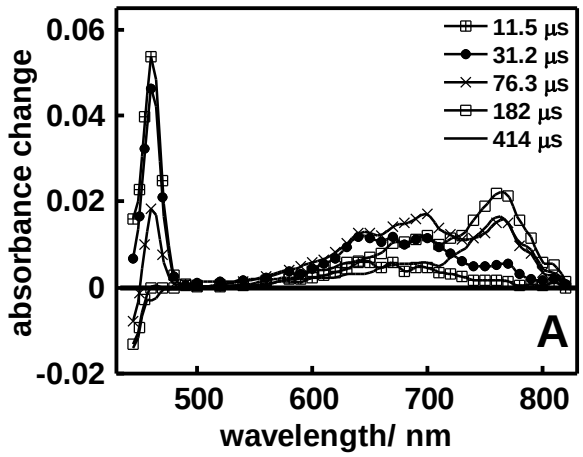

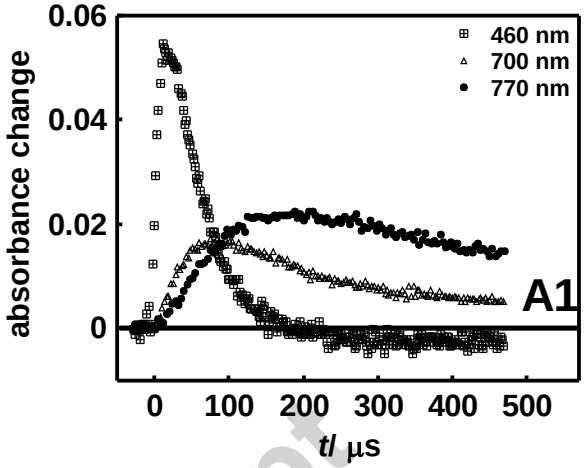

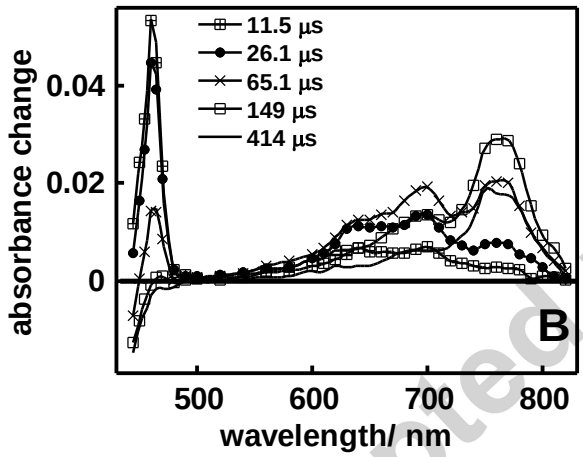

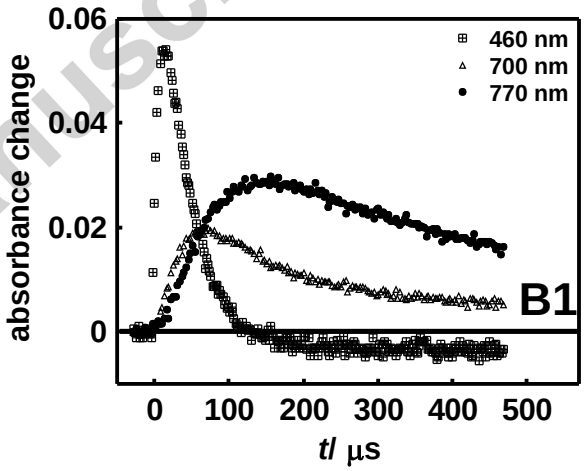

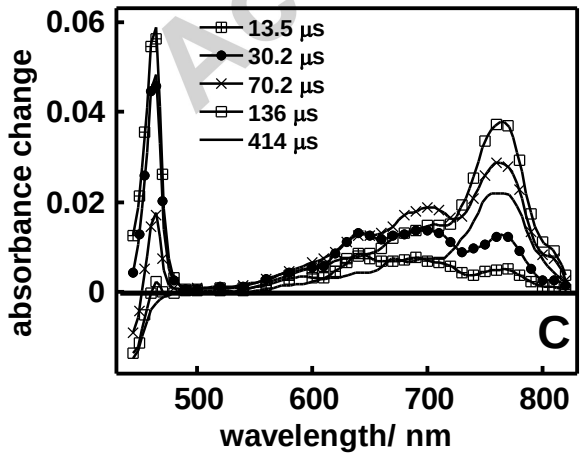

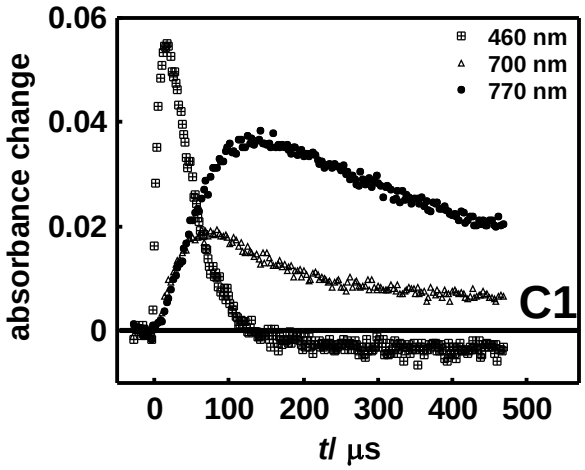

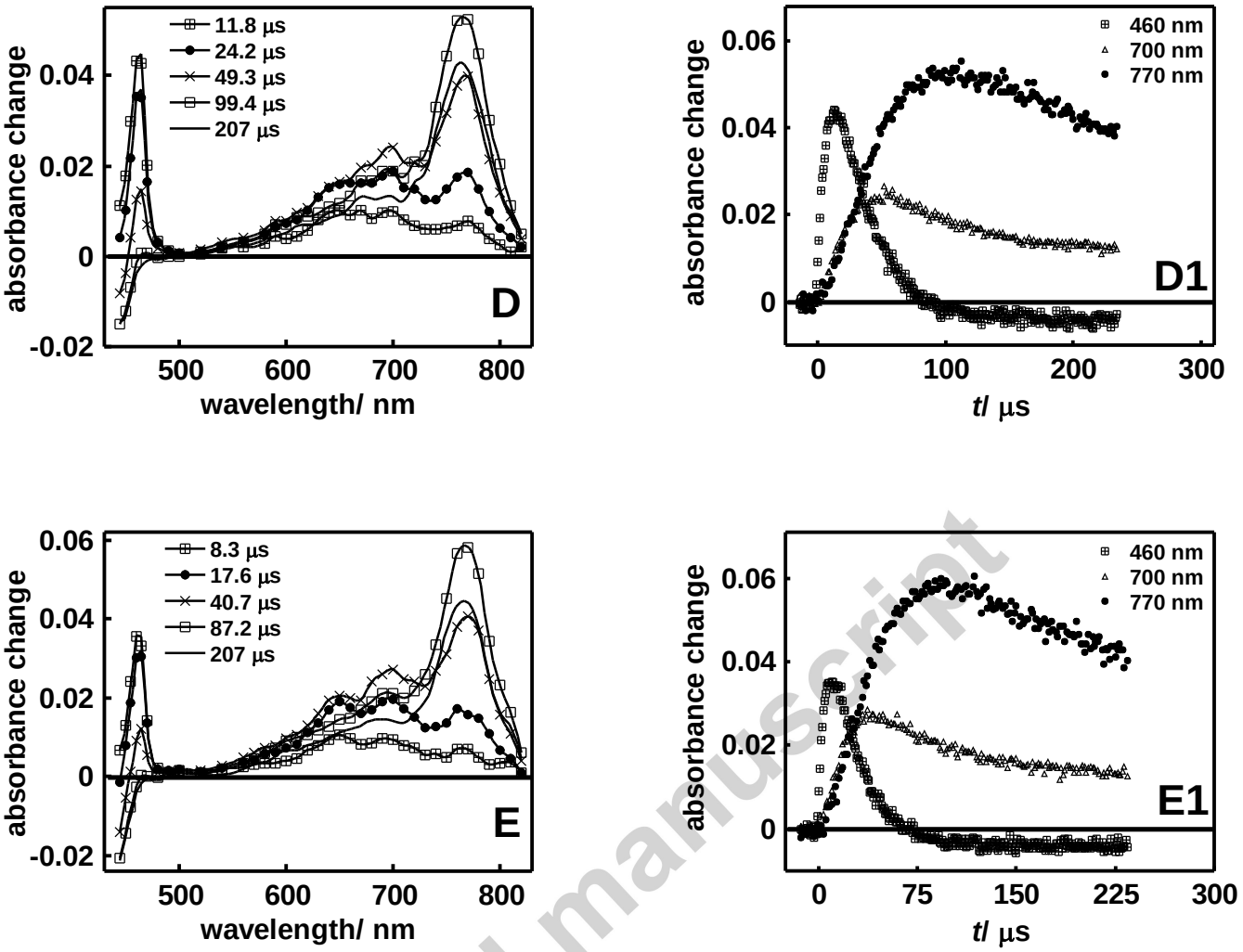

Fig. 2. Transient absorption spectra (Figs. A-E) and transient absorption profiles at 460, 700 and 770 nm (Figs. A1-E1) obtained following LFP (266 nm) of air-saturated solution of APPHCl (2.9 x 10^{-3} M) and 77DH (~4.0 x 10^{-5} M) in SDS microemulsions A, B, C, D and E, respectively (Laser energy = 2.5 mJ, see Table 1).

(2-column fitting image)

The transient spectra in Figs. 2 and S1 show the formation of three distinct transients at 460, 700 and 770 nm. In a previous study [5] of the reaction of

acylperoxyl radicals ($AcylOO^{\bullet}$), generated from α–cleavage of ketones in air-saturated methanolic solution, with 77DH, similar transients have been observed and were attributed to $AcylOO\text{-}77DH^{\bullet}$ (at 460 nm), an ion pair ($AcylOO^{-}$ $77DH^{\bullet+}$) or isomeric derivative of $77DH^{\bullet+}$ (at 700 nm) and $77DH^{\bullet+}$ (at 770 nm). $AcylOO^{\bullet}$ radicals react with 77DH to form addition radicals ($AcylOO\text{-}77DH^{\bullet}$), which decay to form (1) several oxidation products *e.g.* epoxides via S_Hi reaction (Pathway ii in Schemes 4 and 5) [26c] and/or (2) NIR1, $AcylOO^{-}$ $77DH^{\bullet+}$ or isomeric derivative of $77DH^{\bullet+}$, in polar solvents (Pathway i in Scheme 4). Subsequently, the decay of NIR1 species is accompanied by the formation of $77DH^{\bullet+}$ (Pathway iii in Scheme 4). As a further support for the proposed mechanism (Scheme 4), the growth profile at 700 nm shows sigmoidal behavior at early times, which is indicative that this species is formed from an intermediate in a consecutive reaction (*i.e.* transient at 700 nm (NIR1) corresponds to C in the sequence A → B → C, where B is the addition radical at 460 nm and A is the parent carotenoid). In non-polar solvents, the reaction gives rise to $AcylOO\text{-}77DH^{\bullet}$ only since its conversion to polar and/or ionic intermediates such as NIR1 and $77DH^{\bullet+}$ is prohibited due to the high energy barrier for their formation in non-polar solvents [5]. Therefore, on the basis of the results of this study [5], a similar interpretation can be attributed to the reaction of $ACP^{\bullet}$ with 77DH in SDS microemulsions.

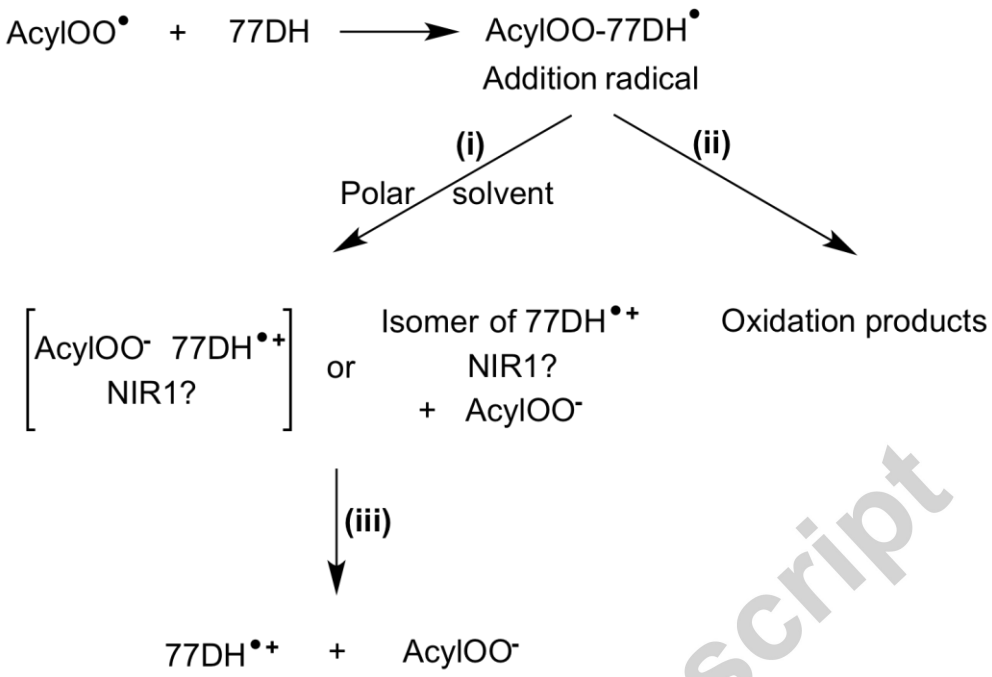

Scheme 4

As shown in Figs. 2A-2E, it is clear that the relative proportions of water and cyclohexane have a strong effect on the absorption ratio of NIR1 species to $77DH^{\bullet+}$. As the water concentration in the microemulsion composition increases, the absorption ratio of NIR1 species to $77DH^{\bullet+}$ is significantly reduced. The plots of the absorption ratio of NIR1 species to $77DH^{\bullet+}$ *versus* the concentration of water (or cyclohexane) in the SDS microemulsion are shown in Figs. 3, 4, S2 and S3. Moreover, by increasing the water concentration in the microemulsion composition, the observed rate constants for ACP-$77DH^{\bullet}$ decay, NIR1 formation, NIR1 decay and $77DH^{\bullet+}$ formation are significantly enhanced (See Tables S1 and S2 and Figs. 5, 6, S4-S7). These observations are in support of the mechanism described in Scheme 4. Similar observations have been reported for the reactions of 77DH with $AcylOO^{\bullet}$ in a series of alcohols (methanol, ethanol, 1-

butanol, 1-pentanol and 1-decanol) where the absorption ratio of NIR1 species to $77DH^{\bullet+}$ decreases as the polarity of the solvent increases [5,11].

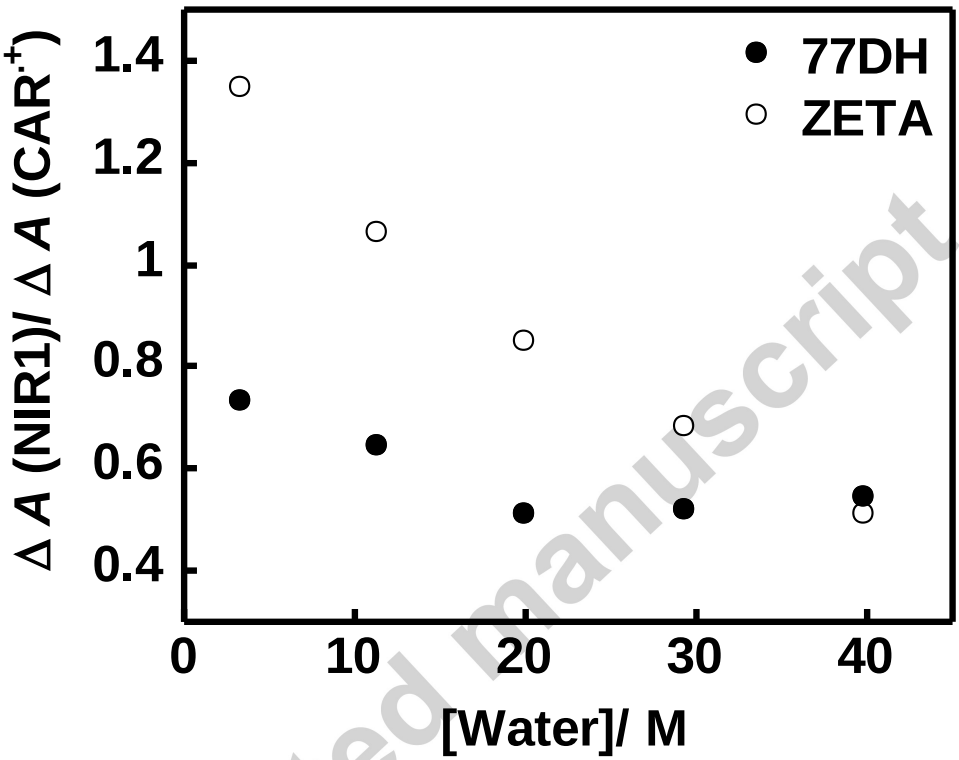

Fig. 3. Plot of the absorbance ratio of NIR1 to $CAR^{\bullet+}$, formed from the reaction of $ACP^{\bullet}$ (generated from LFP of APPHCl) and 77DH or ZETA, *versus* water concentration in different SDS microemulsions.

(single-column fitting image)

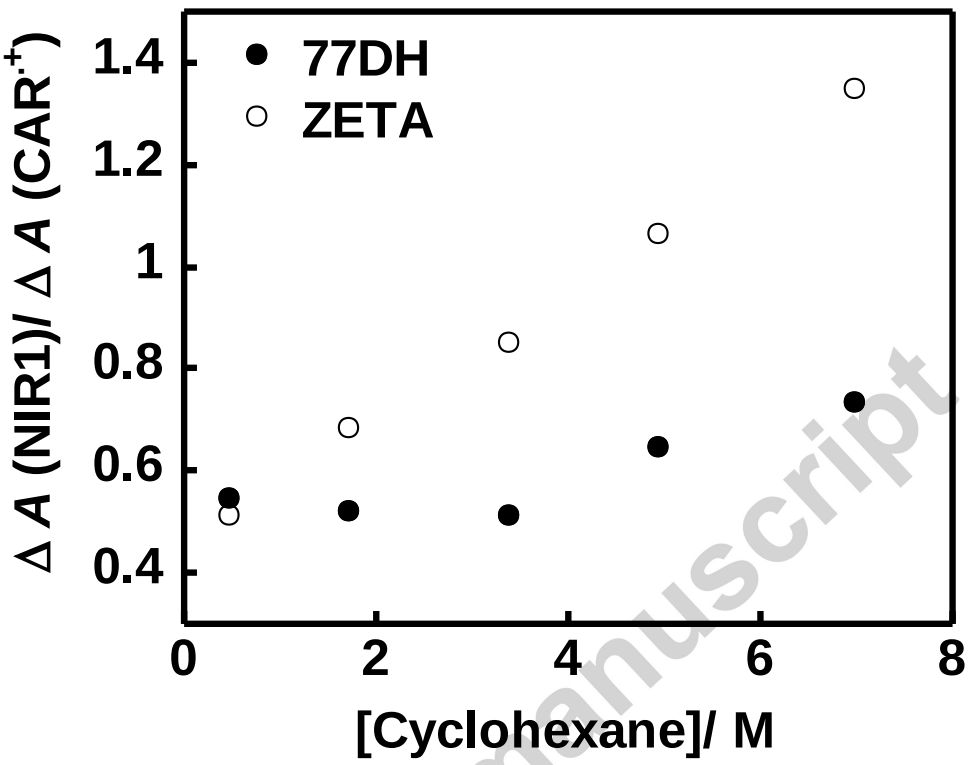

Fig. 4. Plot of the absorbance ratio of NIR1 to $CAR^{\bullet+}$, formed from the reaction of $ACP^{\bullet}$ (generated from LFP of APPHCl) and 77DH or ZETA, *versus* cyclohexane concentration in different SDS microemulsions.

(single-column fitting image)

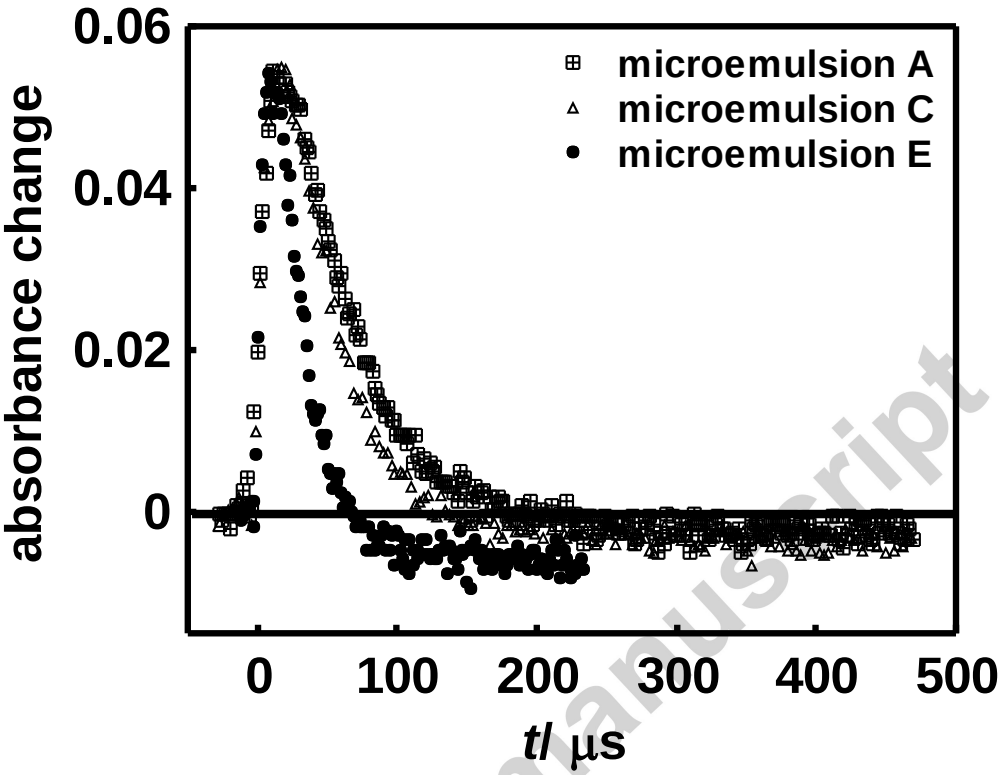

Fig. 5. Normalized transient absorption profiles at 460 nm (ACP-77DH$^{\bullet}$) obtained following LFP (266 nm) of air-saturated solution of APPHCl (2.9 x 10^{-3} M) and 77DH (~4.0 x 10^{-5} M) in SDS microemulsions A, C and E, respectively (Laser energy = 2.5 mJ, see Table 1).

(single-column fitting image)

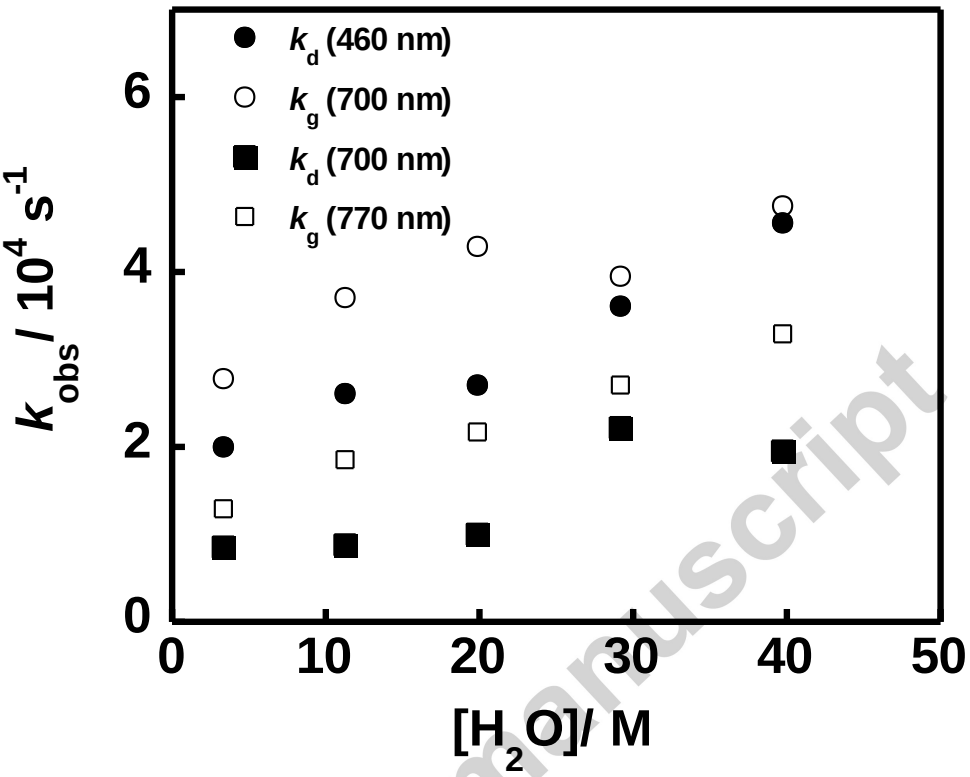

Fig. 6. Plot of the observed rate constants (k_{obs}) for the decay (or growth) of the radical processes involving ACP$^{\bullet}$ (generated from LFP of APPHCl) and 77DH *versus* water concentration in different SDS microemulsions. k_d and k_g are the observed rate constant for the 1st order decay and growth at the corresponding wavelength.

(single-column fitting image)

The reactions of 77DH with either water or lipid-soluble peroxyl radical precursors show a similar trend in the yields and the kinetics of the transients formed (See Tables S1 and S2 and Figs. 2 and S1). This could be attributed to

the rapid equilibration of $ACP^{\bullet}$ between the pseudo-phases in comparison with the $ACP^{\bullet}$ decay. Similarly, the independence of singlet oxygen ($^1O_2$) quenching kinetics on the site of generation has been ascribed to the rapid equilibration of $^1O_2$ between the two phases or pseudophases in micelles [28,29], microemulsions [21, 24] and liposomes [30]. This could be due to the presence of the $ACP^{\bullet}$ precursors in the interfacial region because of their amphiphilic characters. Charged molecules (*e.g.* rose begal) and ketones (*e.g.* perinaphthenone and phenyl pyridyl ketones) have been reported to reside in the interfacial region of micelles and microemulsions [24,28,31,32].

The results from LFP (266 nm) of 77DH and APPHCl or 11DPA in air-saturated CTAC microemulsions A and E are shown in Figs. 7 and S8. Similar transients were observed at 460, 700 and 770 nm. The influence of microemulsion composition is great since in microemulsion A there is almost no formation of $77DH^{\bullet+}$, however in microemulsion E the yield of $77DH^{\bullet+}$ is even higher than the NIR1 species. By comparing Fig. 2A with Fig. 7A (or Fig. S1A with S8A), it can be concluded that the type of surfactant in the microemulsion has a substantial influence on the polarity of the microenvironment of the 77DH. At similar microemulsion composition, it appears that the SDS microemulsion has a more polar microenvironment around 77DH than that of CTAC microemulsion. This could be attributed to the electrostatic repulsion between the positive charges on $77DH^{\bullet+}$ and CTAC surfactant molecules, which inhibits the formation of $77DH^{\bullet+}$. Also, CTAC has a longer alkyl chain than that of SDS, which may cause the 77DH to reside even further away from the interface (Fig. 1).

Therefore, the formation of $77DH^{\bullet+}$ is inhibited by the presence of positively charged head groups at the O/W interface. By analogy to the reactions of 77DH with peroxyl radical precursors in SDS microemulsions, the variation of the nature of the peroxyl radical precursors used (either 11DPA or APPHCl) does not show any significant difference in the behavior of the transients formed (Figs. 7 and S8).

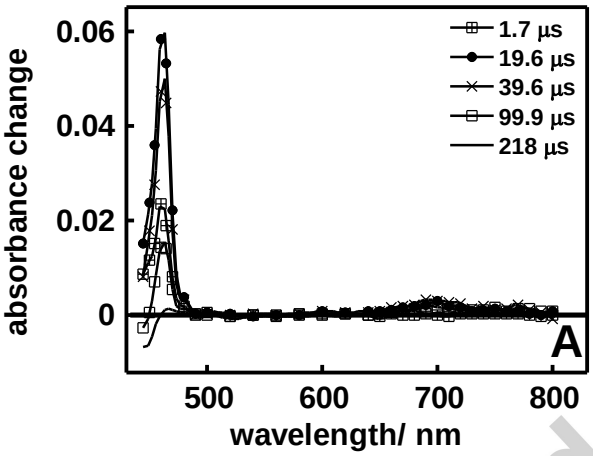

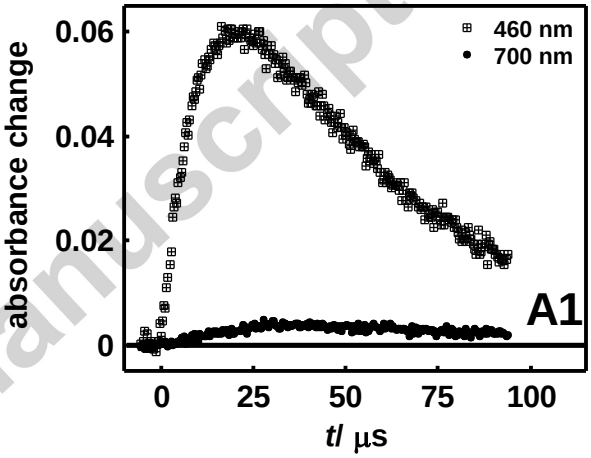

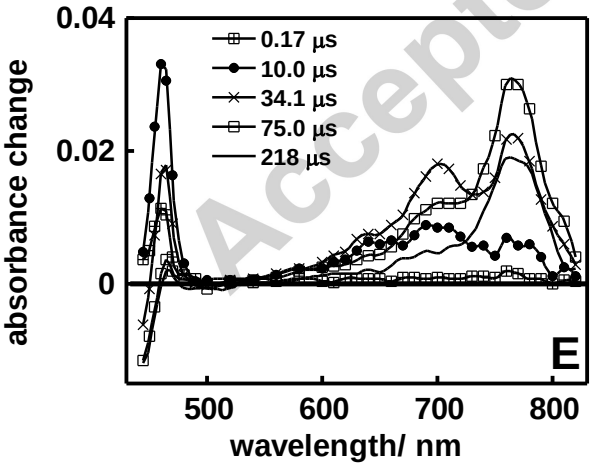

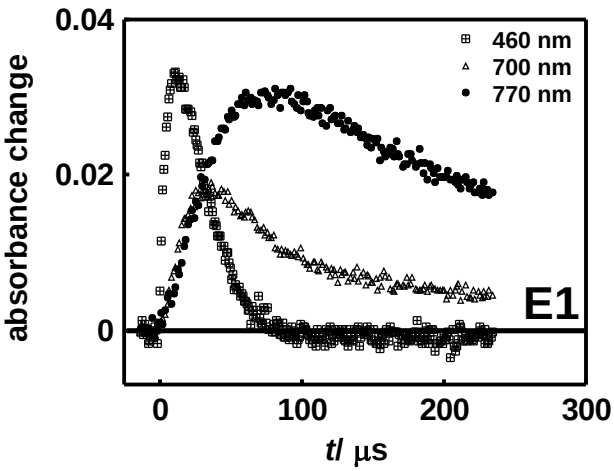

Fig. 7. Transient absorption spectra (Figs. A and E) and transient absorption profiles at 460, 700 and 770 nm, (Figs. A1 and E1) obtained following LFP (266 nm) of air-saturated solution of APPHCl (2.9 x 10^{-3} M) and 77DH (~4.0 x 10^{-5} M) in CTAC microemulsions A and E, respectively (Laser energy = 2.0 mJ, see Table 1).

(2-column fitting image)

(ii) ζ-carotene (ZETA). LFP (266 nm) of ZETA and APPHCl or 11DPA in air-saturated SDS microemulsions is shown in Figs. 8 and S9. The transient spectra show the formation of two distinct transients at 660 and 730-740 nm. In a previous study [5] for the reaction of acylperoxyl radicals (AcylOO$^{\bullet}$) with ZETA in a series of alcohols (methanol, ethanol, 1-butanol, 1-pentanol and 1-decanol), similar transients have been reported and attributed to ion pair (AcylOO^{-} ZETA$^{\bullet+}$) or isomeric derivative of ZETA$^{\bullet+}$ (NIR1, at 660 nm) and ZETA$^{\bullet+}$ (at 740 nm). Therefore, the transients observed in microemulsion can be attributed to ion pair (ACP^{-}ZETA$^{\bullet+}$) or isomeric derivative of ZETA$^{\bullet+}$ (at 660 nm) and ZETA$^{\bullet+}$ (at 730-740 nm) respectively. The presence of the sigmoidal behavior at early times in the transient profiles shown in Fig. 8 provides an evidence for consecutive reaction mechanism proposed in Scheme 4. Similarly, in support of this mechanism (Scheme 4), the microemulsion composition shows a strong influence on the absorption ratio of NIR1 species to ZETA$^{\bullet+}$ (Figs. 3, 4, S2 and S3). Furthermore, the observed rate constants for NIR1 decay and ZETA$^{\bullet+}$ formation increase with increasing the water concentration in the microemulsion

composition (See Figs. S10-S13 and Tables S3 and S4). The absence of an absorption band for the ACP-ZETA$^{\bullet}$ can be attributed to the great overlap between the spectra of this addition radical and ZETA. The lack of spectral resolution of the addition radical absorption of ZETA and many other carotenoids was previously observed during the study of acylperoxyl radicals (AcylOO$^{\bullet}$) with various carotenoids [5].

In Figs. 3 and S2, the dependence of the absorption ratio of NIR1 species to 77DH$^{\bullet+}$ on water content in the microemulsion is less than that observed for the corresponding transients of ZETA [33]. The increased dependence of absorption ratio of NIR1 species to ZETA$^{\bullet+}$ on microemulsion composition can be used as a basis for a new method to probe the polarity of the microenvironment of the carotenoid under investigation. In a previous study [11], a plot of the absorption ratio of NIR1 species to ZETA$^{\bullet+}$ *versus* the dielectric constant (ε) of the alcohol was reported. Using this plot and the values of the absorption ratio of NIR1 species to ZETA$^{\bullet+}$ in microemulsion, numerical values for the polarity of the microenvironments at different microemulsion compositions can be calculated. Moreover, in Figs. 8A and S9A (or Figs. 2A and S1A), the observed low yields of ZETA$^{\bullet+}$ (or 77DH$^{\bullet+}$) in oil-rich SDS microemulsions are in agreement with the results of Szymula [34], who has reported that β-carotene shows resistance toward oxidation in oil-rich SDS microemulsion and this has been attributed to the hydrophobic barrier of SDS association structures that hinder electron transfer from β-carotene. Similar to that observed with 77DH, the nature of the

peroxyl radical precursor used shows only a small influence on the behavior of the transients formed (Figs. 8 and S9 and Tables S3 and S4).

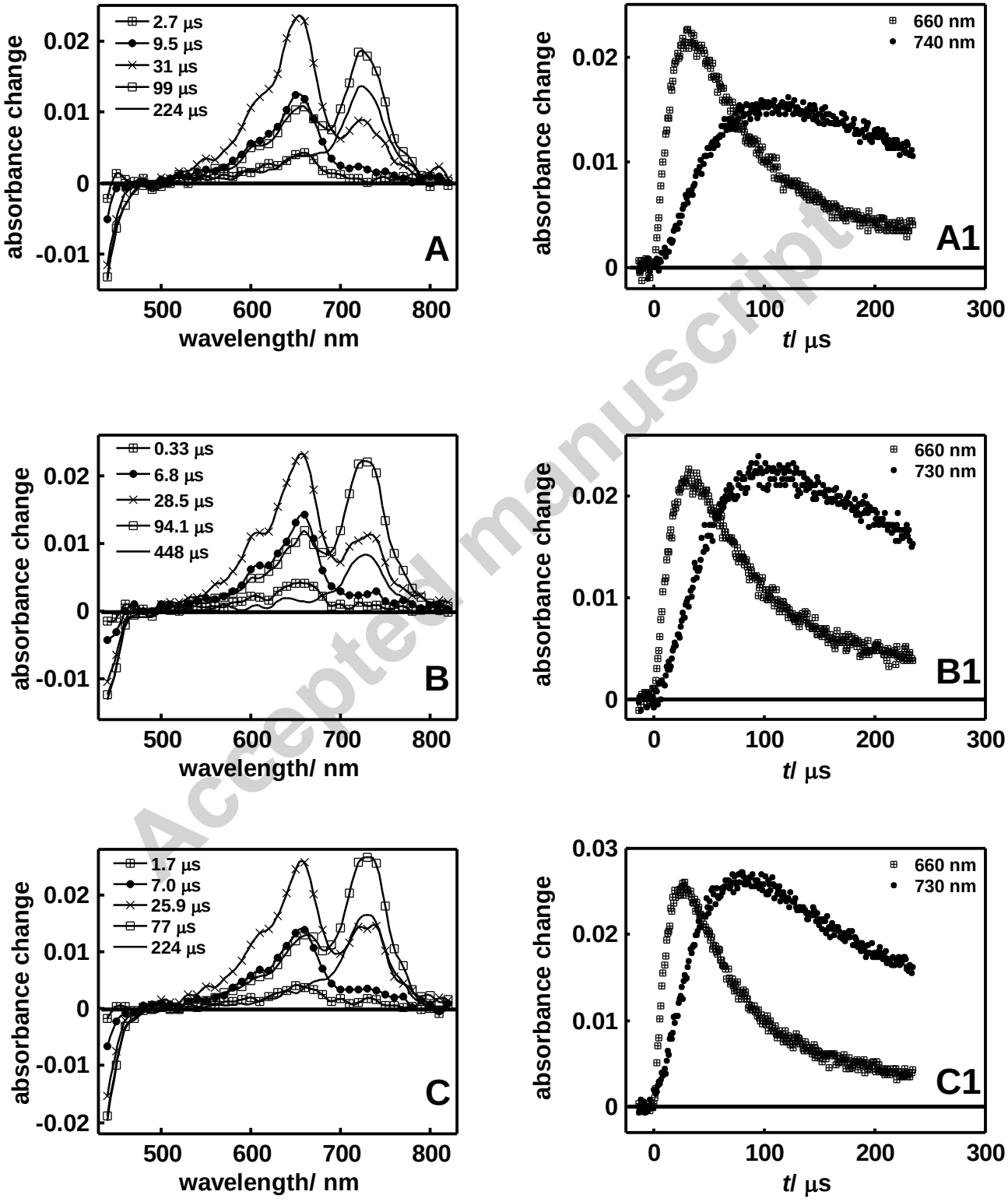

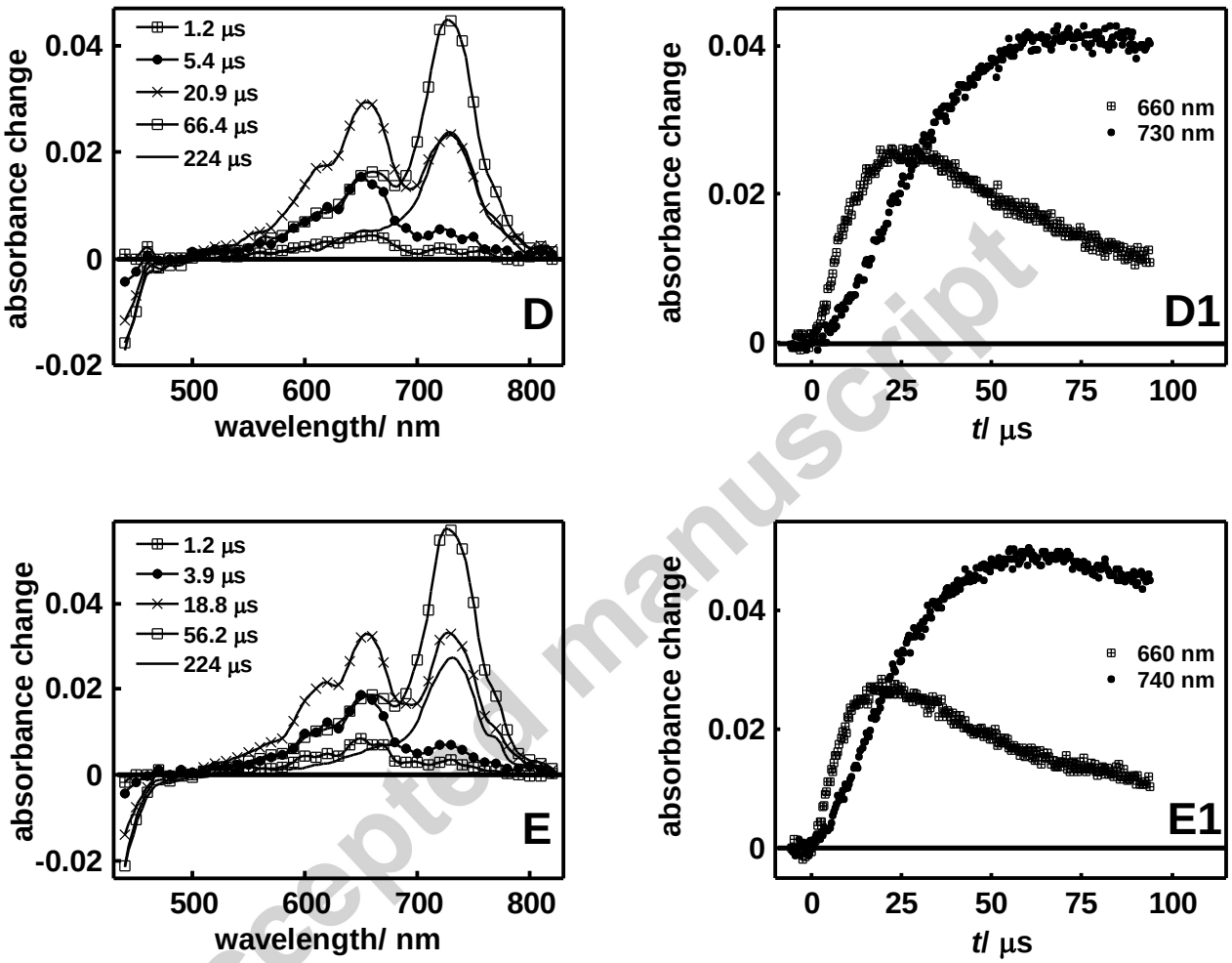

Fig. 8. Transient absorption spectra, (Figs. A-E) and transient absorption profiles at 660 and 730 nm (or 740 nm), (Figs. A1-E1) obtained following LFP (266 nm) of air-saturated solution of APPHCl (2.9 x 10^{-3} M) and ZETA (~ 3.5 x 10^{-5} M) in SDS microemulsions A, B, C, D and E, respectively (Laser energy = 3.5 mJ, see Table 1).

(2-column fitting image)

LFP (266 nm) of ZETA and APPHCl or 11DPA in air-saturated CTAC microemulsions A and E gives rise to two transients at 660 and 740 nm respectively (Figs. 9 and S14). The lower quantum yield of $ZETA^{\bullet+}$ in CTAC microemulsions (Figs. 9A and S14A), compared with that in SDS microemulsions (Figs. 8A and S9A) clearly indicate that there is a substantial effect for the type of the surfactant used in the microemulsion on the absorption ratio of NIR1 species to $ZETA^{\bullet+}$ (*i.e.* on the polarity of the microenvironment around ZETA in microemulsion). These results clearly establish that the microenvironment around carotenoid in CTAC microemulsions is less polar than that in SDS microemulsion at similar microemulsion compositions. Similar observations were obtained from the study of the reaction of $ACP^{\bullet}$ with 77DH in SDS and CTAC microemulsions (Figs. 2 and 7). Furthermore, the peroxyl radical reactions with ZETA in CTAC microemulsions are independent on the nature of peroxyl radical precursors used (Figs. 9 and S14).

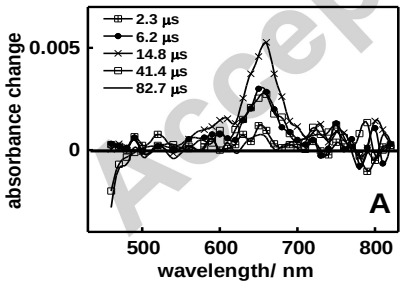

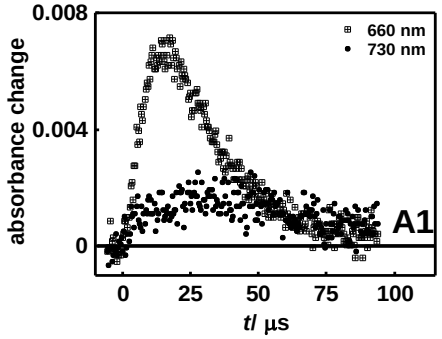

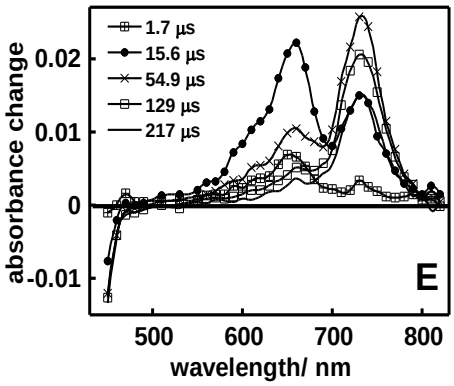

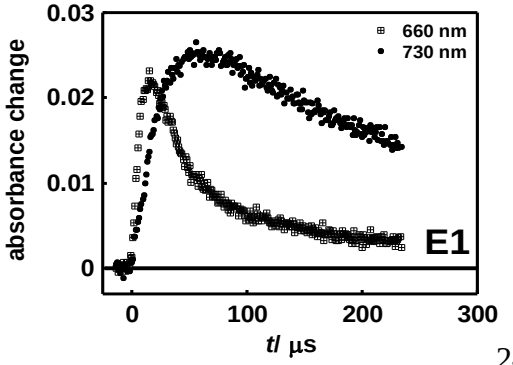

Fig. 9. Transient absorption spectra, (Figs. A and E) and transient absorption profiles at 660 and 730 nm (Figs. A1 and E1) obtained following LFP (266 nm) of air-saturated solution of APPHCl (2.9 x 10^{-3} M) and ZETA (~ 3.0 x 10^{-5} M) in CTAC microemulsions A and E, respectively (Laser energy = 3.5 mJ, see Table1).

(2-column fitting image)

(c) Influence of media composition on the prooxidant-antioxidant properties of carotenoids.

An antioxidant can be defined as any substance that, when present at low concentration compared with those of an oxidizable substrate, significantly delays or prevents oxidation of that substrate [35]. Some compounds act as antioxidants under certain conditions, however, if these conditions change, they can propagate the oxidation of the substrate (*i.e.* they become prooxidants) or they may lose some of their antioxidant efficiency. For carotenoids, it has been reported that β–carotene (β–CAR) acts as an antioxidant at low oxygen concentration, however, under high oxygen concentration, the antioxidant activity of β–CAR is reduced [36-40] and in some cases it acts as prooxidant [38, 41]. The different intermediates formed from the reactions of peroxyl radicals ($ROO^{\bullet}$) with carotenoids (CAR) are shown in Scheme 5. These intermediates are ROO-CAR-$OO^{\bullet}$ (Pathway iii), alkoxyl radical ($RO^{\bullet}$) (Pathway ii) and carotenoid radical cation ($CAR^{\bullet+}$) (Pathway i). The hydrogen-abstraction pathway is omitted from

Scheme 5 since a recent theoretical study has shown that the reaction barrier for the peroxyl radical addition to CAR to form ROO-CAR$^{\bullet}$ is smaller than that for its hydrogen abstraction from CAR [42].

The chemistry of ROO-CAR-OO$^{\bullet}$, has not been thoroughly investigated. However, if ROO-CAR-OO$^{\bullet}$ has similar reactivity to lipidperoxyl radicals (Lipid-OO$^{\bullet}$), it can abstract hydrogen atoms from lipids to form lipid radicals (Lipid$^{\bullet}$), which will start the lipid peroxidation process (Pathways vi and vii) [37,43]. Also, carotenoids can be oxidized via their reactions with ROO-CAR-OO$^{\bullet}$ (Pathway v) [37,43]. The alkoxyl radical (Pathway ii) is generated via S_Hi reaction of ROO-CAR$^{\bullet}$ to form an epoxide [5,39,44]. This radical (RO$^{\bullet}$) can abstract hydrogen atoms from lipids to initiate lipid peroxidation in a similar way to that described earlier for ROO-CAR-OO$^{\bullet}$ (Pathways vi and vii) [45,46]. It is important to emphasize that alkoxyl radicals have a stronger tendency toward hydrogen abstraction than peroxyl radicals therefore their formation will enhance lipid peroxidation process [42].

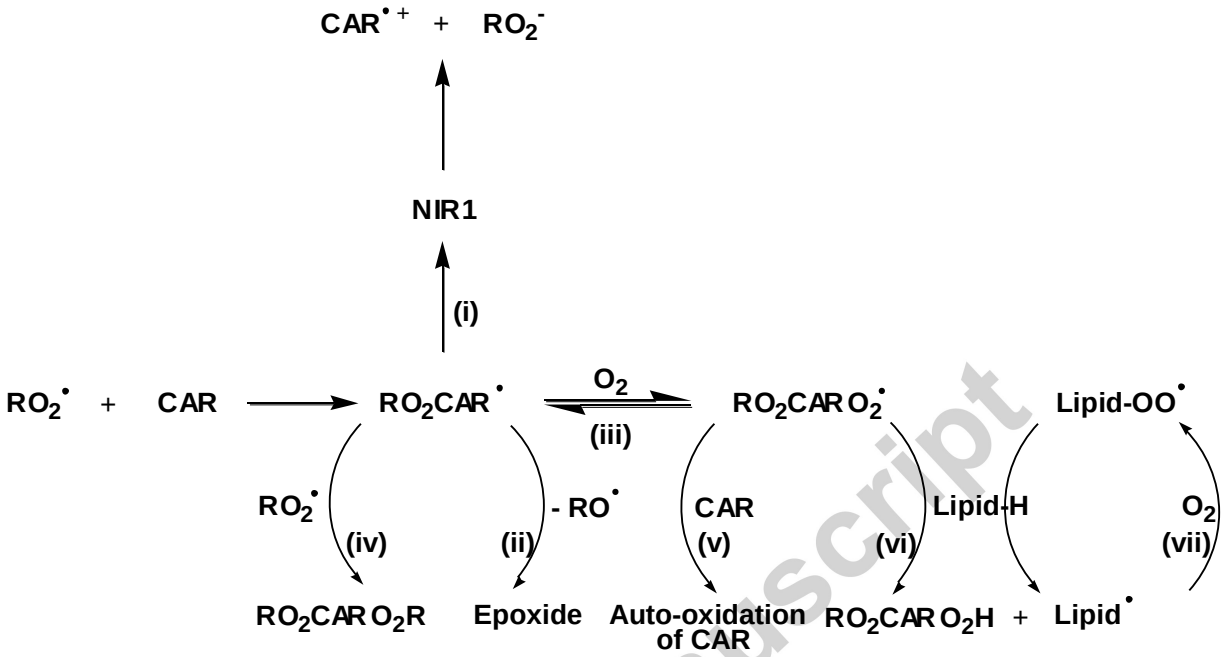

Scheme 5

For carotenoid radical cations ($CAR^{\bullet+}$), it has been reported that various $CAR^{\bullet+}$, generated via pathway i (Scheme 5), are able to oxidize both tyrosine (TyrOH) and cysteine (CySH) (k ~10^4 and 10^6 M^{-1} s^{-1}, respectively) (Eqs. 4 and 5) [13,47-50]. Also, certain carotenoid radical cations react reversibly with tryptophan (TrpH) to form the tryptophan radical cation (Eq. 6) [47,48] in a pH-dependent process. Therefore, if these amino acids are part of protein or enzyme, their functions may be affected by these oxidation reactions. However, in the presence of antioxidants such as vitamin C or E (AscH [51-53] or TOH [54,55]), $CAR^{\bullet+}$ can be reduced to the parent carotenoid (Eqs. 7 and 8).

$$CAR^{\bullet+} + TyrOH \longrightarrow CAR + TyrO^{\bullet} + H^{+} \quad (4)$$

$$CAR^{\bullet+} + CysH \longrightarrow CAR + Cys^{\bullet} + H^{+} \quad (5)$$

$$CAR^{\bullet+} + TrpH \rightleftharpoons CAR + Trp^{\bullet+} + H^{+} \quad (6)$$

$$CAR^{\bullet+} + AscH \longrightarrow CAR + Asc^{\bullet} + H^{+} \quad (7)$$

$$CAR^{\bullet+} + TOH \longrightarrow CAR + TO^{\bullet} + H^{+} \quad (8)$$

The oxygen concentration dependence of the switch between prooxidant and antioxidant properties of β–carotene can be attributed to the reversible oxygen addition to ROO-CAR$^{\bullet}$ (Scheme 5, pathway iii), which converts this unreactive addition radical to a reactive peroxyl radical (ROO-CAR-OO$^{\bullet}$) [4,11,37,39,56]. The factors that control the oxygen addition to carotenoid radicals (Scheme 5, pathway iii) are the oxygen concentration, the rate constant of oxygen addition, the carotenoid chain length and the type of peroxyl radical [4,5].

In W/O microemulsion, the yield of CAR$^{\bullet+}$ is substantially reduced especially in the case of CTAC microemulsions (Figs. 7 and 9). Therefore, the main oxidizing species will be either ROO-CAR-OO$^{\bullet}$ or RO$^{\bullet}$. However, if pathway iv [39,44] is the only important pathway for the decay of ROO-CAR$^{\bullet}$, carotenoids will act as antioxidants. In O/W microemulsion, the formation of CAR$^{\bullet+}$ is significantly enhanced therefore CAR$^{\bullet+}$, RO$^{\bullet}$ and ROO-CAR-OO$^{\bullet}$ can act as oxidizing intermediates. In the previous discussion, it was shown that composition of the microemulsion has a significant effect on the rate constants of different pathways and the yields of different intermediates formed, therefore, it can be concluded that microemulsion composition will have a great impact on the

pro-oxidant-antioxidant activity of the carotenoids. Taken together, it should be highlighted that in addition to the media properties, there are many factors, which have an influence on the pro-oxidant-antioxidant activity of the carotenoids. These factors are oxygen concentration, orientation and location of the carotenoid within biological membranes, carotenoid structure, interaction with other antioxidants and carotenoid concentration [11,53,57-60].

Conclusions

The composition and the type of surfactant used in the microemulsion have significant influences on the polarity of the microenvironment and thereby the quantum yield of various transients formed. In this study, we indicated that the absorption ratio of NIR1 species to $CAR^{\bullet+}$ can be used to probe and compare the polarities of the microenvironments in different microemulsions. Moreover, our results suggest that the peroxyl radical reactions with carotenoids in SDS or CTAC microemulsions are independent on the nature (water or lipid-soluble) of peroxyl radical precursors used. Finally, the flexibility of changing the polarity of the microenvironment of the target in microemulsions by changing the microemulsion composition can facilitate the study of the effect of the media polarity on the any reaction especially where there is a solubility restriction for any component involved in the reaction.

Supporting Information

Kinetic and spectral data of 7,7'-dihydro-β-carotene (77DH) and ζ-carotene (ZETA) with 1, 1-diphenylacetone (11DPA) or 4-acetyl-4-phenylpiperidine hydrochloride (APPHCl) in various SDS and CTAC microemulsions are provided.

Acknowledgements

The authors are grateful to the Leverhulme Trust (Research Grant F/00130F) for financial support and to DSM Nutritional Products for supplying the carotenoids used in this work.

References

[1] Everett, S. A.; Dennis, M. F.; Patel, K. B.; Maddix, S.; Kundu, S. C.; Willson, R. L. Scavenging of nitrogen dioxide, thiyl, and sulfonyl free radicals by the nutritional antioxidant β-carotene. *J. Biol. Chem.* **271**:3988-3994; 1996.

[2] Mortensen, A.; Skibsted, L. H.; Sampson, J.; Rice-Evans, C.; Everett, S. A. Comparative mechanisms and rates of free radical scavenging by carotenoid antioxidants. *FEBS Lett.* **418**:91-97; 1997.

[3] Everett, S. A.; Kundu, S. C.; Maddix, S.; Willson, R. L. Mechanisms of free-radical scavenging by the nutritional antioxidant β-carotene. *Biochem. Soc. Trans.* **23**:230S; 1995.

[4] (a) El-Agamey, A. and McGarvey, D. J. First direct observation of reversible oxygen addition to a carotenoid-derived carbon-centered neutral radical. *Org. Lett.* **7**:3957-3960; 2005. (b) El-Agamey, A. and McGarvey, D. J. The reactivity of carotenoid radicals with oxygen. *Free Rad. Res.* **41**:295-302; 2007.

[5] El-Agamey, A. and McGarvey, D. J. Evidence for a lack of reactivity of carotenoid addition radicals towards oxygen: A laser flash photolysis study of the reactions of carotenoids with acylperoxyl radicals in polar and non-polar solvents. *J. Am. Chem. Soc.* **125**:3330-3340; 2003.

[6] Mortensen, A. Scavenging of benzylperoxyl radicals by carotenoids. *Free Rad. Res.* **36**:211-216; 2002.

[7] Mortensen, A. Scavenging of acetylperoxyl radicals and quenching of triplet diacetyl by β-carotene: mechanisms and kinetics. *J. Photochem. Photobiol. B: Biol.* **61**:62-67; 2001.

[8] Mortensen, A.; Skibsted, L. H. Kinetics of parallel electron transfer from β-carotene to phenoxyl radical and adduct formation between phenoxyl radical and β-carotene. *Free Rad. Res.* **25**:515-523; 1996.

[9] Mortensen, A.; Skibsted, L. H. Importance of carotenoid structure in radical-scavenging reactions. *J. Agric. Food Chem.* **45**:2970-2977; 1997.

[10] Mortensen, A. Mechanism and kinetics of scavenging of the phenylthiyl radical by carotenoids. A laser flash photolysis study. *Asian Chem. Lett.* **4**:135-143; 2000.

[11] El-Agamey, A.; Lowe, G. M.; McGarvey, D. J.; Mortensen, A.; Phillip, D. M.; Truscott, T. G.; Young, A. J. Carotenoid radical chemistry and antioxidant/pro-oxidant properties. *Arch. Biochem. Biophys.* **430**:37-48; 2004.

[12] Edge, R.; Truscott, T. G. *Carotenoid radicals and the interaction of carotenoids with active oxygen species.* In: Frank, H. A.; Young, A. J.; Britton, G.;

Cogdell, R. J., eds. *The photochemistry of carotenoids*, 1st ed., Dordrecht: Kluwer Academic Publishers; **1999**: 223-234.

[13] El-Agamey, A.; Cantrell, A.; Land, E. J.; McGarvey, D. J.; Truscott, T. G. Are dietary carotenoids beneficial? Reactions of carotenoids with oxy-radicals and singlet oxygen. *Photochem. Photobiol. Sci.* **3**:802-811; 2004.

[14] Krinsky, N. I.; Yeum, K. –J. Carotenoid-radical interactions. *Biochem. Biophys. Res. Commun.* **305**:754-760; 2003.

[15] Edge, R.; McGarvey, D. J.; Truscott, T. G. The carotenoids as anti-oxidants – a review. *J. Photochem. Photobiol. B: Biol.* **41**:189-200; 1997.

[16] El-Agamey, A. and McGarvey, D. J. Carotenoid addition radicals do not react with molecular oxygen: Aspects of carotenoid reactions with acylperoxyl radicals in polar and non-polar media. *Free Rad. Res.* **36**:97-100 (Suppl. S); 2002.

[17] D`Aquino, M.; Dunster, C.; Willson, R. L. Vitamin A and glutathione-mediated free radical damage: competing reactions with polyunsaturated fatty acids and vitamin C. *Biochem. Biophys. Res. Commun.* **161**:1199-1203; 1989.

[18] Hill, T. J.; Land, E. J.; McGarvey, D. J.; Schalch, W.; Tinkler, J. H.; Truscott, T. G. Interactions between carotenoids and the $CCl_3O_2^{\bullet}$ radical. *J. Am. Chem. Soc.* **117**:8322-8326; 1995.

[19] (a) Adhikari, S.; Kapoor, S.; Chattopadhyay, S.; Mukherjee, T. Pulse radiolytic oxidation of β-carotene with halogenated alkylperoxyl radicals in a quaternary microemulsion: formation of retinol. *Biophys. Chem.* **88**:111-117; 2000. (b) Rozanowska, M.; Cantrell, A.; Edge, R.; Land, E. J.; Sarna, T.;

Truscott, T. G. Pulse radiolysis study of the interaction of retinoids with peroxyl radicals. *Free Rad. Biol. Med.* **39**:1399-1405; 2005.

[20] (a) Li, K.; Wang, M.; Wang, J.; Zhu, R.; Sun, D.; Sun, X.; Wang, S.-L. Photoionization of oxidized coenzyme Q in microemulsion: laser flash photolysis study in biomembrane-like system. *Photochem. Photobiol.* **89**:61-67; 2013. (b) Li, K.; Wang, M.; Wang, T.; Sun, D.; Zhu, R.; Sun, X.; Wu, X.; Wang, S.-L. Interaction of retinoic acid radical cation with lysozyme and antioxidants: laser flash photolysis study in microemulsion. *Photochem. Photobiol.* **89**:1064-1070; 2013.

[21] Martinez, C. G.; Braun, A. M.; Oliveros, E. Effect of the media on the quantum yield of singlet oxygen ($O_2(^1\Delta_g)$) production by 9H-fluoren-9-one: microheterogeneous systems. *Helv.Chim. Acta* **87**:382-393; 2004.

[22] Adhikari, S.; Joshi, R.; Mukherjee, T. Radiation chemistry in microemulsion. *J. Indian Chem. Soc.* **78**:573-577; 2001.

[23] (a) De Gennes, P. G.; Taupin, C. Microemulsions and the flexibility of oil/water interfaces. *J. Phys. Chem.* **86**:2294-2304; 1982. (b) Strey, R.; Winkler, J.; Magid, L. Small-angle neutron scattering from diffuse interfaces. 1. Mono- and bilayers in the water-octane-$C_{12}E_5$ system. *J. Phys. Chem.* **95**:7502-7507; 1991.

[24] Martinez, L. A.; Martinez, C. G.; Klopotek, B. B.; Lang, J.; Neuner, A.; Braun, A. M.; Oliveros, E. Nonradiative and radiative deactivation of singlet molecular oxygen ($O_2(a^1\Delta_g)$) in micellar media and micrpemulsions. *J. Photochem. Photobiol. B: Biol.* **58**:94-107; 2000.

[25] 4-Acetyl-4-phenylpiperidine hydrochloride (APPHCl) is water-soluble and so is predominantly in the aqueous phase.

[26] (a) El-Agamey, A. Laser flash photolysis of new water-soluble peroxyl radical precursor. *J. Photochem. Photobiol. A: Chem.* **203**:13-17; 2009. (b) Tinkler, J. H.; Tavender, S. M.; Parker, A. W.; McGarvey, D. J.; Mulroy, L.; Truscott, T. G. Investigation of carotenoid radical cations and triplet states by laser flash photolysis and time-resolved resonance Raman spectroscopy: observation of competitive energy and electron transfer. *J. Am. Chem. Soc.* **118**:1756-1761; 1996. (c) Mordi, R. C.; Walton, J. C.; Burton, G. W.; Hughes, L.; Ingold, K. U.; Lindsay, D. A.; Moffatt, D. J. Oxidative degradation of β-carotene and β-apo-8`-carotenal. Tetrahedron **49**:911–928; 1993.

[27] El-Agamey, A.; McGarvey, D. J. Acyl/aroylperoxyl radicals: a comparative study of the reactivity of peroxyl radicals resulting from the α-cleavage of ketones. *Phys. Chem. Chem. Phys.* **4**:1611-1617; 2002.

[28] Lee, P. C.; Rodgers, M. A. J. Singlet molecular oxygen in micellar systems. 1. Distribution equilibria between hydrophobic and hydrophilic compartments. *J. Phys. Chem.* **87**:4894-4898; 1983.

[29] Rodgers, M. A. J.; Lee, P. C. Singlet molecular oxygen in micellar systems. 2. Quenching behaviour in AOT reverse micelles. *J. Phys. Chem.* **88**:3480-3484; 1984.

[30] Cantrell, A.; McGarvey, D. J.; Truscott, T. G.; Rancan, F.; Bohm, F. Singlet oxygen quenching by dietary carotenoids in a model membrane environment. *Arch. Biochem. Biophys.* **412**:47-54; 2003.

[31] (a) Favaro, G.; Ortica, F. Micellar effects on absorption spectra and protolytic equilibria of phenyl-pyridyl-ketones. *Spectrochimica Acta Part A* **47**:1721-1726; 1991. (b) Montenegro, M. A.; Nazareno, M. A.; Durantini, E. N.; Borsarelli, C. D. Singlet molecular oxygen quenching ability of carotenoids in a reverse-micelle membrane mimetic system. *Photochem. Photobiol.* **75**:353-361; 2002.

[32] Martinez, L. A.; Braun, A. M.; Oliveros, E. Effect of the microenvironment on the efficiency of singlet oxygen ($O_2(^1\Delta_g)$) production by photosensitizing anti-inflammatory drugs. *J. Photochem. Photobiol. B: Biol.* **45**:103-112; 1998.

[33] This is probably due to the greater overlap between the two NIR bands in the case of 77DH.

[34] Szymula, M. Atmospheric oxidation of beta-carotene in aqueous, pentanol, SDS microemulsion systems in the presence and absence of vitamin C. *Journal of Dispersion Science and Technology* **25**:129-137; 2004.

[35] Halliwell, B. How to characterize a biological antioxidant. *Free Rad. Res. Commun.* **9**:1-32; 1990.

[36] Vile G. F.; Winterbourn, C. C. Inhibition of adriamycin-promoted microsomal lipid peroxidation by β-carotene, α-tocopherol and retinol at high and low oxygen partial pressures. *FEBS Lett.* **238**:353-356; 1988.

[37] Tsuchihashi, H.; Kigoshi, M.; Iwatsuki, M.; Niki, E. Action of β-carotene as an antioxidant against lipid peroxidation. *Arch. Biochem. Biophys.* **323**:137-147; 1995.

[38] Zhang, P.; Omaye, S. T. β-Carotene and protein oxidation: effects of ascorbic acid and α-tocopherol. *Toxicology* **146**:37-47; 2000.

[39] Kennedy, T. A.; Liebler, D. C. Peroxyl radical scavenging by β-carotene in lipid bilayers. *J. Biol. Chem.* **267**:4658-4663; 1992.

[40] Martin, H. -D., Jäger, C., Ruck, C., Schmidt, M., Walsh, R. and Paust, J. Anti- and prooxidant properties of carotenoids. *J. Prakt. Chem.* **341**:302-308; 1999.

[41] Palozza, P.; Luberto, C.; Calviello, G.; Ricci, P.; Bartoli, G. M. Antioxidant and prooxidant role of β-carotene in murine normal and tumor thymocytes: effects of oxygen partial pressure. *Free Rad. Biol. Med.* **22**:1065-1073; 1997.

[42] Guo, J.-J.; Hu, C.-H. Mechanism of chain termination in lipid peroxidation by carotenes: a theoretical study. *J. Phys. Chem. B* **114**:16948-16958; 2010.

[43] Palozza, P. Prooxidant actions of carotenoids in biologic systems. *Nutr. Rev.* **56**:257-265; 1998.

[44] Liebler, D. C. *Antioxidant reactions of carotenoids.* In: Canfield, L. M.; Krinsky, N. I.; Olson, J. A., eds. *Carotenoids in human health*, *Ann. New York Acad. Sci.,* volume 691. New York: The New York Academy of Sciences; **1993**: 20-31.

[45] Small, Jr. R. D.; Scaiano, J. C. Absolute rates of hydrogen abstraction by tert-butoxy radicals. *J. Am. Chem. Soc.* **100**:296-298; 1978.

[46] Small, Jr. R. D.; Scaiano, J. C. Radical processes in lipids. A laser photolysis study of *t*-butoxy radical reactivity toward fatty acids. *Photochem. Photobiol.* **29**:49-51; 1979.

[47] Edge, R.; Land, E. J.; McGarvey, D. J.; Burke, M.; Truscott, T. G. The reduction potential of the β-carotene$^{\bullet+}$/□β-carotene couple in an aqueous micro-heterogeneous environment. *FEBS Lett.* **471**:125-127; 2000.

[48] Burke, M.; Edge, R.; Land, E. J.; McGarvey, D. J.; Truscott, T. G. One-electron reduction potentials of dietary carotenoid radical cations in aqueous micellar environments. *FEBS Lett.* **500**:132-136; 2001.

[49] Burke, M. *Pulsed radiation studies of carotenoid radicals and excited states*, PhD Thesis, Keele University; **2001**: 104-133.

[50] Edge, R.; Truscott, T. G. Carotenoids-free radical interactions. *The Spectrum* **13**:12-20; 2000.

[51] Burke, M.; Edge, R.; Land, E. J.; Truscott, T. G. Characterisation of carotenoid radical cations in liposomal environments: interaction with vitamin C. *J. Photochem. Photobiol. B: Biol.* **60**:1-6; 2001.

[52] Böhm, F.; Edge, R.; Land, E. J.; McGarvey, D. J.; Truscott, T. G. Carotenoids enhance vitamin E antioxidant efficiency. *J. Am. Chem. Soc.* **119**:621-622; 1997.

[53] Young, A. J.; Lowe, G. M. Antioxidant and prooxidant properties of carotenoids. *Arch. Biochem. Biophys.* **385**:20-27; 2001.

[54] Mortensen, A.; Skibsted, L. H. Relative stability of carotenoid radical cations and homologue tocopheroxyl radicals. A real time kinetic study of antioxidant hierarchy. *FEBS Lett.* **417**:261-266; 1997.

[55] Mortensen, A.; Skibsted, L. H. Real time detection of reactions between radicals of lycopene and tocopherol homologues. *Free Rad. Res.* **27**:229-234; 1997.

[56] Burton, G. W.; Ingold, K. U. β-Carotene: an unusual type of lipid antioxidant. *Science* **224**:569-573; 1984.

[57] Rice-Evans, C. A.; Sampson, J.; Bramley, P. M.; Holloway, D. E. Why do we expect carotenoids to be antioxidants in vivo?. *Free Rad. Res.* **26**:381-398; 1997.

[58] Woodall, A. A.; Britton, G.; Jackson, M. J. Carotenoids and protection of phospholipids in solution or in liposomes against oxidation by peroxyl radicals: relationship between carotenoid structure and protective ability. *Biochim. Biophys. Acta* **1336**:575-586; 1997.

[59] Britton, G. Structure and properties of carotenoids in relation to function. *FASEB J.* **9**:1551-1558; 1995.

[60] El-Agamey, A.; McGarvey, D. J. *Carotenoid radicals and radical ions.* In: Britton, G.; Liaaen-Jensen, S.; Pfander, H., eds. *Carotenoids Volume 4: natural functions*, Basel: Birkhäuser; **2008**: 119-154.

Highlights

- ❖ Peroxyl radical reactions with carotenoids are greatly affected by microemulsion composition.
- ❖ Type of surfactant used has marked effect on the polarity of the microenvironment.
- ❖ The transients' absorption ratio can be used to probe the polarity of the microenvironment.

The nature of peroxyl radical precursors used has small effect on the reactions.

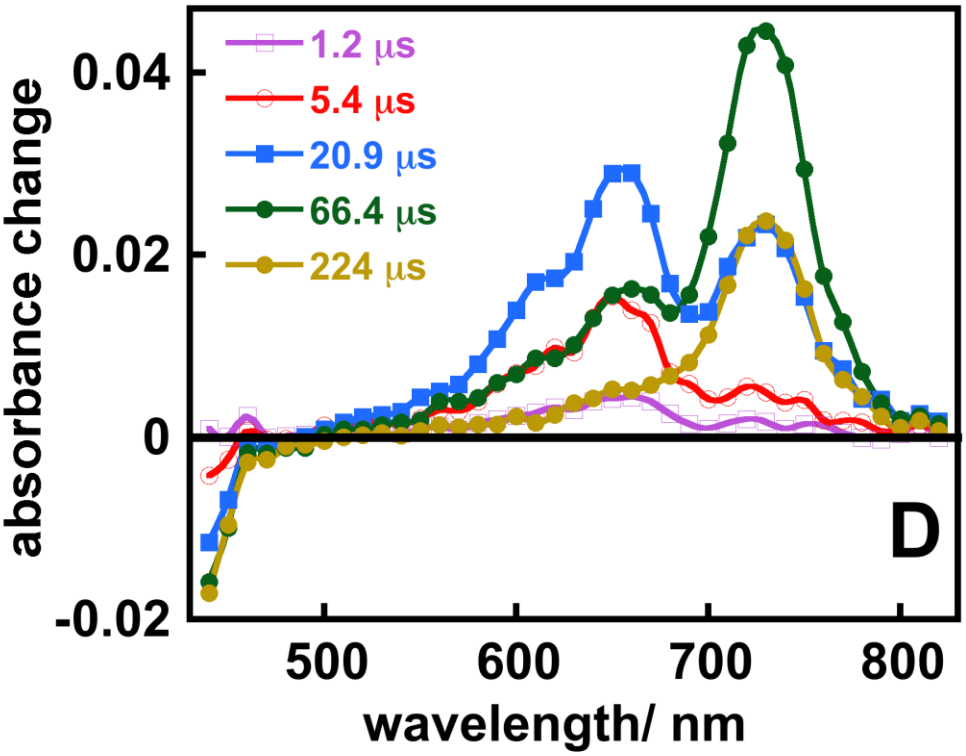
1.2 μs
5.4 μs
20.9 μs
66.4 μs
224 μs
absorbance change
0.04
0.02
0
-0.02
500
600
700
800
wavelength/ nm
D

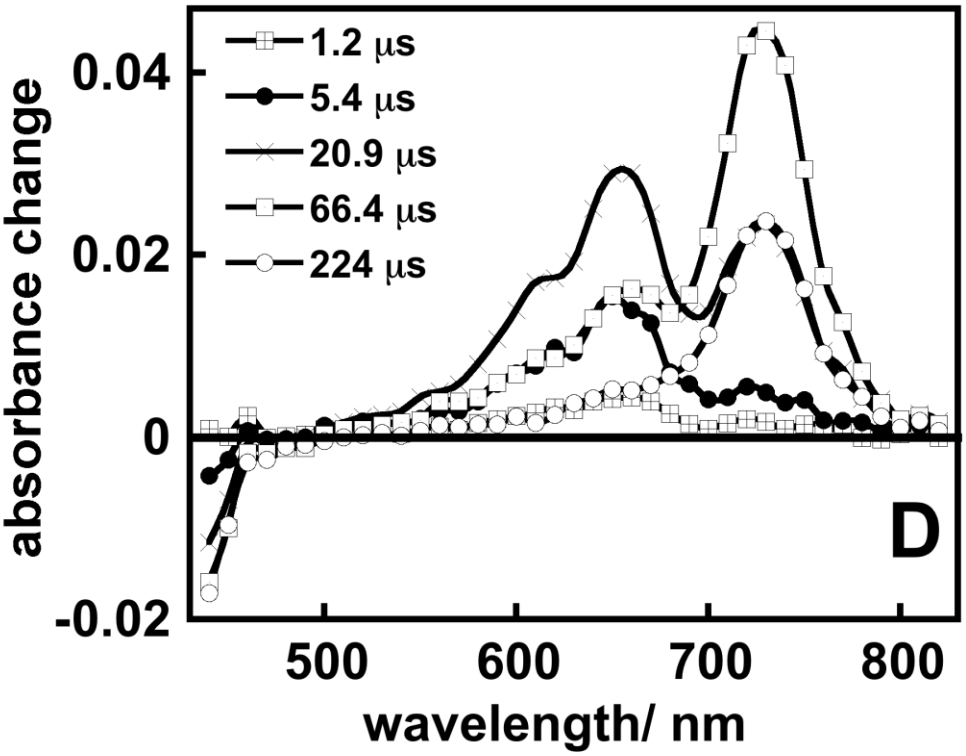
1.2 μs
5.4 μs
20.9 μs
66.4 μs
224 μs
absorbance change
0.04
0.02
0
-0.02
500
600
700
800
wavelength/ nm
D

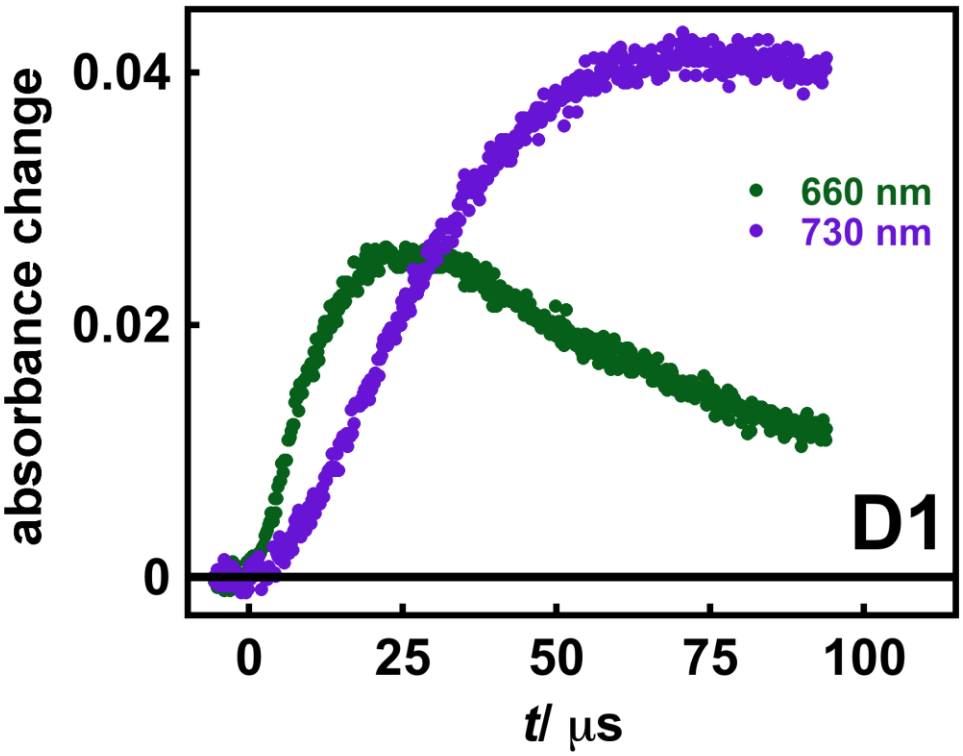

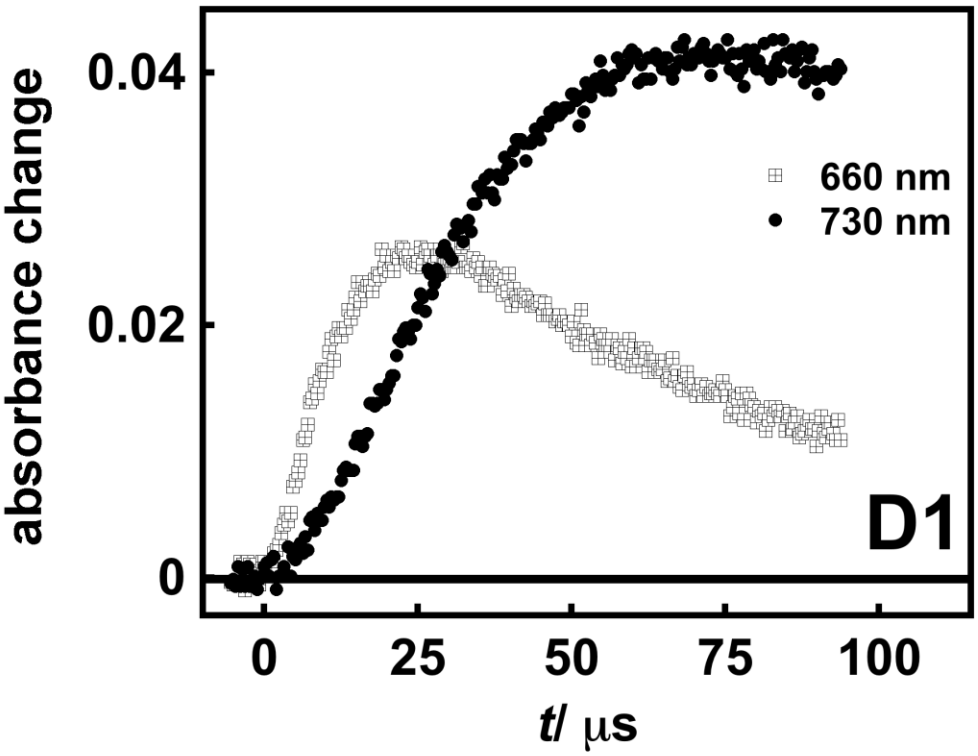

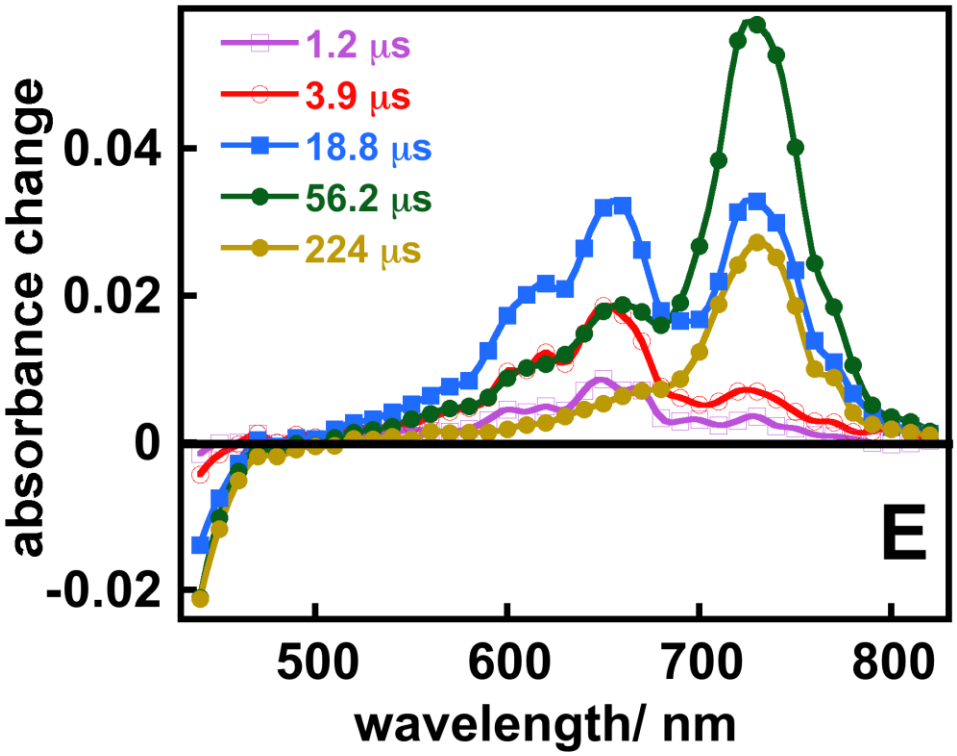
1.2 μs
3.9 μs
18.8 μs
56.2 μs
224 μs
absorbance change
0.04
0.02
0
-0.02
500
600
700
800
wavelength/ nm
E

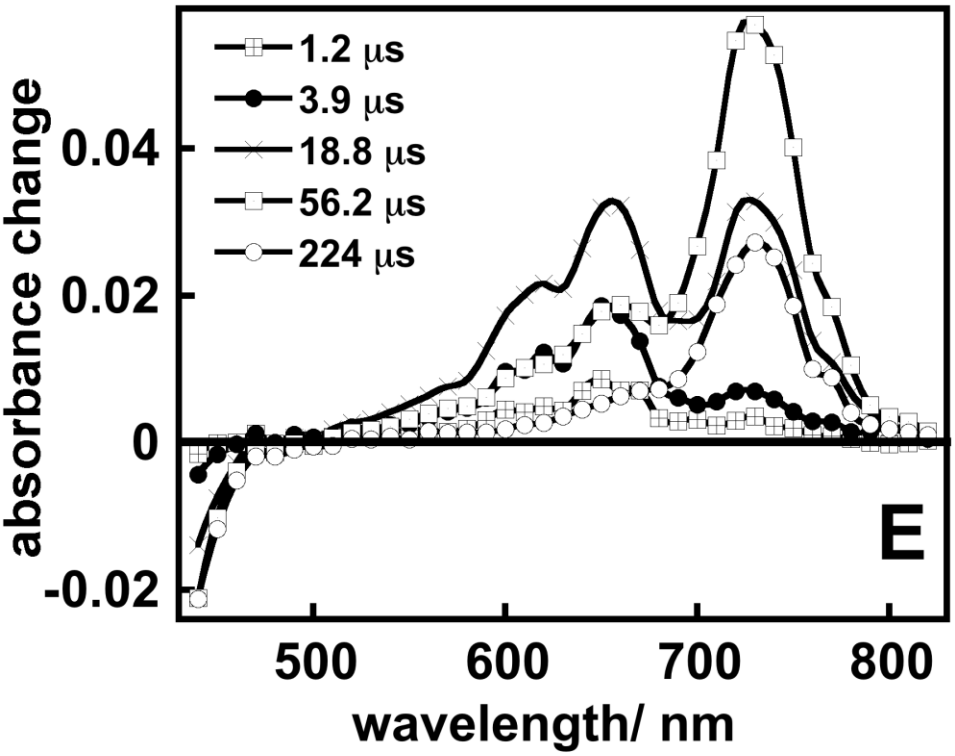
1.2 μs
3.9 μs
18.8 μs
56.2 μs
224 μs
absorbance change
0.04
0.02
0
-0.02
500
600
700
800
wavelength/ nm
E

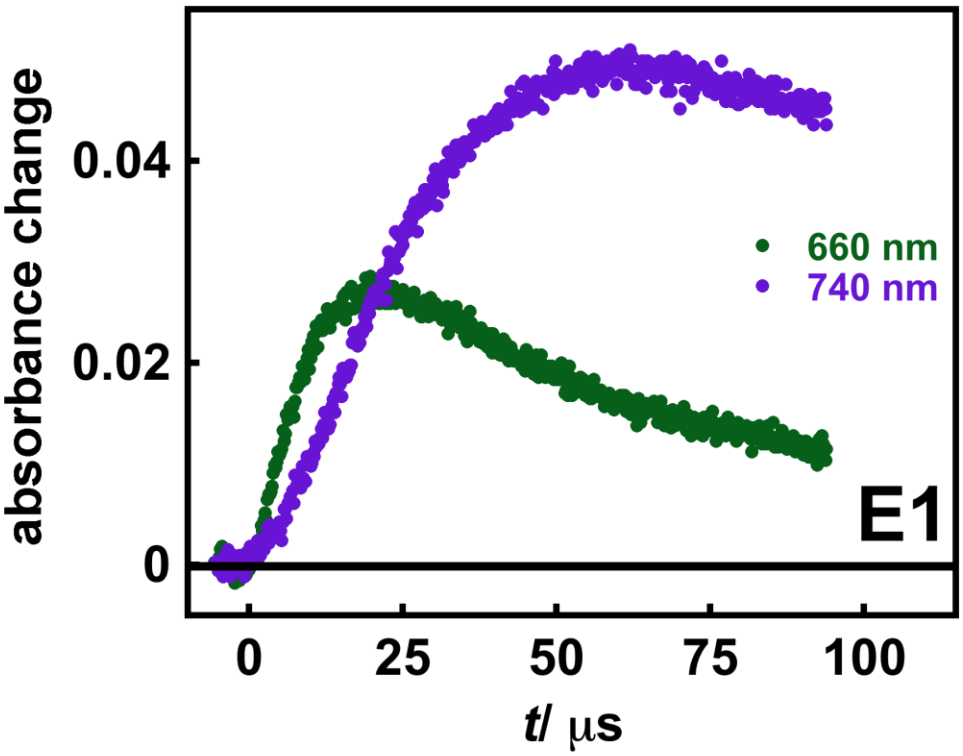

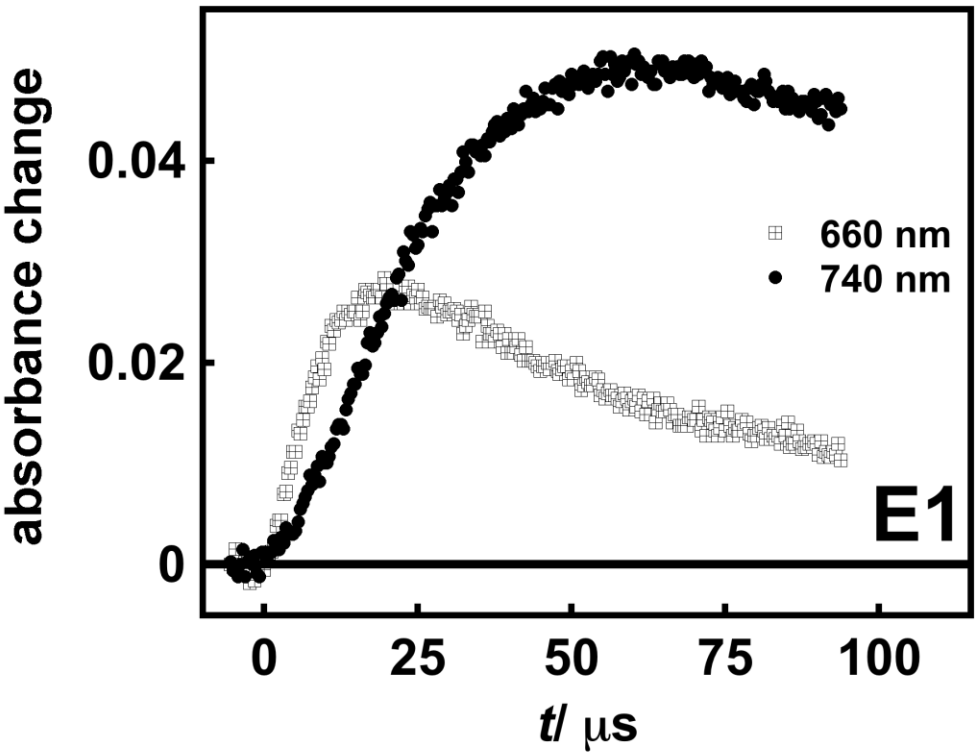

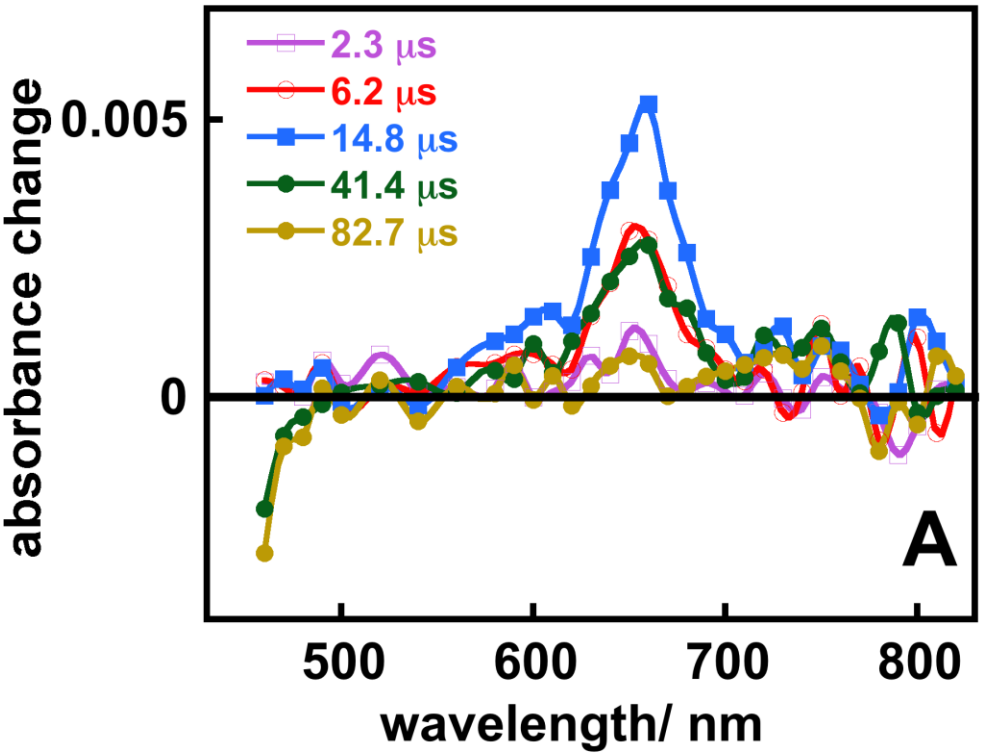
2.3 μs
6.2 μs
14.8 μs
41.4 μs
82.7 μs
0.005
0
absorbance change
A
500
600
700
800
wavelength/ nm

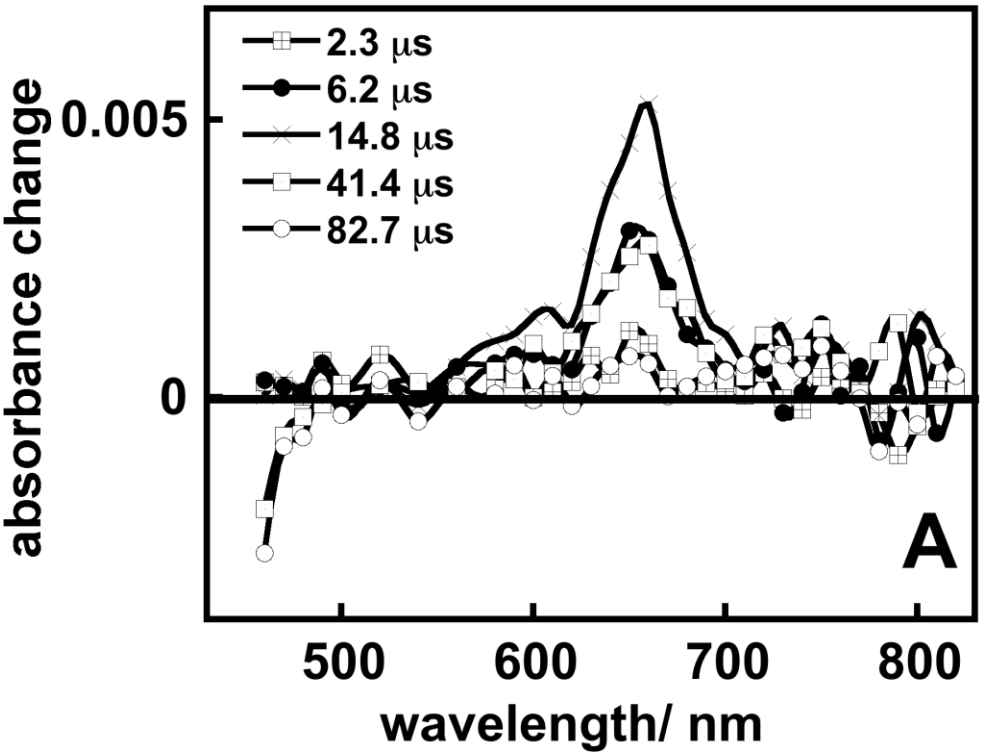
2.3 μs
6.2 μs
14.8 μs
41.4 μs
82.7 μs
absorbance change
0.005
0
A
500
600
700
800
wavelength/ nm

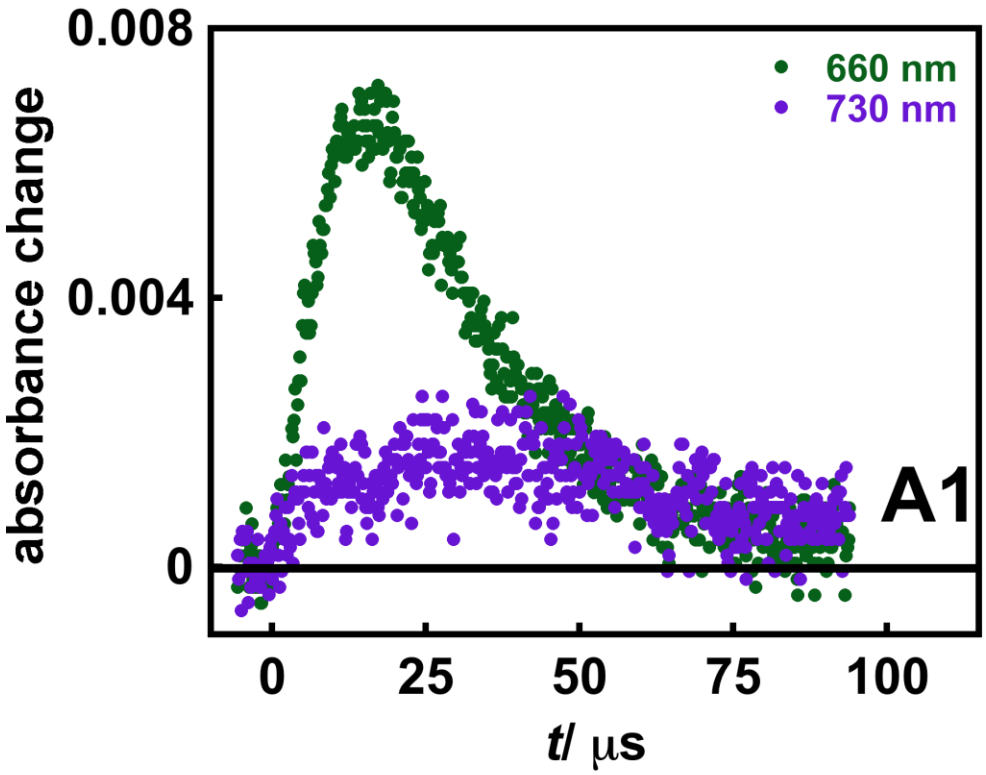
0.008
0.004
0
absorbance change
660 nm
730 nm
A1
0
25
50
75
100
t/ μs

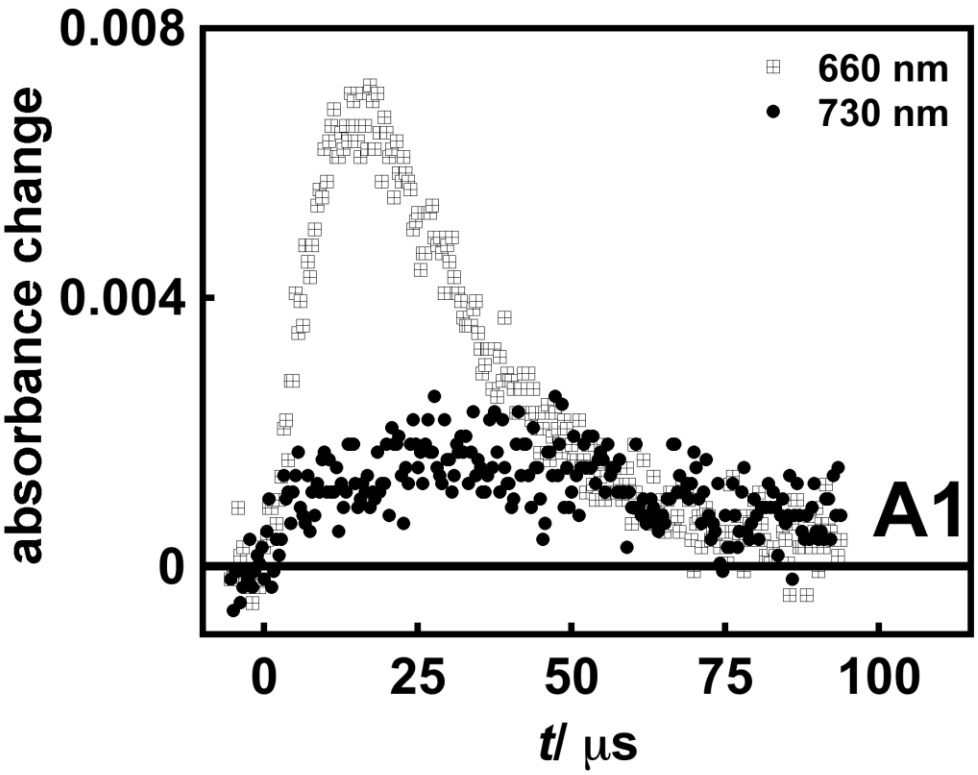
0.008
0.004
0
absorbance change
660 nm
730 nm
A1
0
25
50
75
100
t/ μs

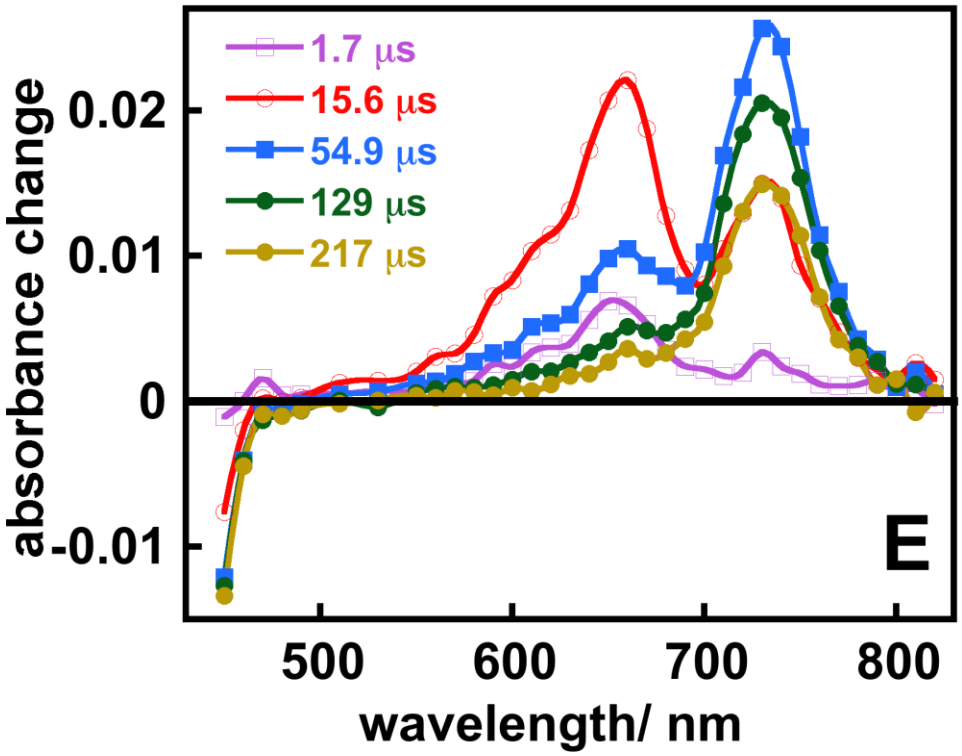
1.7 μs
15.6 μs
54.9 μs
129 μs
217 μs
absorbance change
0.02
0.01
0
-0.01
500
600
700
800
wavelength/ nm
E

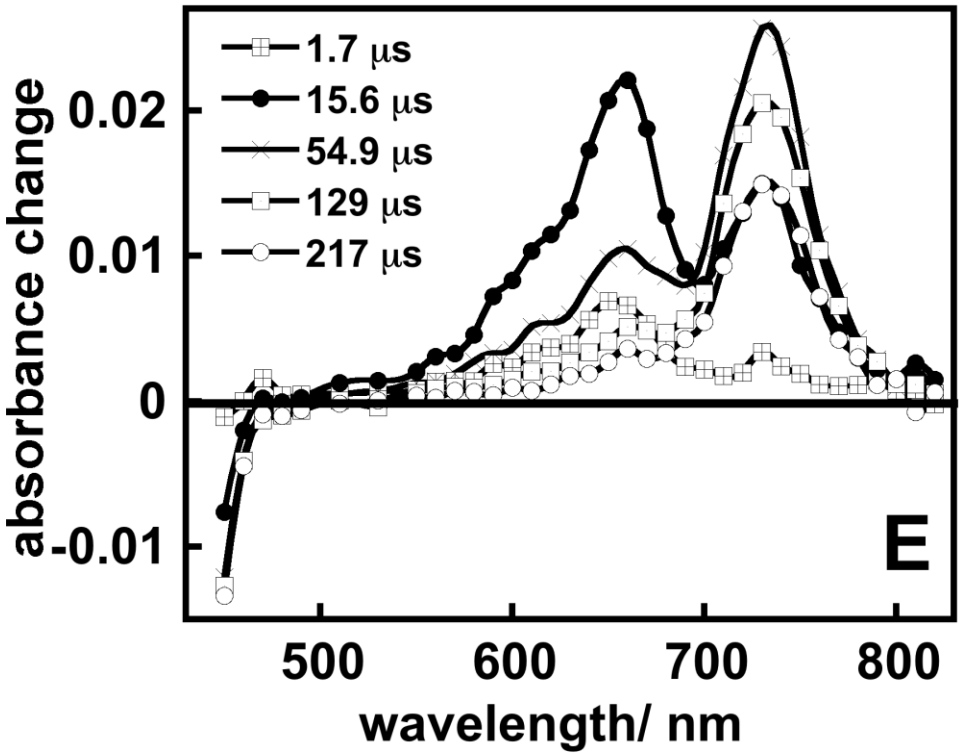
1.7 μs
15.6 μs
54.9 μs
129 μs
217 μs
absorbance change
0.02
0.01
0
-0.01
E
500
600
700
800
wavelength/ nm

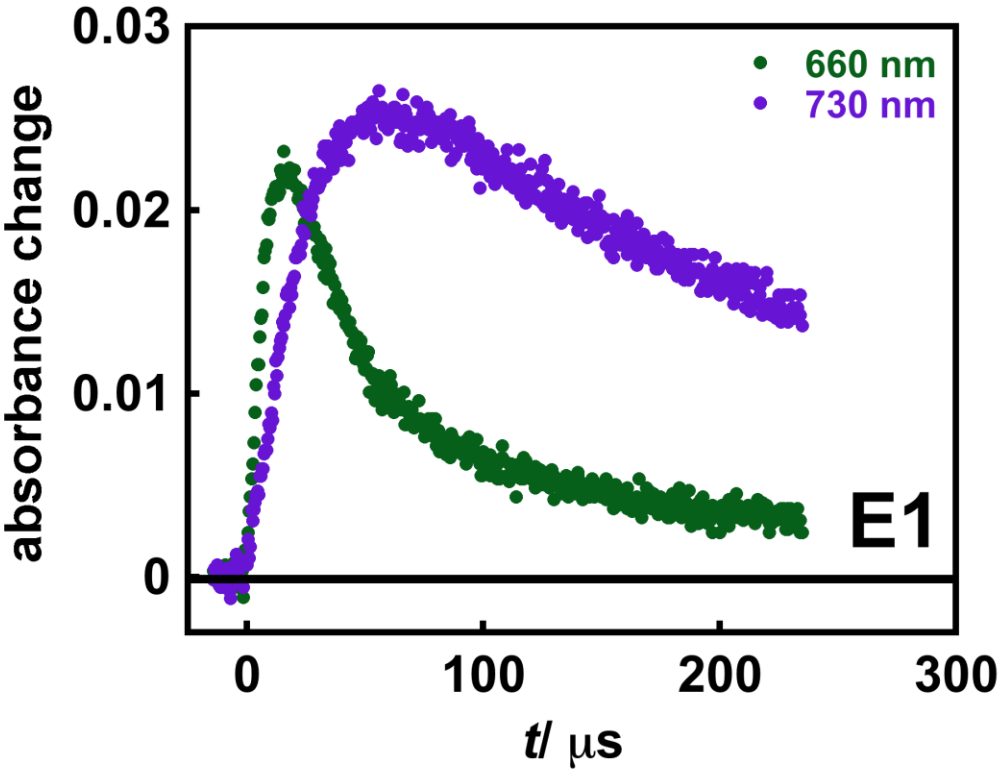
0.03
0.02
0.01
0
absorbance change
660 nm
730 nm
E1
0
100
200
300
t/ μs

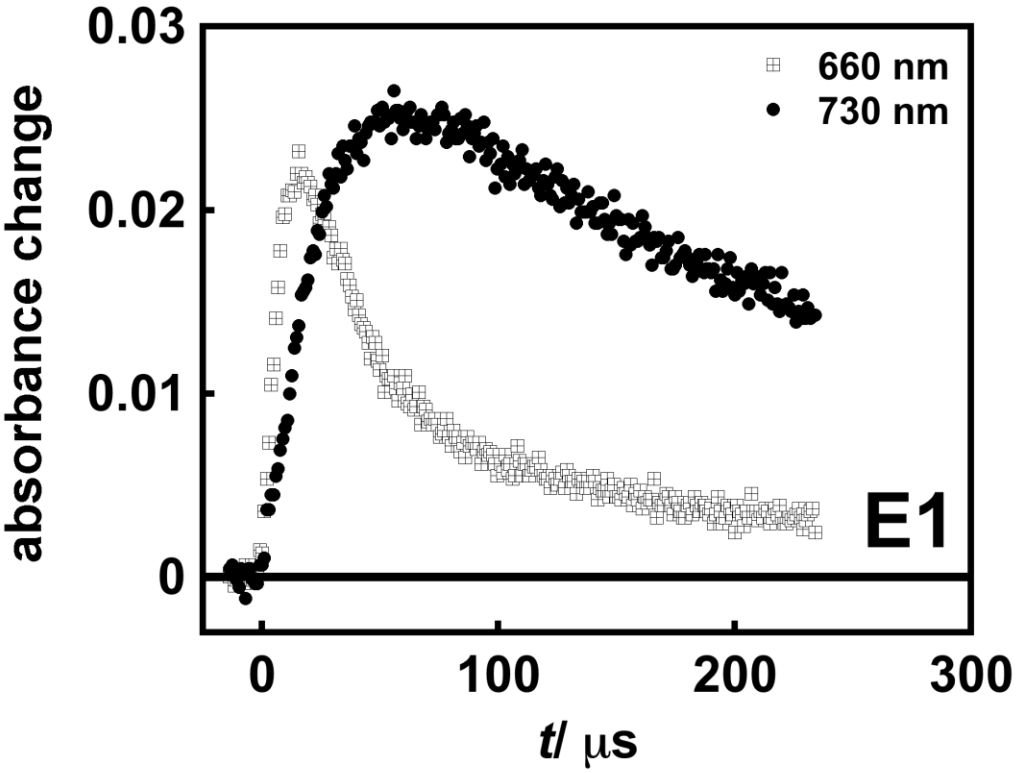
0.03
0.02
0.01
0
absorbance change
660 nm
730 nm
E1
0
100
200
300
t/ μs

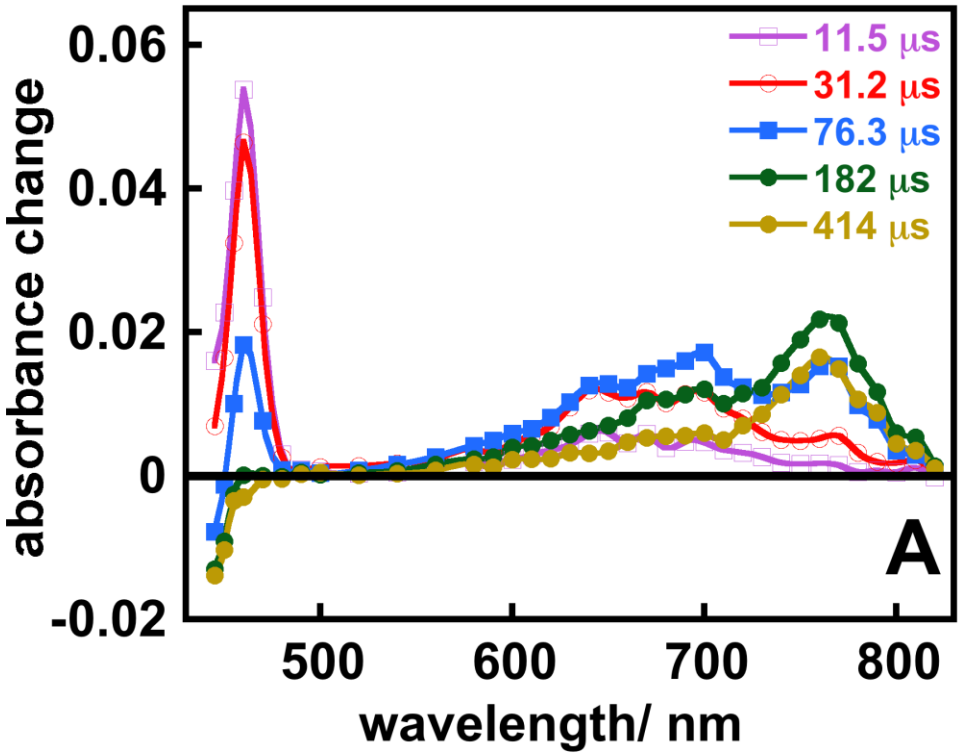
0.06
0.04
0.02
0
-0.02
absorbance change
500
600
700
800
wavelength/ nm
11.5 µs
31.2 µs
76.3 µs
182 µs
414 µs
A

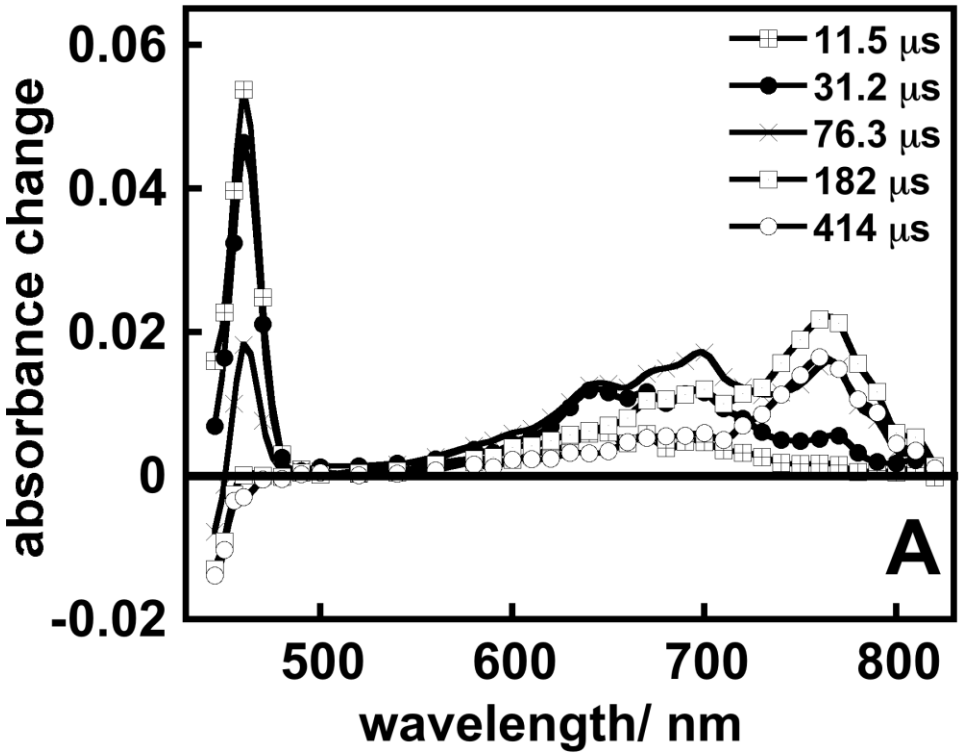
0.06
0.04
0.02
0
-0.02
absorbance change
500
600
700
800
wavelength/ nm
11.5 μs
31.2 μs
76.3 μs
182 μs
414 μs
A

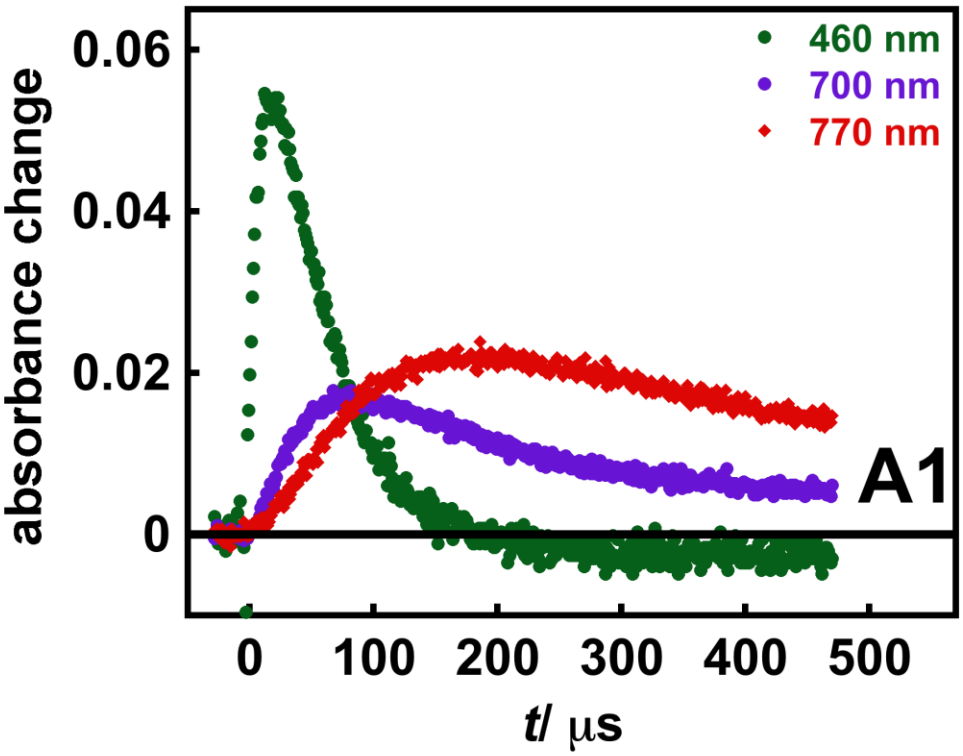
absorbance change
0.06
0.04
0.02
0
460 nm
700 nm
770 nm
A1
0
100
200
300
400
500
t/ μs

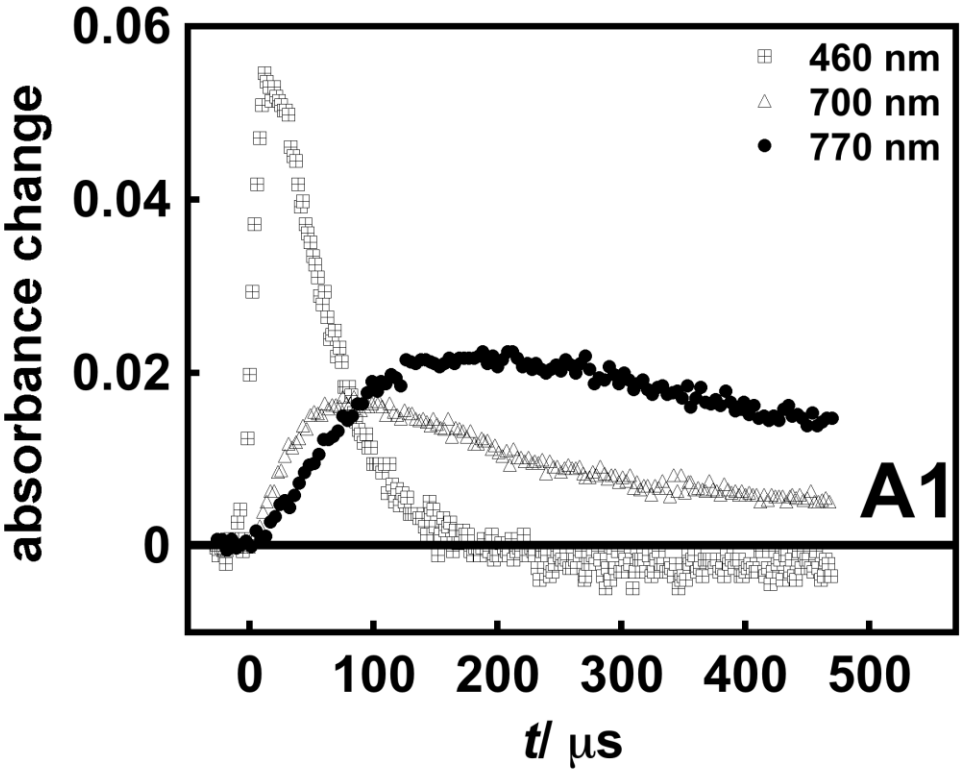
0.06
0.04
0.02
0
absorbance change
460 nm
700 nm
770 nm
A1
0
100
200
300
400
500
t/ μs

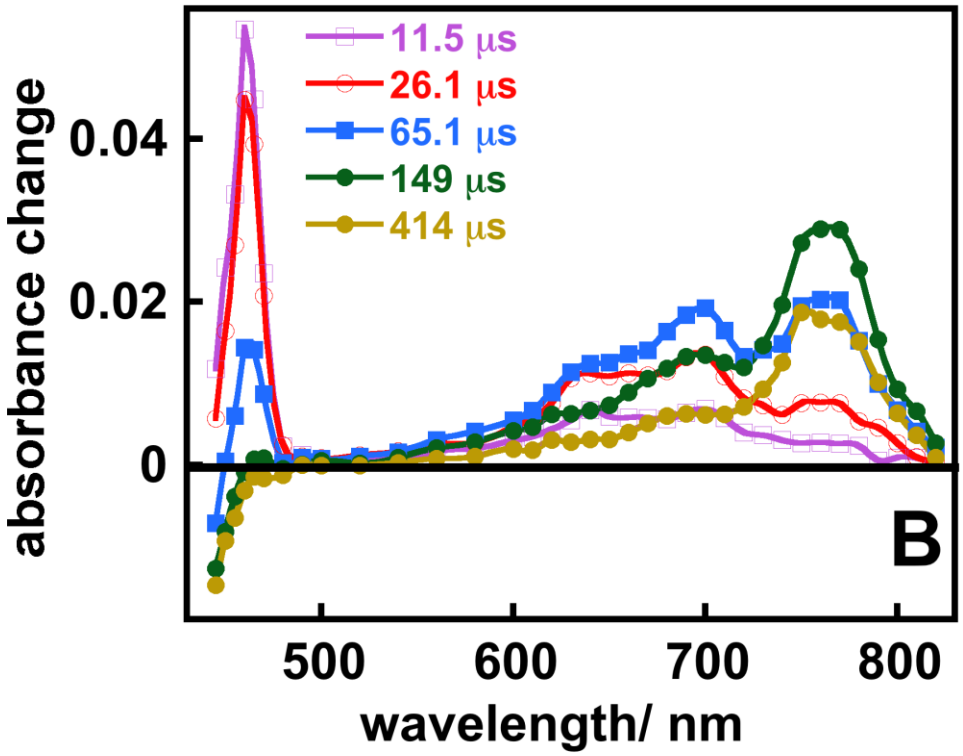
11.5 μs
26.1 μs
65.1 μs
149 μs
414 μs
absorbance change
0.04
0.02
0
B
500
600
700
800
wavelength/ nm

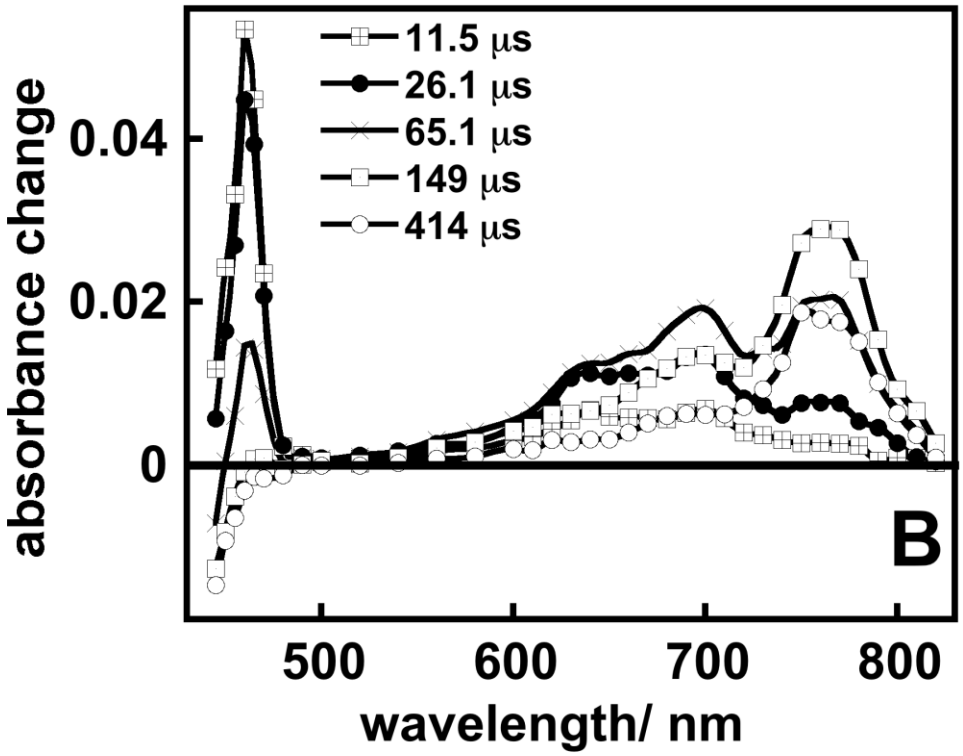
11.5 μs
26.1 μs
65.1 μs
149 μs
414 μs
absorbance change
0.04
0.02
0
B
500
600
700
800
wavelength/ nm

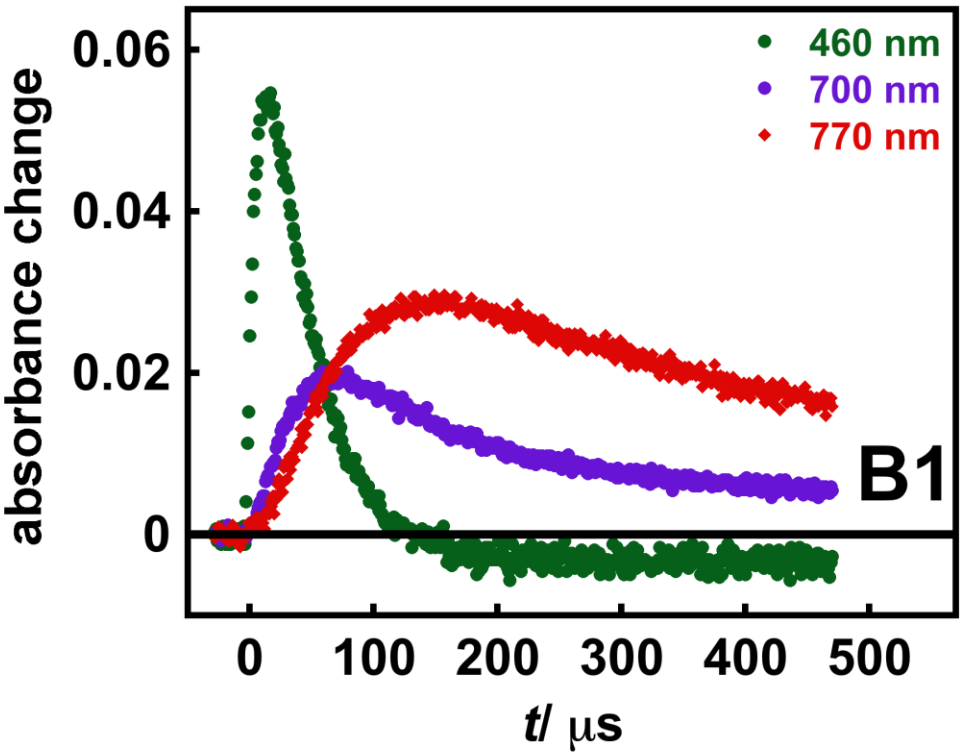
absorbance change
0.06
0.04
0.02
0
460 nm
700 nm
770 nm
B1
0
100
200
300
400
500
t/ μs

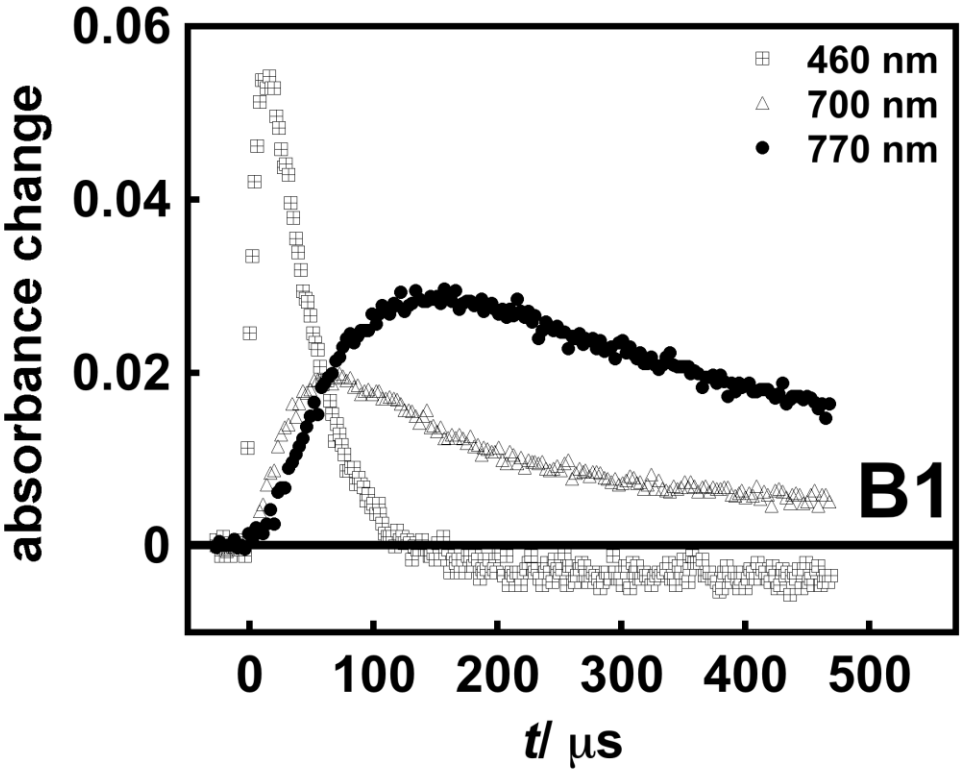
0.06
0.04
0.02
0
absorbance change
460 nm
700 nm
770 nm
B1
0
100
200
300
400
500
t/ μs

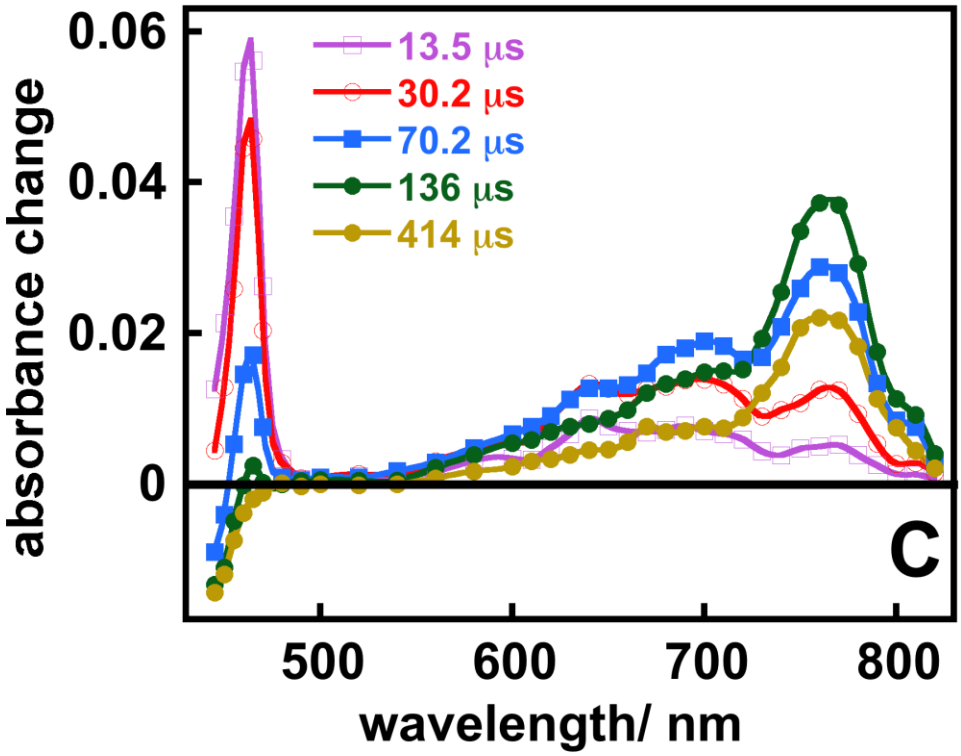
0.06
0.04
0.02
0
absorbance change
13.5 μs
30.2 μs
70.2 μs
136 μs
414 μs
C
500
600
700
800
wavelength/ nm

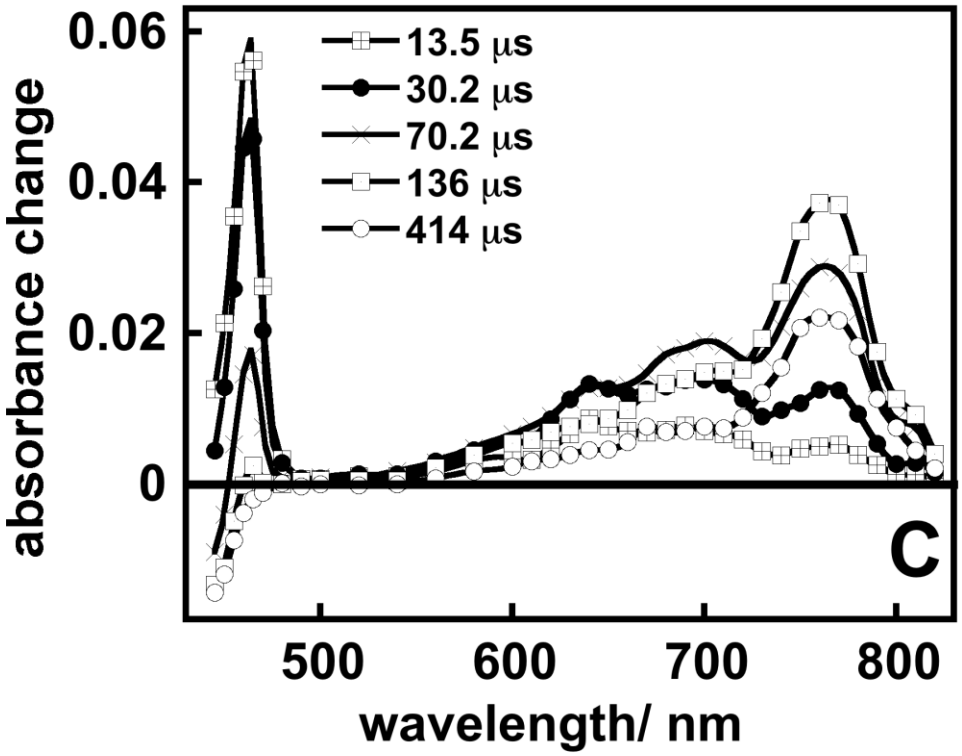
0.06
0.04
0.02
0
absorbance change
13.5 μs
30.2 μs
70.2 μs
136 μs
414 μs
C
500
600
700
800
wavelength/ nm

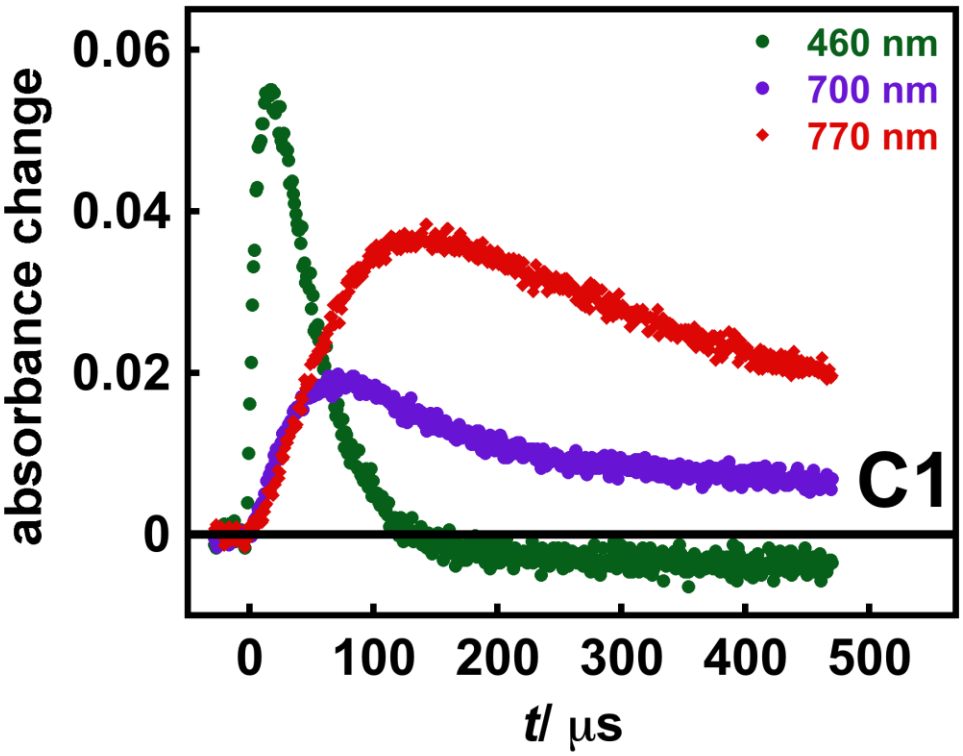
absorbance change
0.06
0.04
0.02
0
460 nm
700 nm
770 nm
C1
0
100
200
300
400
500
t/ μs

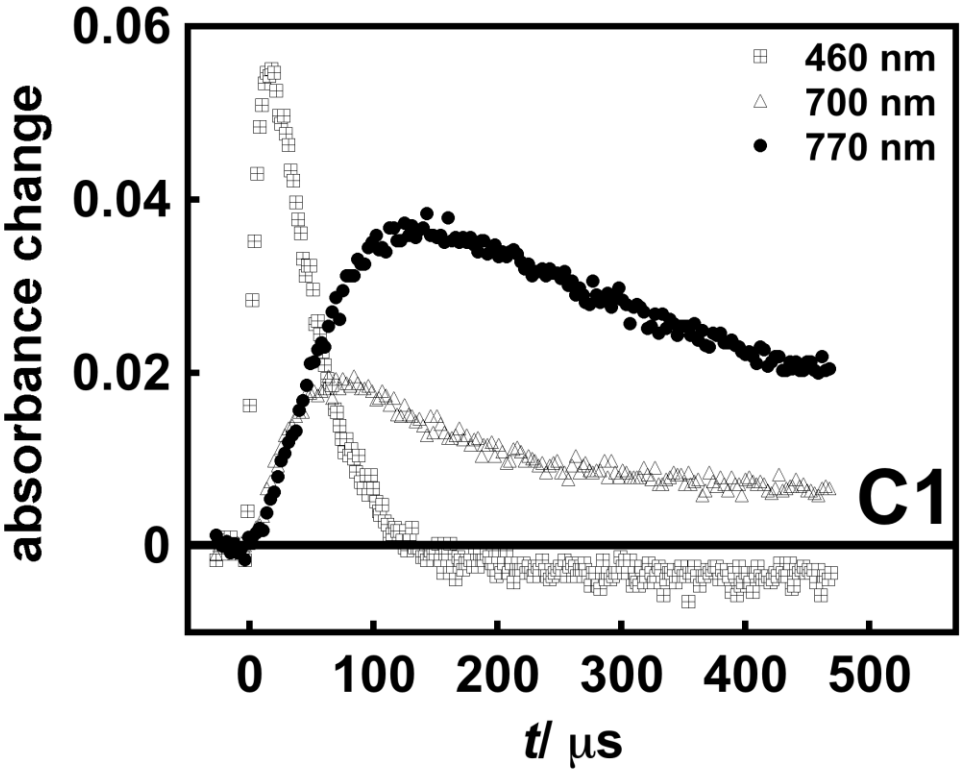
0.06
0.04
0.02
0
absorbance change
460 nm
700 nm
770 nm
C1
0
100
200
300
400
500
t/ μs

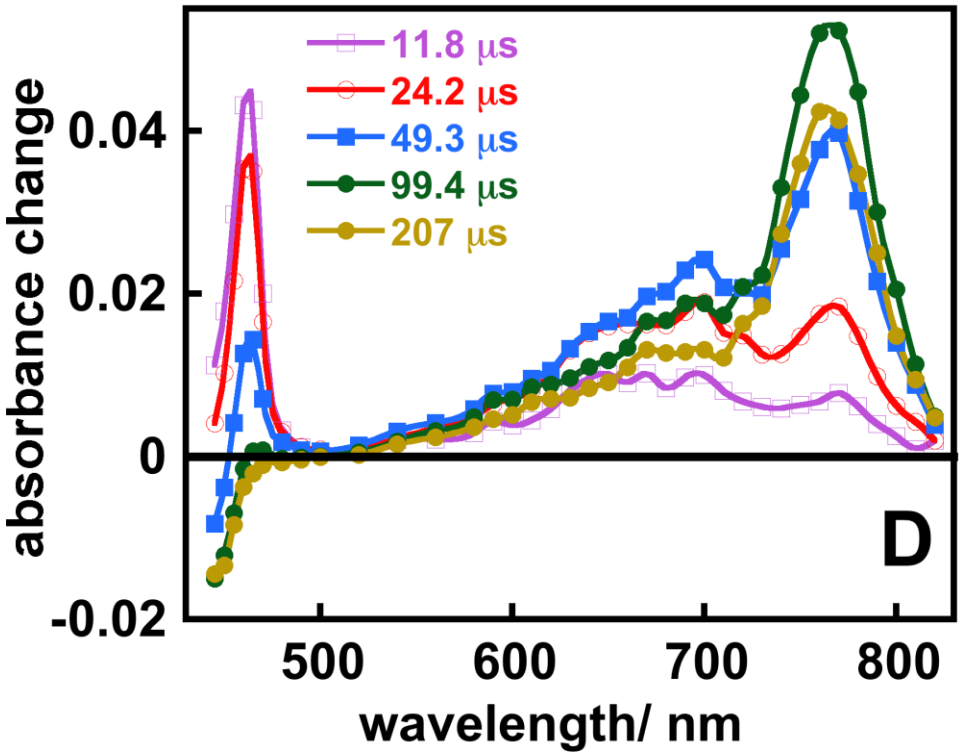
11.8 µs
24.2 µs
49.3 µs
99.4 µs
207 µs
absorbance change
0.04
0.02
0
-0.02
500
600
700
800
wavelength/ nm
D

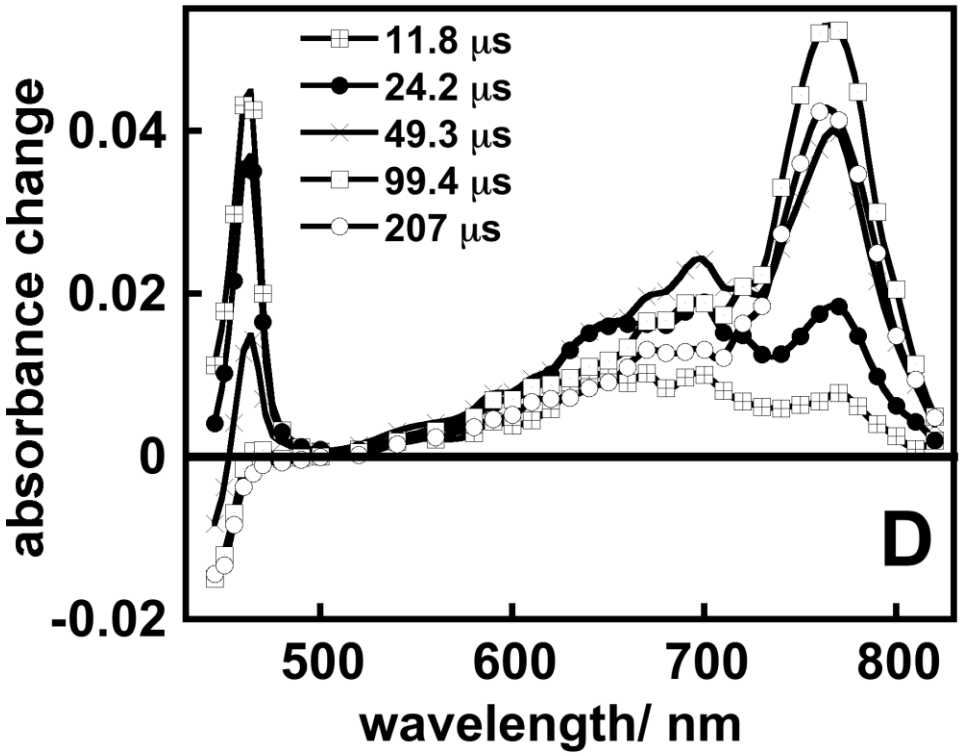
11.8 μs
24.2 μs
49.3 μs
99.4 μs
207 μs
absorbance change
0.04
0.02
0
-0.02
500
600
700
800
wavelength/ nm
D

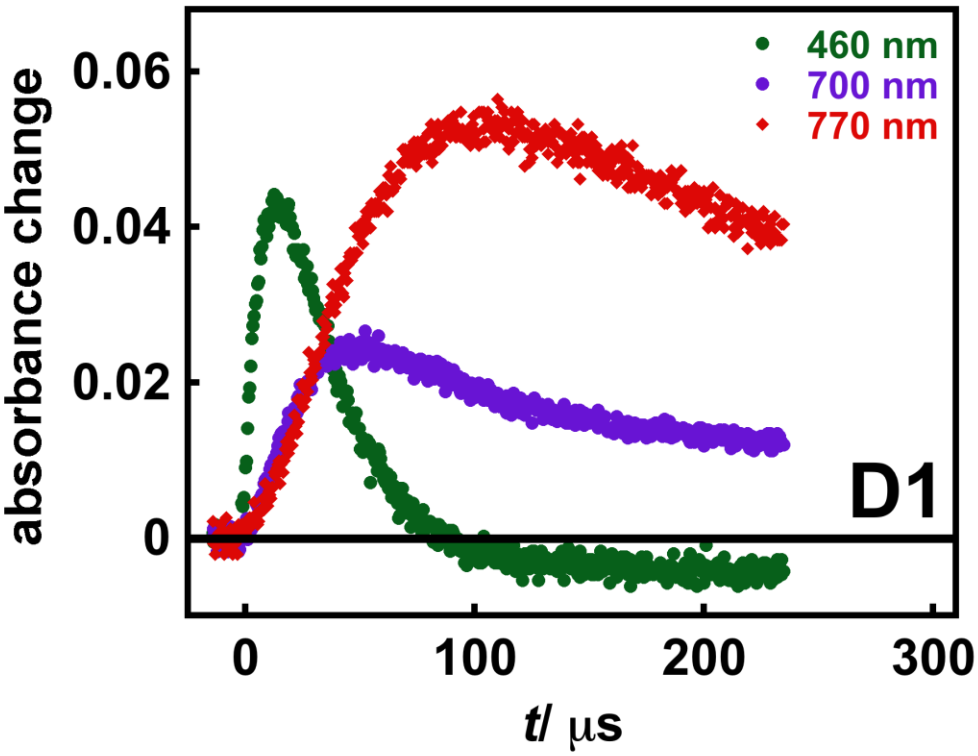
460 nm
700 nm
770 nm
D1
absorbance change
0.06
0.04
0.02
0
0
100
200
300
t/ μs

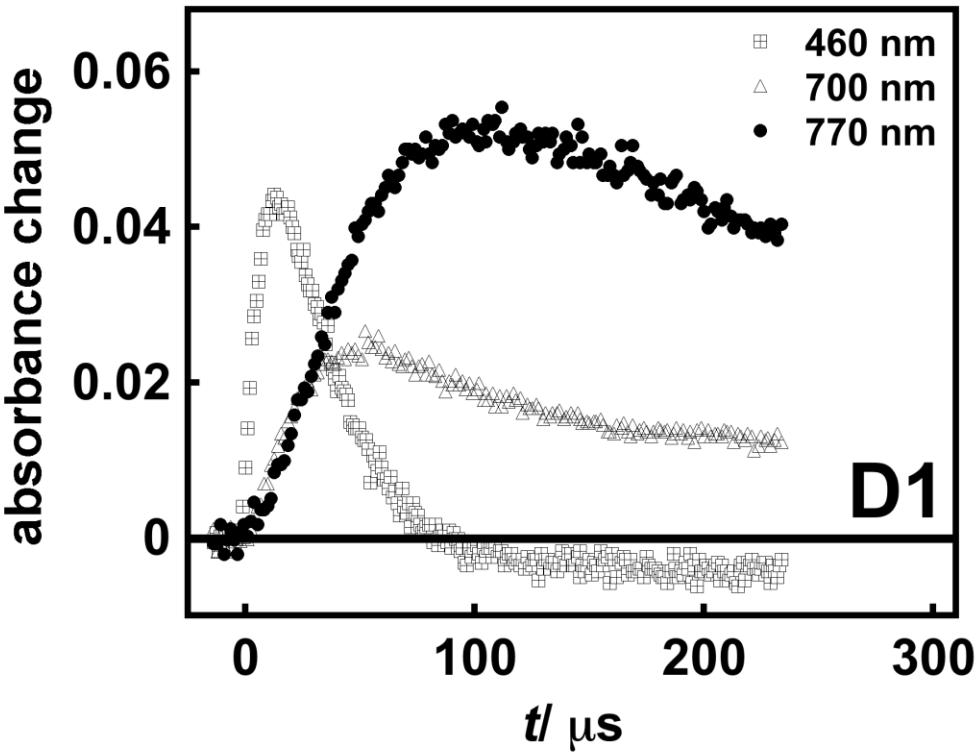
460 nm
700 nm
770 nm
absorbance change
0.06
0.04
0.02
0
D1
0
100
200
300
t/ μs

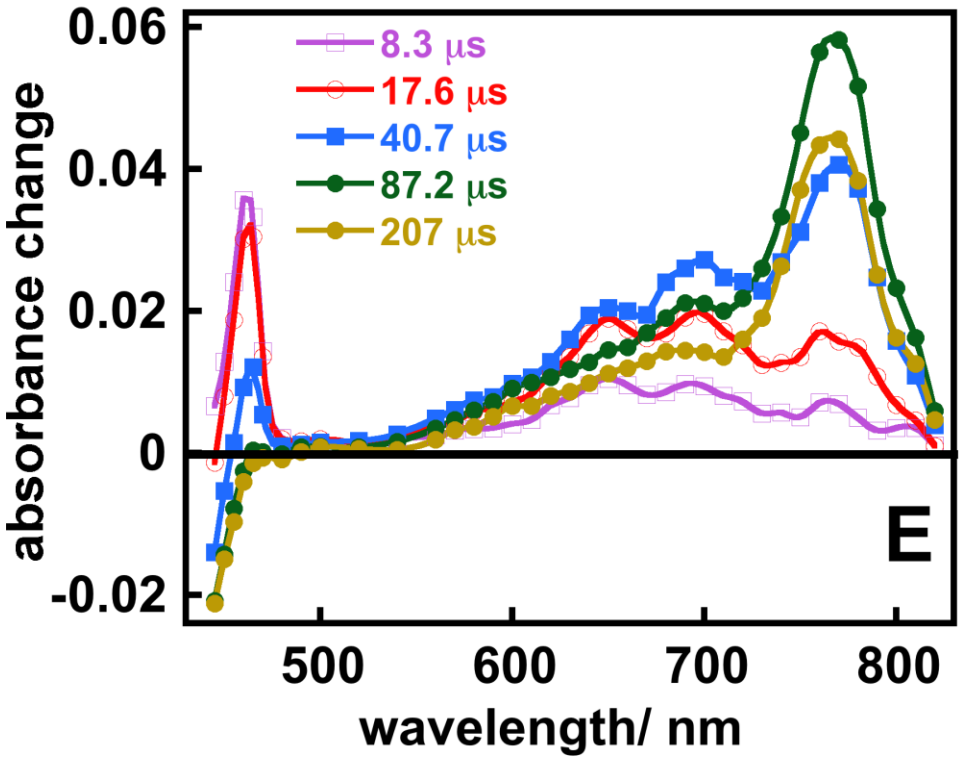
0.06
0.04
0.02
0
-0.02
absorbance change
8.3 µs
17.6 µs
40.7 µs
87.2 µs
207 µs
E
500
600
700
800
wavelength/ nm

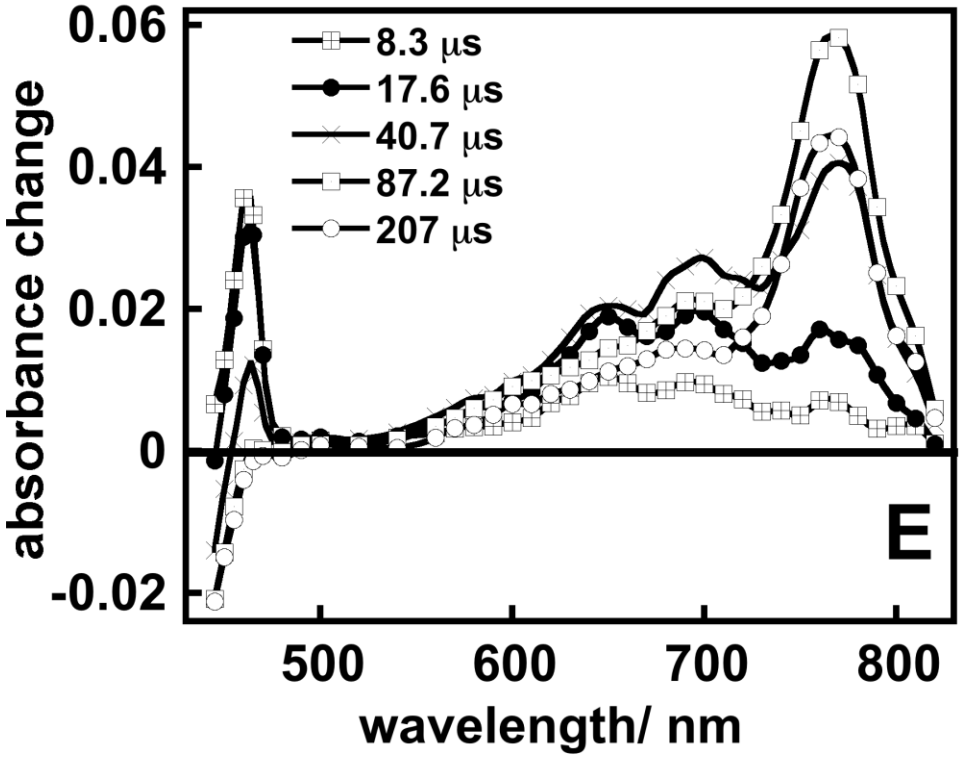
0.06
0.04
0.02
0
-0.02
absorbance change
8.3 μs
17.6 μs
40.7 μs
87.2 μs
207 μs
E
500
600
700
800
wavelength/ nm

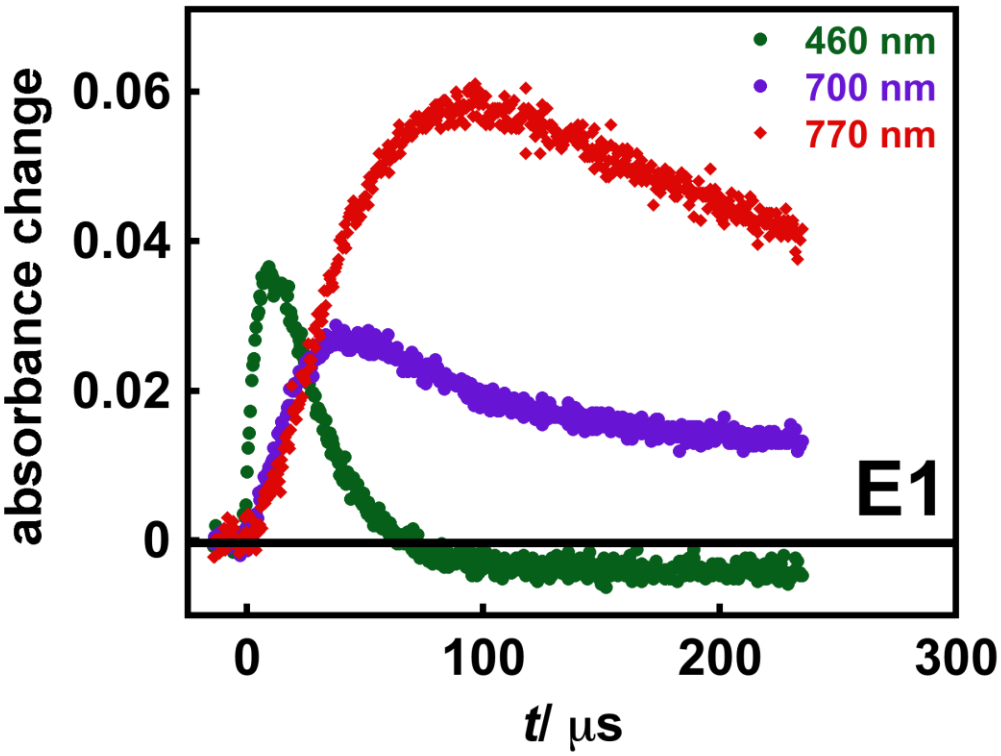
460 nm
700 nm
770 nm
E1
absorbance change
0.06
0.04
0.02
0
0
100
200
300
t/ μs

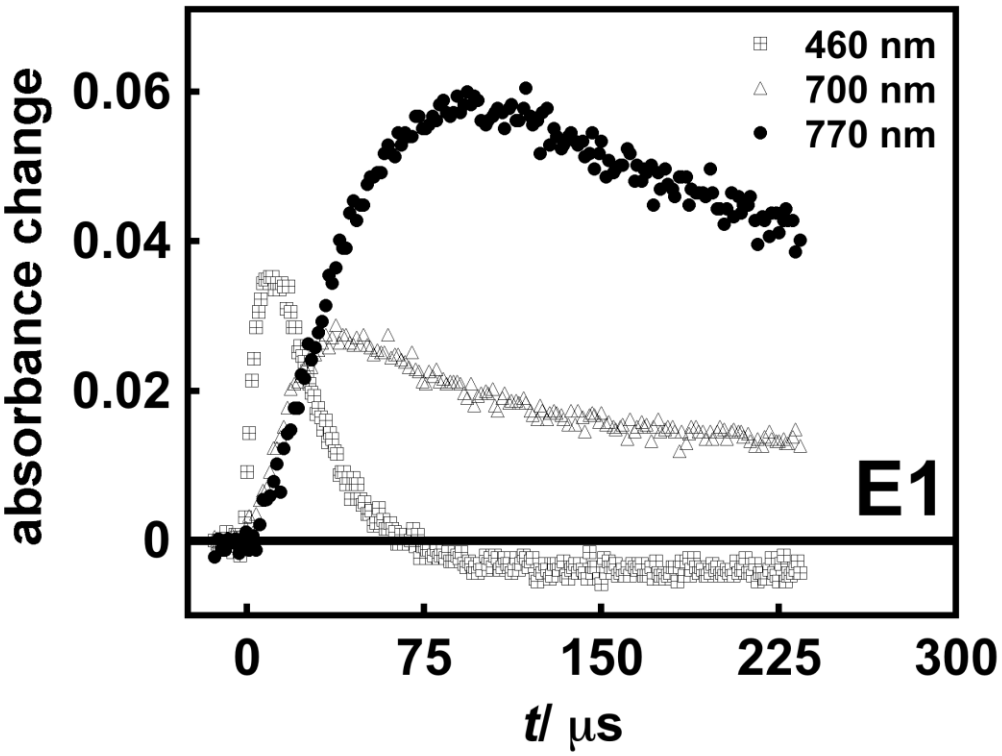
460 nm
700 nm
770 nm
absorbance change
0.06
0.04
0.02
0
E1
0
75
150
225
300
t/ μs

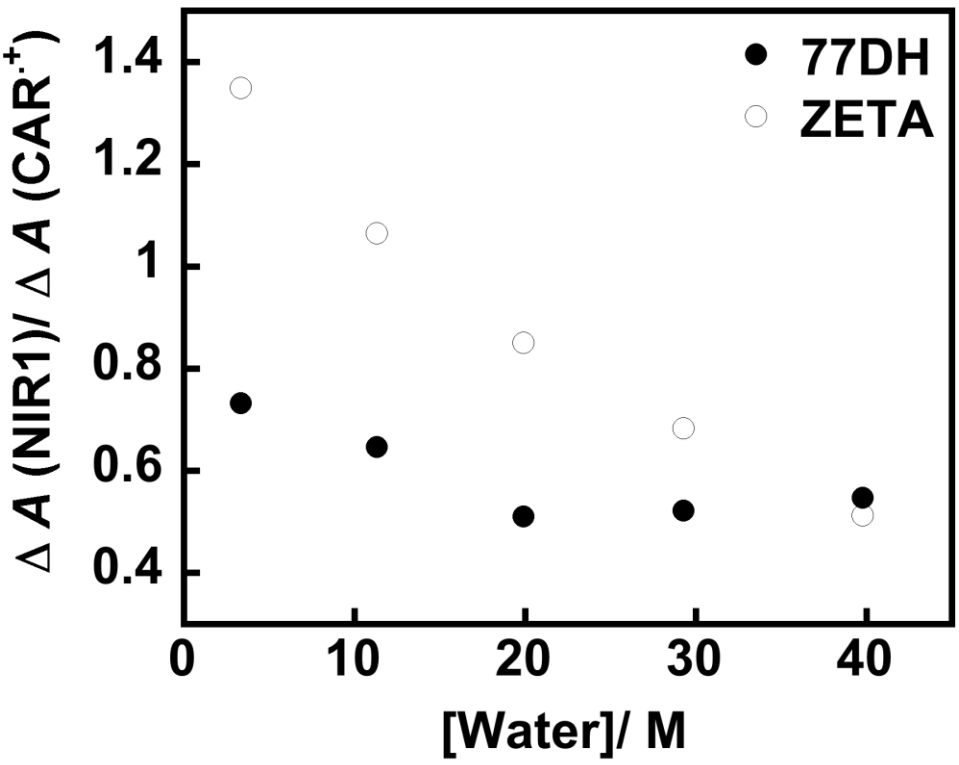

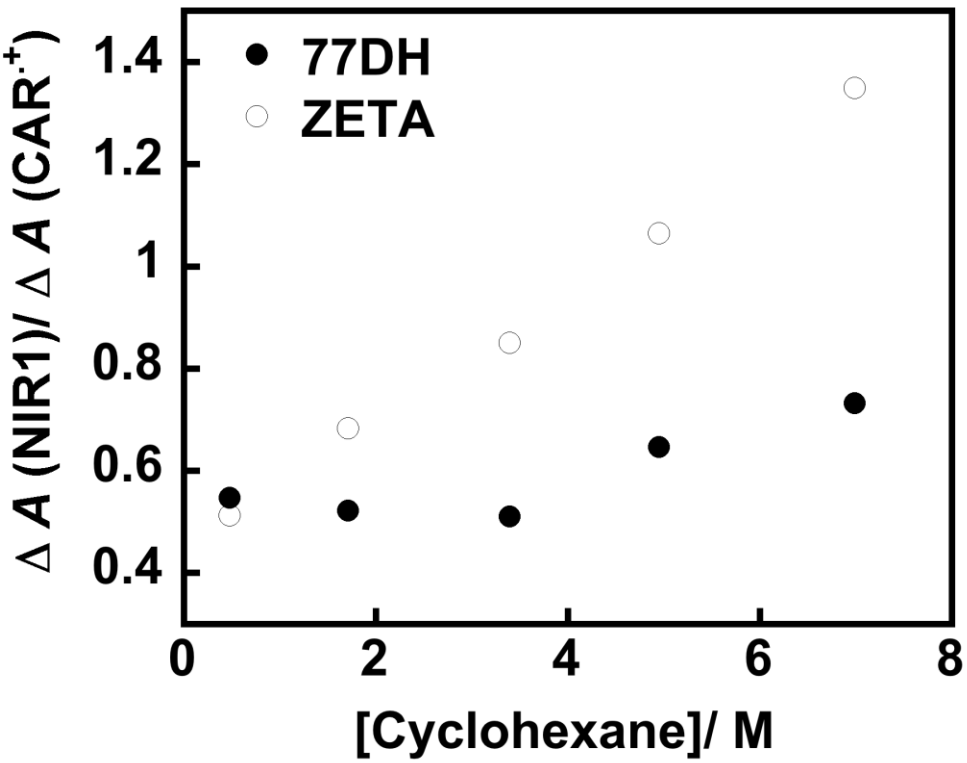

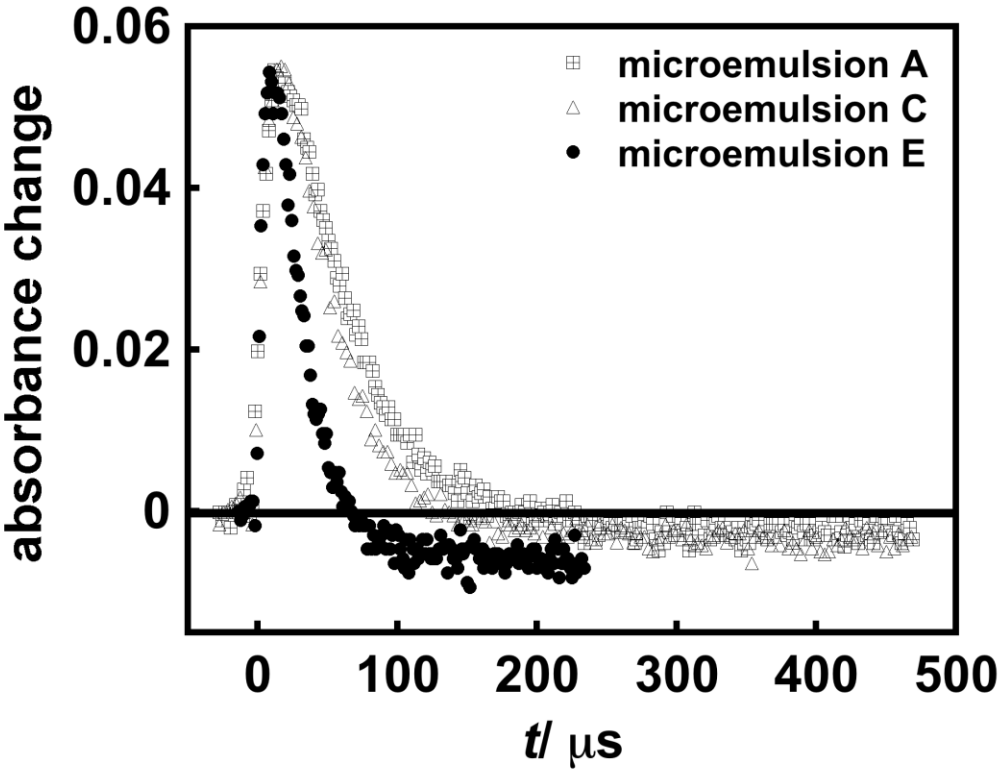
0.06
0.04
0.02
0
absorbance change
microemulsion A
microemulsion C
microemulsion E
0
100
200
300
400
500
t/ μs

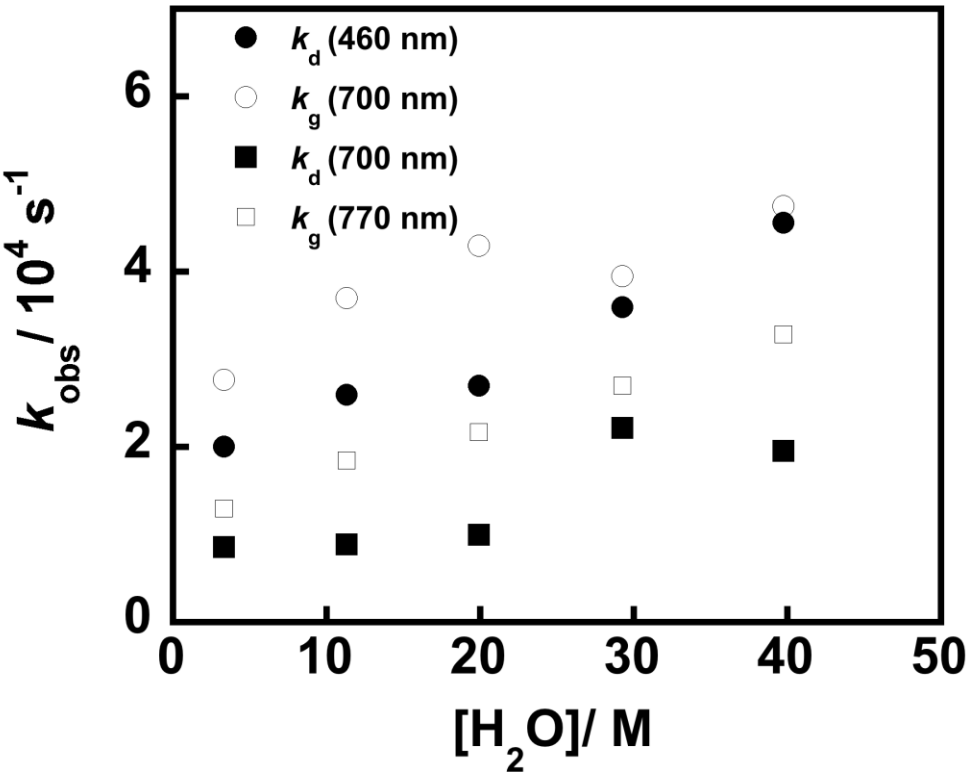
k_d (460 nm)
k_g (700 nm)
k_d (700 nm)
k_g (770 nm)
k_{obs} / 10^4 s^{-1}
0
2
4
6
0
10
20
30
40
50
[H_2O]/ M

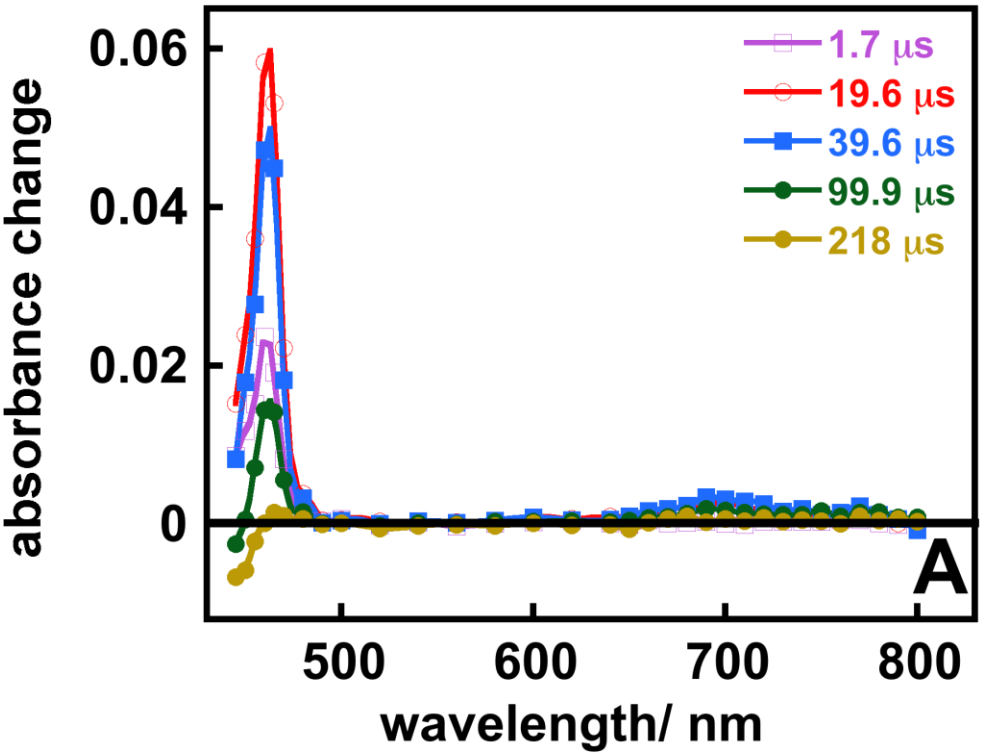
absorbance change
0.06
0.04
0.02
0
500
600
700
800
wavelength/ nm
1.7 μs
19.6 μs
39.6 μs
99.9 μs
218 μs
A

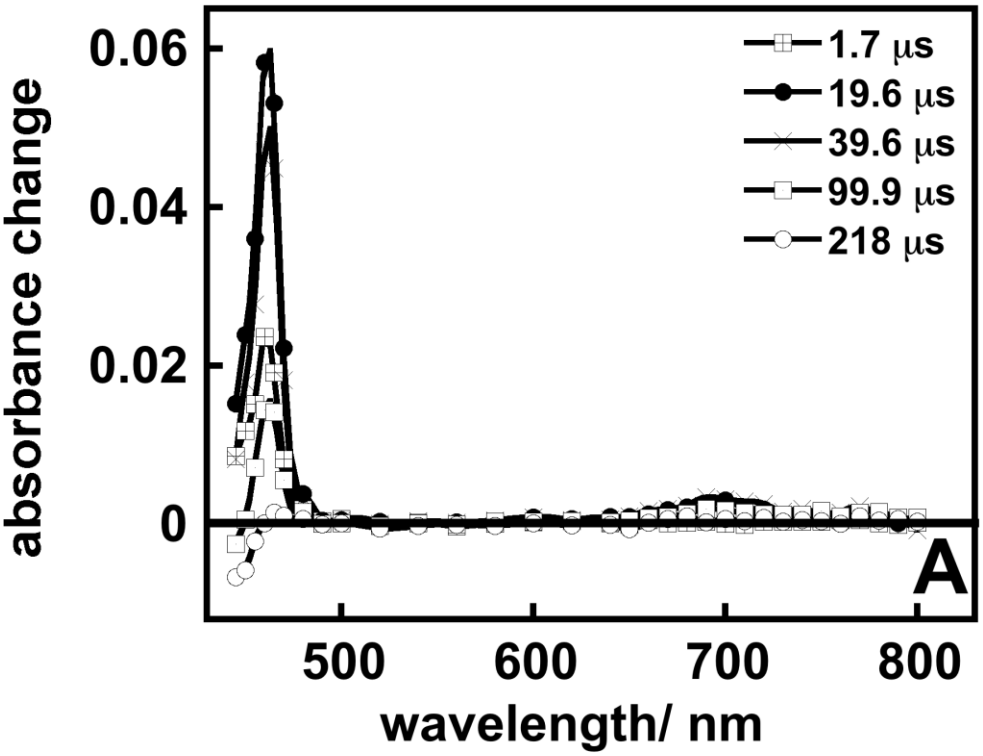
absorbance change
0.06
0.04
0.02
0
500
600
700
800
wavelength/ nm
1.7 μs
19.6 μs
39.6 μs
99.9 μs
218 μs
A

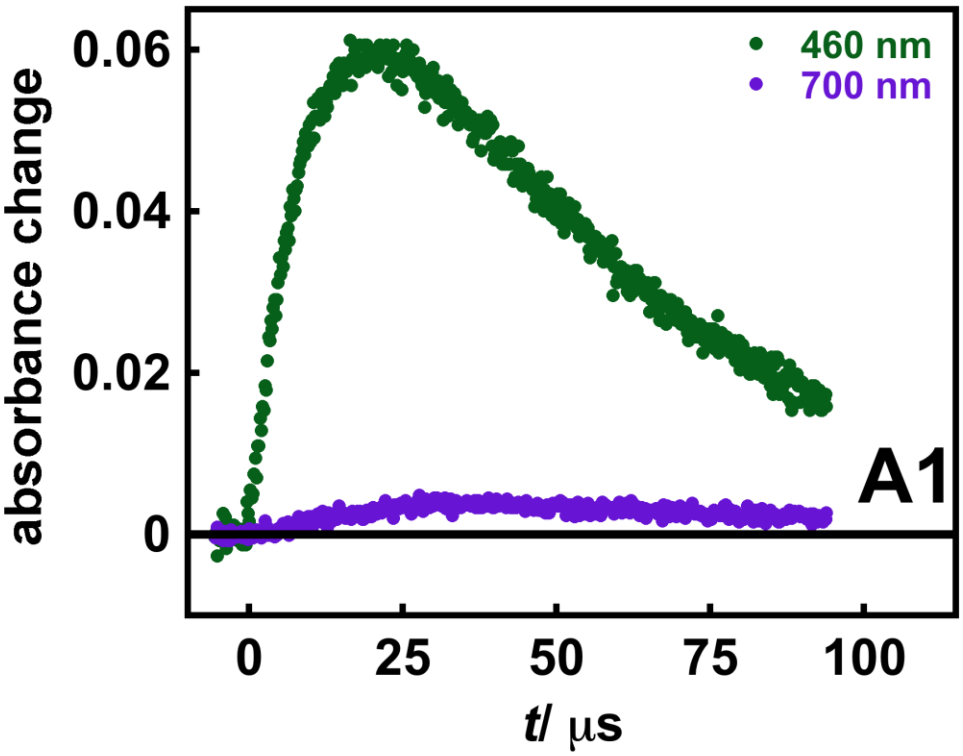
absorbance change
0.06
0.04
0.02
0
460 nm
700 nm
A1
0
25
50
75
100
t/ μs

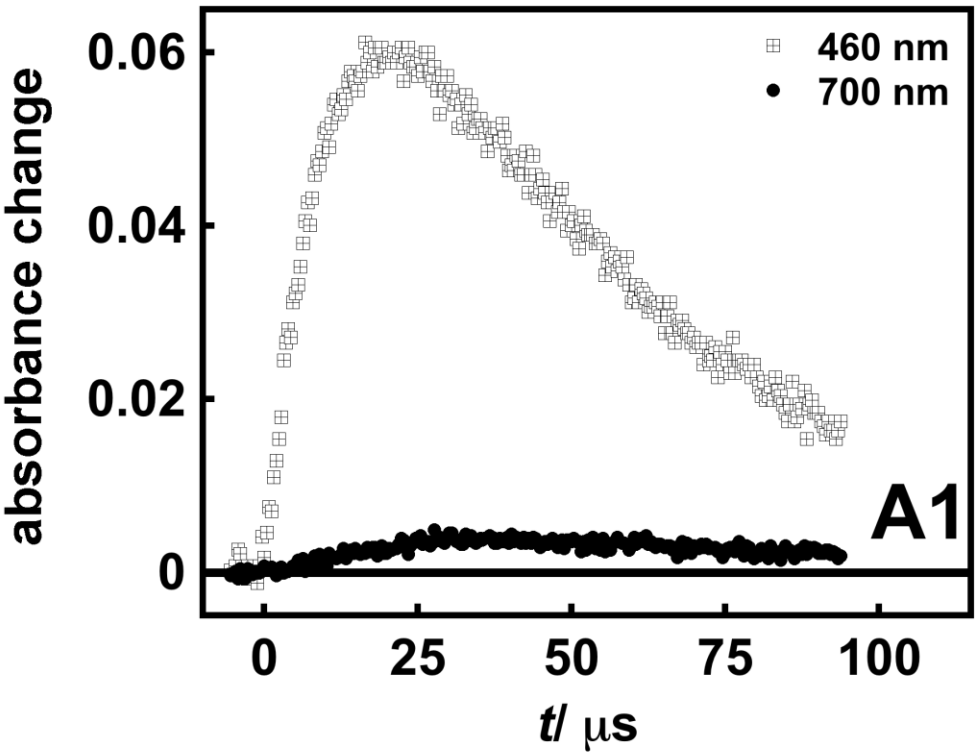
absorbance change
0.06
0.04
0.02
0
460 nm
700 nm
A1
0
25
50
75
100
t/ μs

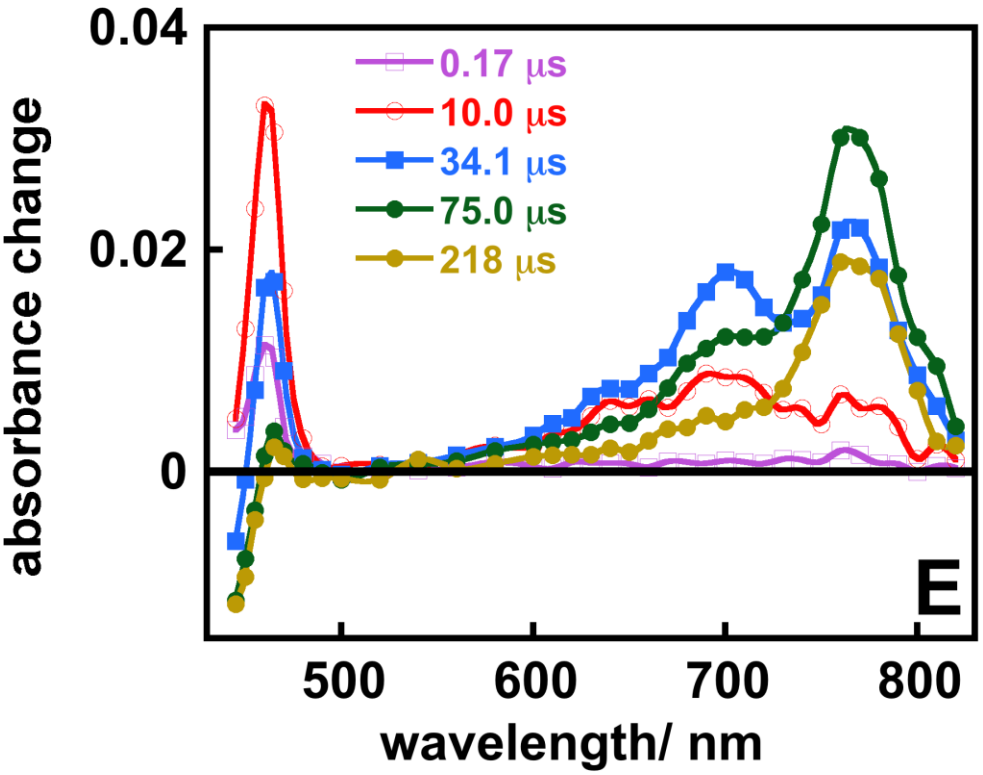
0.04
0.02
0
absorbance change
0.17 μs
10.0 μs
34.1 μs
75.0 μs
218 μs
E
500
600
700
800
wavelength/ nm

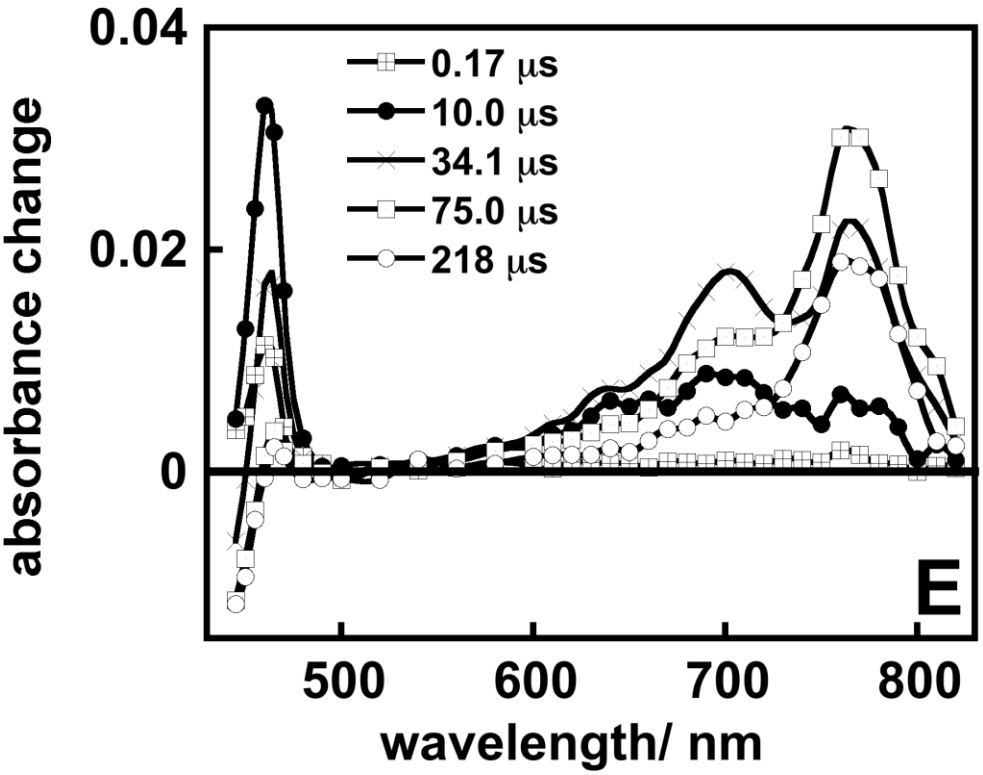
0.04
0.02
0
absorbance change
0.17 μs
10.0 μs
34.1 μs
75.0 μs
218 μs
E
500
600
700
800
wavelength/ nm

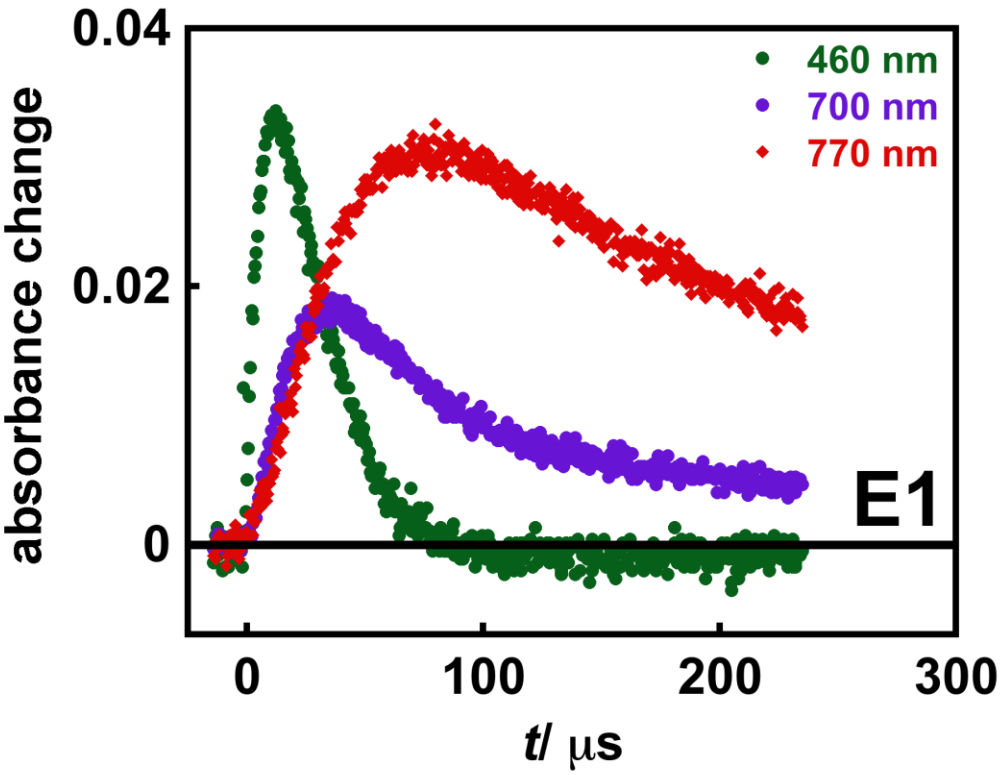
0.04
0.02
0
absorbance change
460 nm
700 nm
770 nm
E1
0
100
200
300
t/ μs

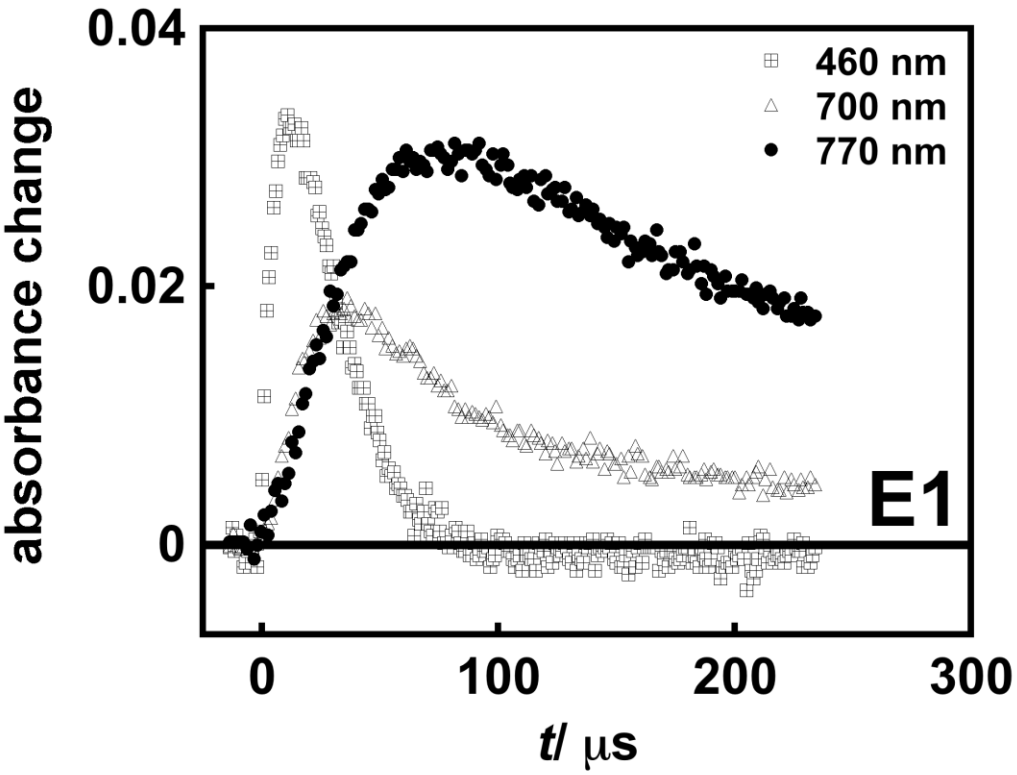
0.04
0.02
0
absorbance change
460 nm
700 nm
770 nm
E1
0
100
200
300
t/ μs

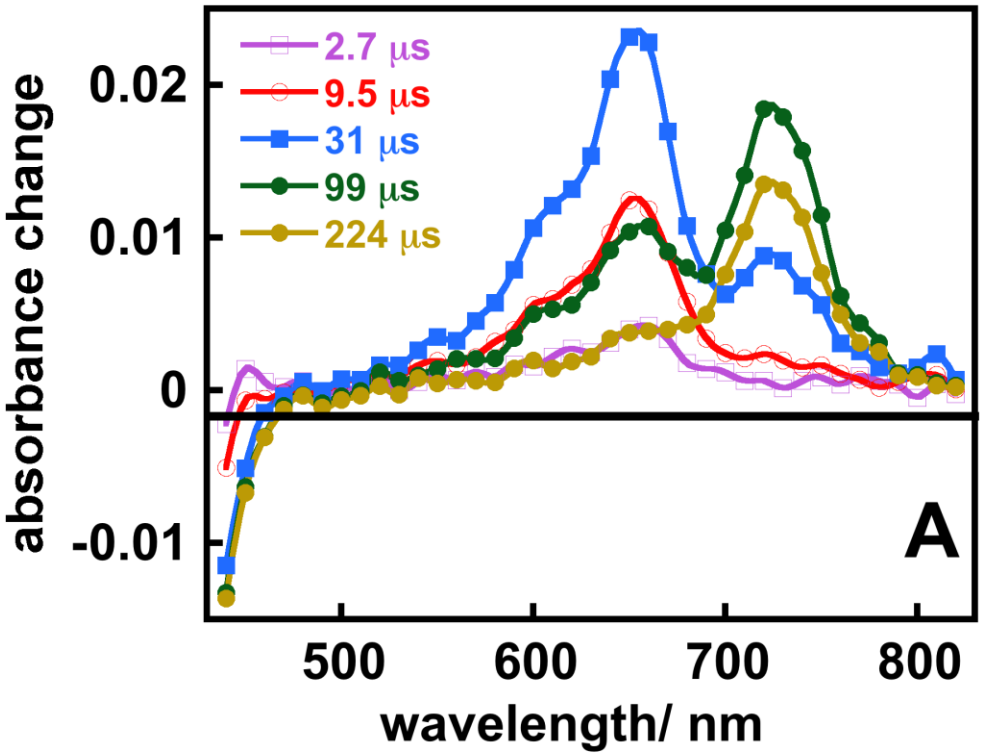
2.7 µs
9.5 µs
31 µs
99 µs
224 µs
absorbance change
0.02
0.01
0
-0.01
A
500
600
700
800
wavelength/ nm

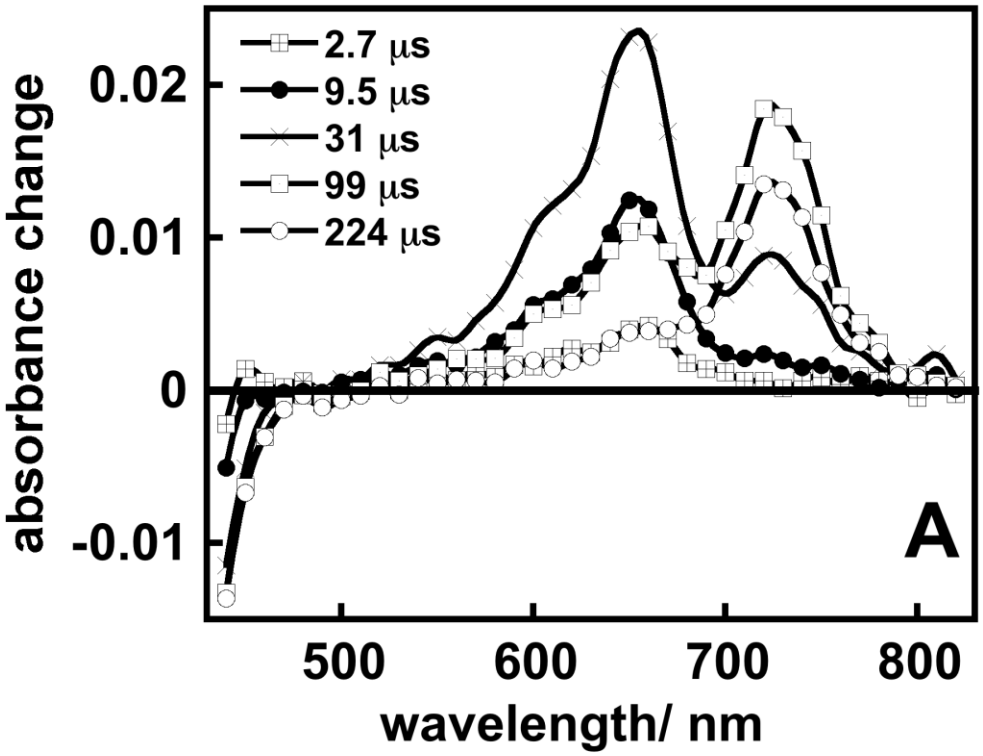
2.7 μs
9.5 μs
31 μs
99 μs
224 μs
absorbance change
0.02
0.01
0
-0.01
A
500
600
700
800
wavelength/ nm

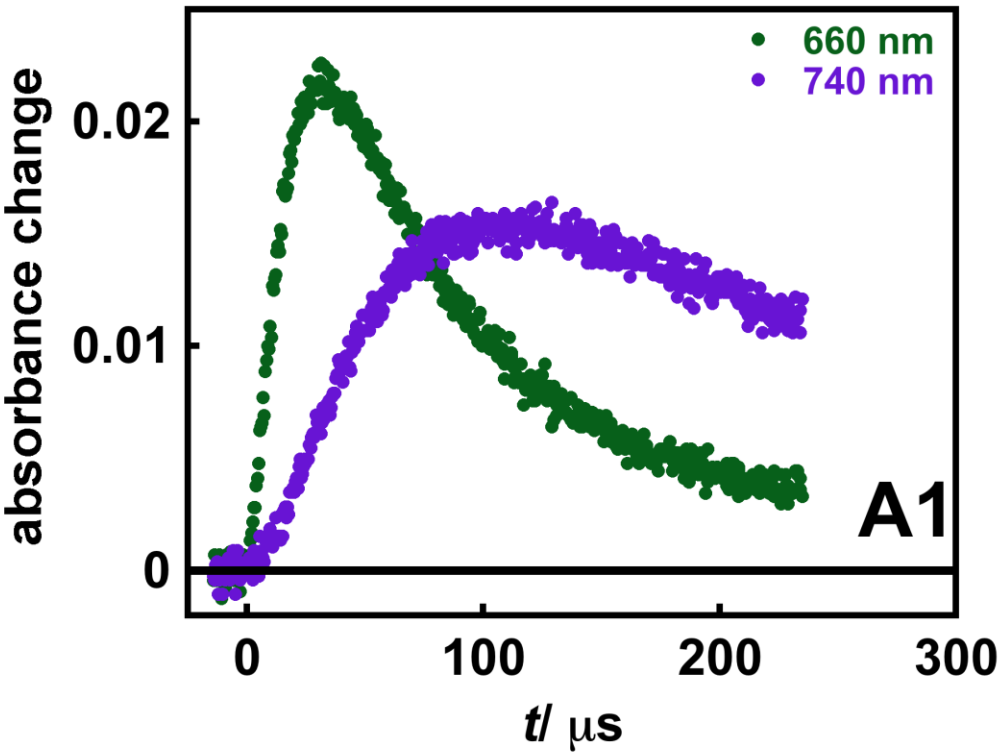

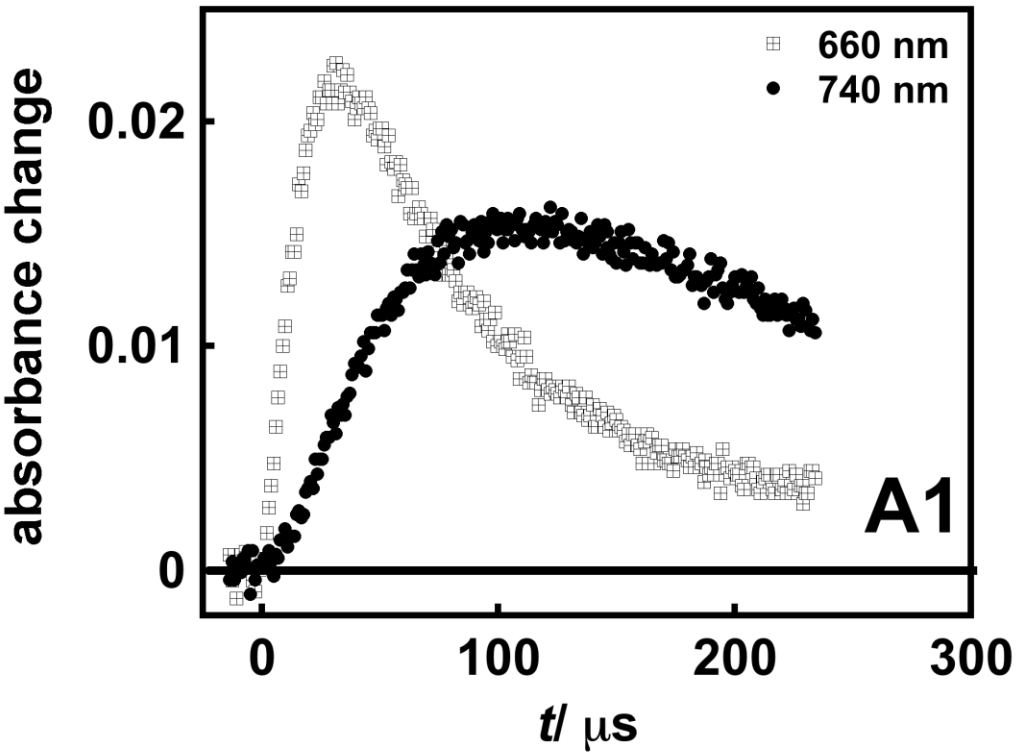

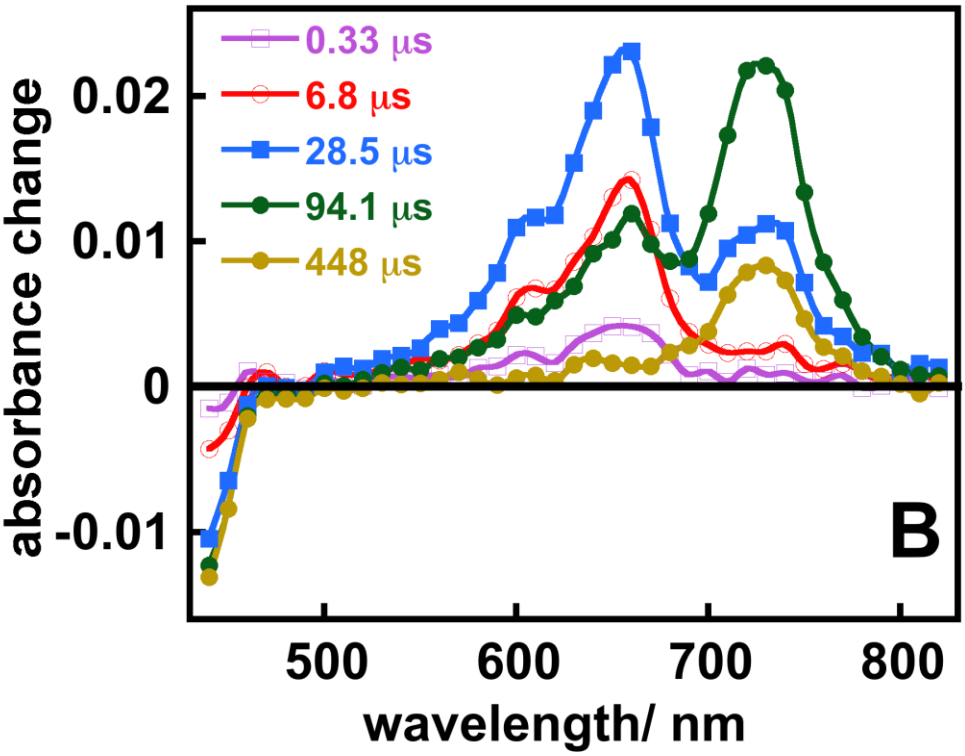
0.33 μs
6.8 μs
28.5 μs
94.1 μs
448 μs
absorbance change
0.02
0.01
0
-0.01
B
500
600
700
800
wavelength/ nm

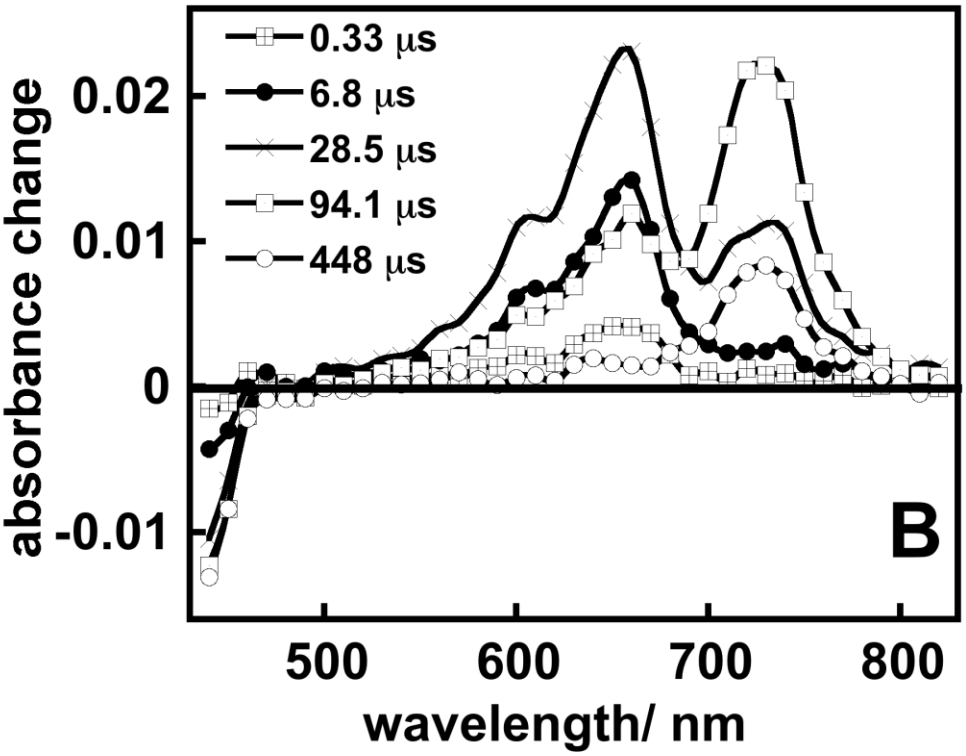
0.33 μs
6.8 μs
28.5 μs
94.1 μs
448 μs
absorbance change
0.02
0.01
0
-0.01
B
500
600
700
800
wavelength/ nm

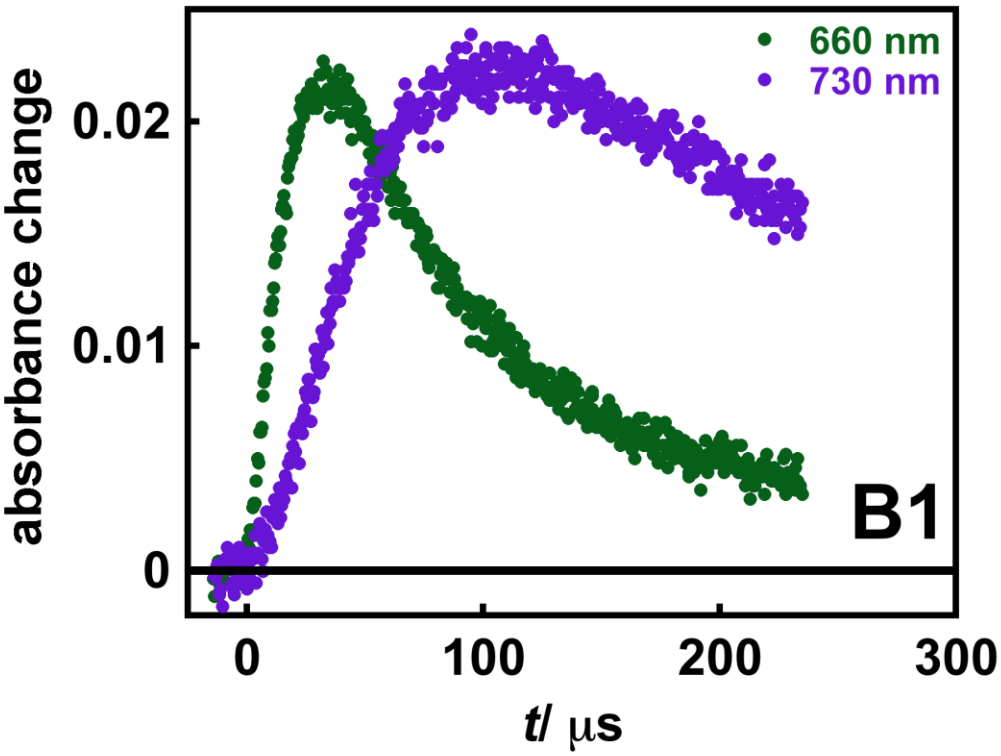

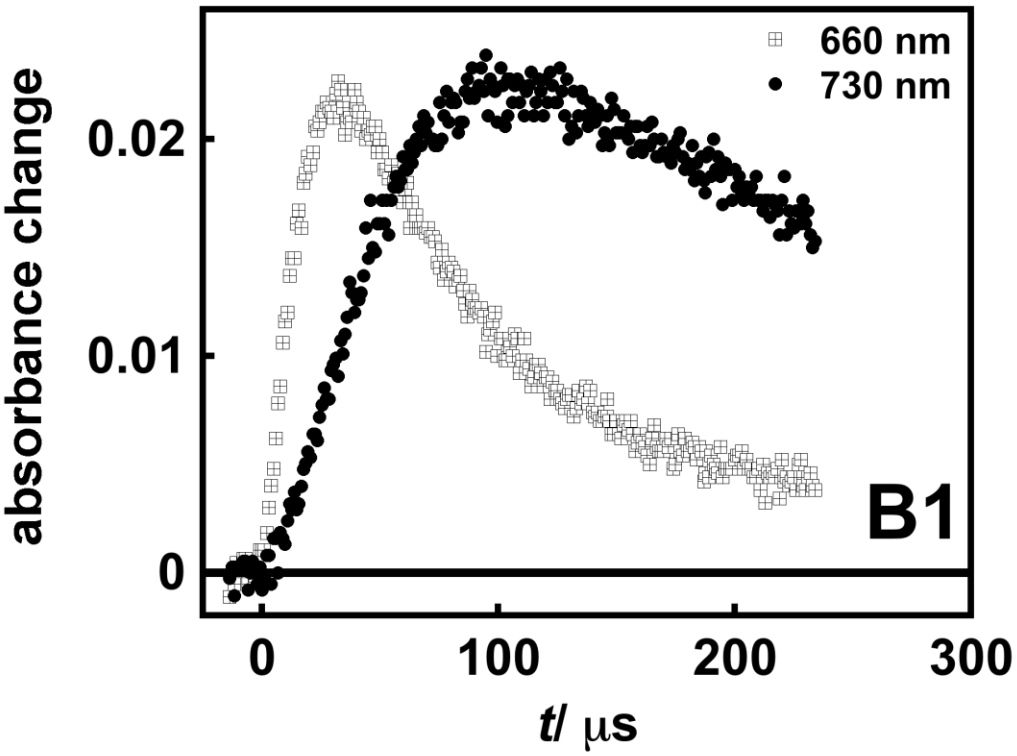

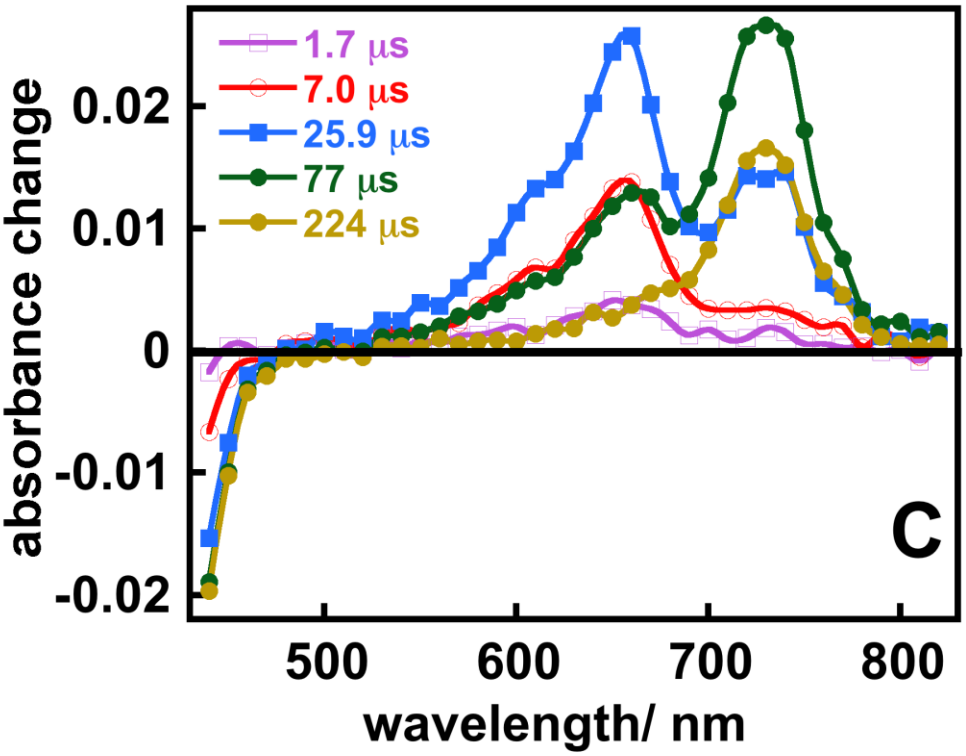
1.7 µs
7.0 µs
25.9 µs
77 µs
224 µs
absorbance change
0.02
0.01
0
-0.01
-0.02
500
600
700
800
wavelength/ nm
C

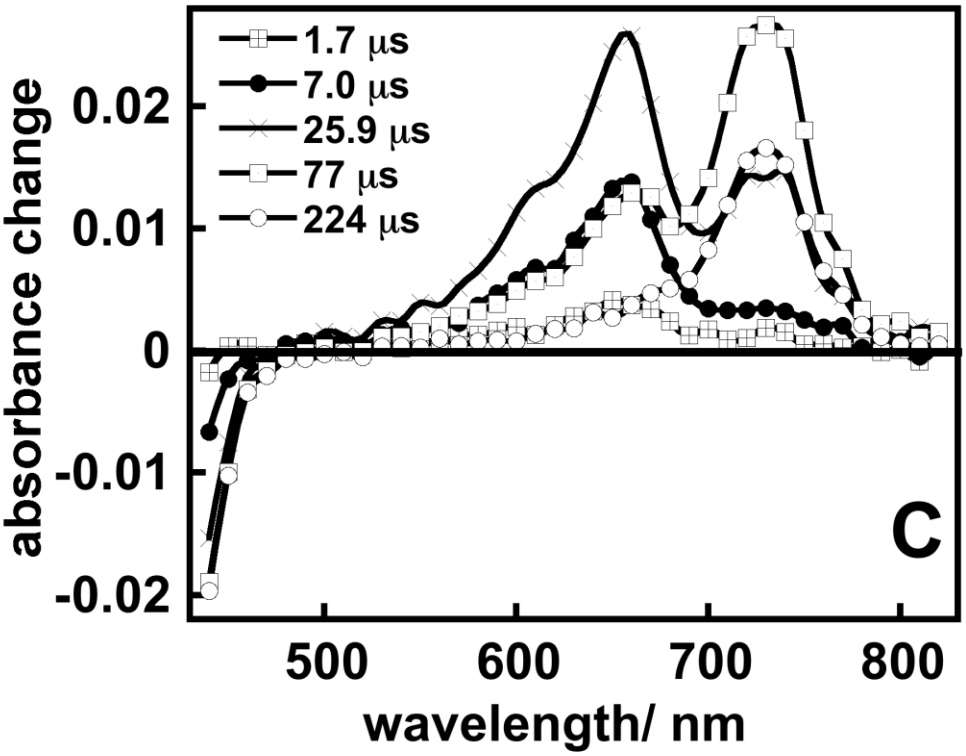
1.7 μs
7.0 μs
25.9 μs
77 μs
224 μs
absorbance change
0.02
0.01
0
-0.01
-0.02
500
600
700
800
wavelength/ nm
C

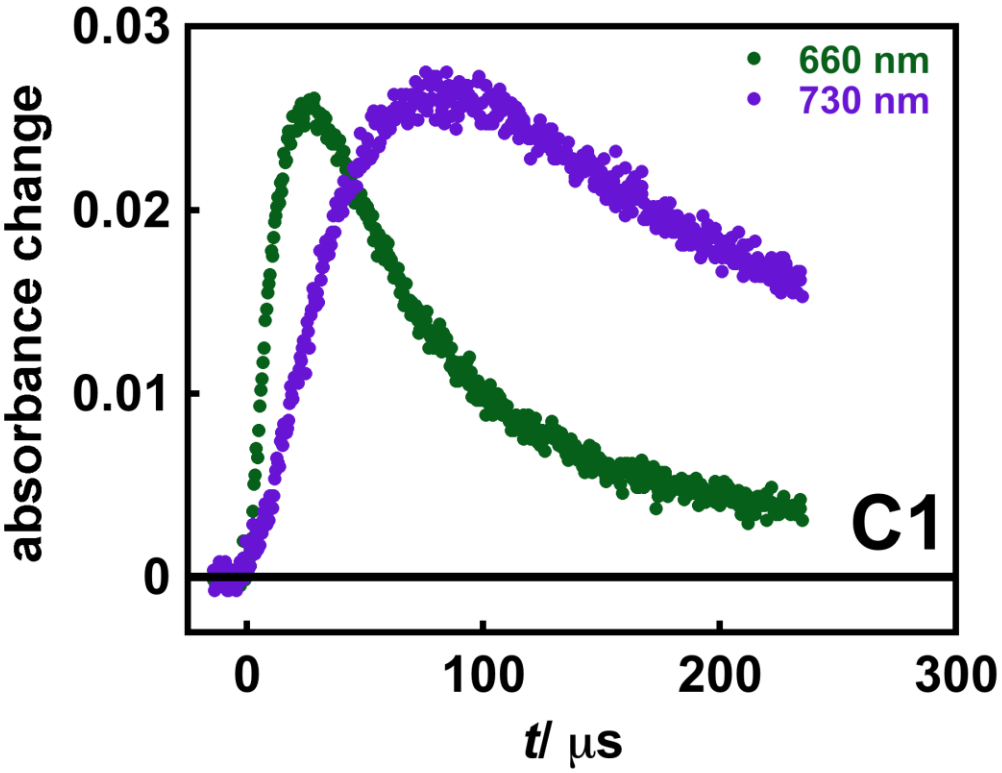
0.03
0.02
0.01
0
absorbance change
660 nm
730 nm
C1
0
100
200
300
t/ μs

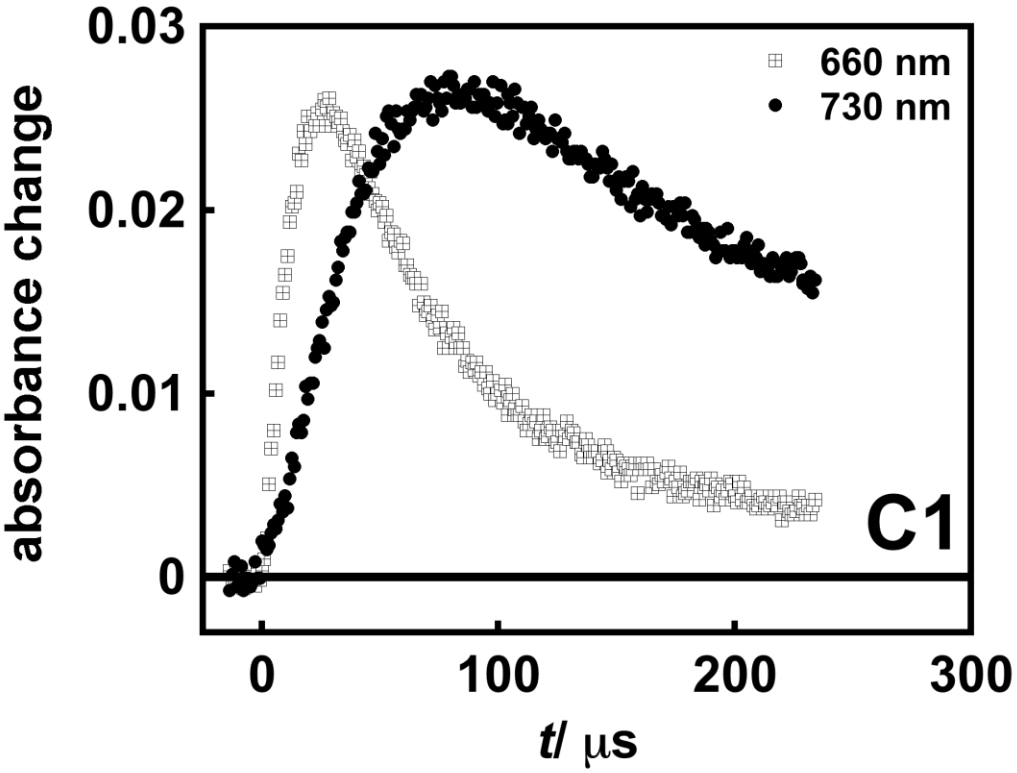
0.03
0.02
0.01
0
absorbance change
660 nm
730 nm
C1
0
100
200
300
t/ μs

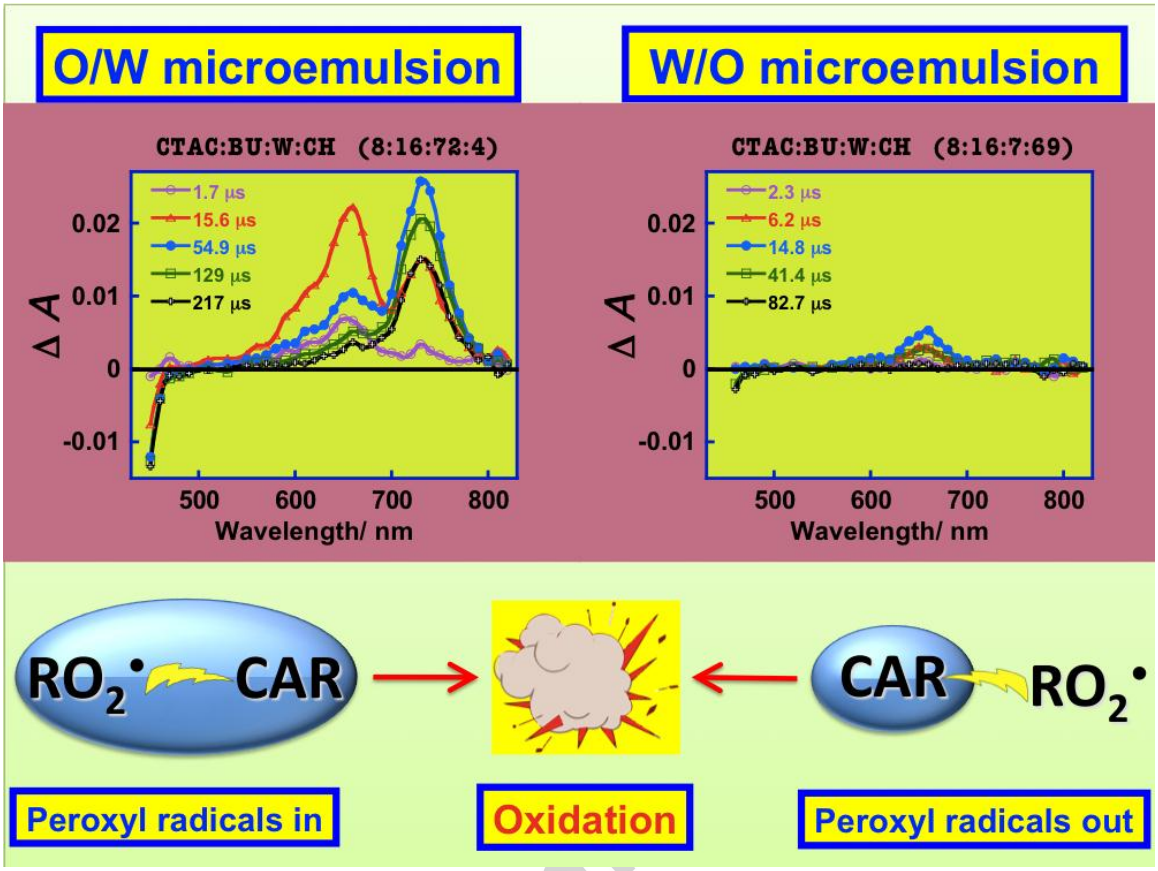
O/W microemulsion
W/O microemulsion
CTAC:BU:W:CH (8:16:72:4)
1.7 µs
15.6 µs
54.9 µs
129 µs
217 µs
0.02
0.01
0
-0.01
Δ A
500
600
700
800
Wavelength/ nm
CTAC:BU:W:CH (8:16:7:69)
2.3 µs
6.2 µs
14.8 µs
41.4 µs
82.7 µs
RO2• CAR
CAR RO2•
Peroxyl radicals in
Oxidation
Peroxyl radicals out